NEUROPATHOLOGICAL EXAMINATIONS IN THE MOUSE BRAIN- INVESTIGATION OF A NEW PHARMACEUTICAL TARGET IN THE CUPRIZONE MODEL AND COMPARATIVE HISTOLOGICAL ANALYSES OF PRIMARY CILIA IN THE PHYSIOLOGICAL CENTRAL NERVOUS SYSTEM

Ph.D. Thesis

Éva Sipos M.D.

Department of Neurology

Medical School of Pécs

University of Pécs, Hungary

Leader of the project: Prof. Sámuel Komoly M.D., Ph.D., Ds.C.

Péter Ács M.D., Ph.D.

Leader of the program: Prof. Sámuel Komoly M.D., Ph.D., Ds.C.

Leader of Doctoral School: Prof. Sámuel Komoly M.D., Ph.D., Ds.C.

Pécs, 2020

TABLE OF CONTENTS

List of Figures

List of Tables

Dissertation Guidance

The dissertation provides in depth and updated information about specific aspects of Multiple Sclerosis and functions of primary cilia in the brain. All data summarized within each chapter has been published as individual projects on its own right. The thesis involves two independent studies centred around novel histopathological findings in the mouse brain. It is important to emphasize that sections of the dissertation aim to highlight current theoretical knowledge in connection with novel experimental data. As such, it is the intention of the author to lay out concise and accessible information for a broad spectrum of readers (researchers, academics, clinicians) who are interested in the development of new therapies and clinical management of neurological disorders in the future.

Abbreviations:

$5HT_6$ –Serotonin receptor 6

AC3- Adenylyl cyclase type 3

APCs- antigen presenting cells

ARC- arcuate nucleus

Arl13b- ADP-ribosylation factor –like protein 13 B

aEAE- actively-induced experimental autoimmune encephalomyelitis

AsPC- astrocytic primary cilia

Bak 1- Bcl-2-Antagonist/Killer 1

BBB- blood-brain-barrier

BBS- Bardet-Biedl syndrome

CC- corpus callosum

CFA- complete Freud's adjuvant

c-Jun- transcription factor c-Jun

CNS- central nervous system

D1r- Dopamine receptor subtype 1

DAB- 3,3′-diaminobenzidine

DAPI- 4′,6′-diamidino-2-phenylindole

DM- dorsomedial nucleus

DMTs- disease-modifying treatments

DRG- dorsal root ganglion

EAE- Experimental autoimmune encephalomyelitis

EB- Ethidium bromide

ERK1/2- extracellular -regulated protein kinase 1/2

FGF-2- fibroblast growth factor 2

GFAP- Glial fibrillary acidic protein

GM- gray matter

GPCR- G protein-coupled receptor

hEAE- humanized experimental autoimmune encephalomyelitis

HPRT-1- hypoxanthine phosphoribosyltransferase 1

IGF-1- insulin-like growth factor 1

IHC- immunohistochemistry

JNK- c-Jun N-terminal kinase

Kiss1r- Kisspeptin receptor 1

KO CTRL- untreated Transient Receptor Potential Ankyrin 1 knockout mice

KO CPZ- cuprizone-treated Transient Receptor Potential Ankyrin 1 knockout mice

LFB/CV- Luxol fast blue-cresyl violet

LPC- Lysophosphatidylcholin/lysolecithin

MAG- myelin-associated glycoprotein

MAPK- mitogen-activated protein kinase

MBP- myelin basic protein

Mch1r- Melanin-concentrating hormone receptor subtype 1

MHC- major histocompatibility complex

NAWM- normal appearing white matter

NeuN- Neuronal specific nuclear protein

NG- nodose ganglion

NG2: chondroitin sulfate proteoglycan 4/ neural/glial antigen 2

NPC- neuronal primary cilia

NPY2r- Neuropeptide Y 2 receptor

NPY5r- Neuropeptide Y 5 receptor

OL- oligodendrocyte

OPC- oligodendrocyte progenitor cells

pAPC- peripheral antigen presenting cells

PBS- phosphate buffered saline

PDGFRα- platelet-derived growth factor receptor α

pEAE- passive or adoptive transfer- induced experimental autoimmune encephalomyelitis

PLP- myelin proteolipid protein

PPMS- primary progressive multiple sclerosis

PRMS- progressive relapsing multiple sclerosis

PVN- paraventricular nucleus

qPCR- quantitative real-time polymerase chain reaction

RRMS- relapsing-remitting multiple sclerosis

SCN- suprachiasmatic nucleus

sEAE- spontaneous experimental autoimmune encephalomyelitis

SPMS- secondary progressive multiple sclerosis

Sstr3- Somatostatin receptor subtype 3

TRG- trigeminal ganglion

TRPA1- Transient Receptor Potential Ankyrin 1

TRPA1 KO- Transient Receptor Potential Ankyrin 1 knockout mice

TRPA1 WT- Transient Receptor Potential Ankyrin 1 wild-type mice

VM- ventromedial nucleus

WM- white matter

WT CPZ- cuprizone-treated Transient Receptor Potential Ankyrin 1 wild-type mice

WT CTRL- untreated Transient Receptor Potential Ankyrin 1 wild-type mice

1. INTRODUCTION

1.1 General overview of Multiple Sclerosis

1.1.1 Epidemiology, aetiology and clinical features of Multiple Sclerosis

Multiple Sclerosis (MS) is a chronic and degenerative disease of the central nervous system (CNS) characterised by inflammation and myelin destruction. MS has been one of the leading causes of neurological disability among young adults particularly in high-income countries. The initial symptoms or onset of the disease is typically diagnosed between the age of 25-35 and generally found to be more prevalent in women than men (female to male ratio varies between 1,5:1 and 2,5:1) (Ascherio et al., 2016). According to the summarizing study by Leray at al (Leray et al., 2016), the prevalence of MS is highest in the population of North America (140/100.000) and Europe (108/100.000), while lowest in Asia (2,2/100.000) and in the sub-Saharan Africa (2,1/100.000). Additionally, they also emphasize a North-South gradient concept reflecting an increasing prevalence of patients in Northern hemisphere such as Scandinavian countries or the United Kingdom. Regardless of the geographical location, up until today, MS ultimately leads to progressive neurological disabilities that have a major impact on the quality of life of the affected population despite of the increasingly available therapeutic approaches applied even in developed countries.

MS is generally considered to rely on a multifactorial aetiology (Ascherio et al., 2016), in which both genetic predisposition and exogenous factors are suggested to play a central role. Statistical data drawn from different studies show a strong association between the frequency of the disease and certain environmental risk factors such as smoking, infections (Ebstein-Bar virus or infectious mononucleosis) as well as the geographical latitude-linked hours of sun exposure or low levels of vitamin D (Ascherio et al., 2010; Degelman et al., 2017; Handel et al., 2011; Harbo et al., 2013; Levin et al., 2010; Marabita et al., 2017; Munger et al., 2006; Nielsen et al., 2007; Pierrot-Deseilligny et al., 2017). The genetic contribution to disease susceptibility has become evident in the last decades. The disease clusters in families, blood-related siblings and relatives of MS patients have a significantly higher risk for MS development (O'Gorman et al., 2013; Robertson et al., 1996). Series of genomic studies highlighted the crucial association between genes encoding human leukocyte antigens (HLA) within the major histocompatibility complex (MHC) and the inflammatory nature of MS (Canto et al., 2018; Compston et al., 1976; Hedström et al., 2017; Hollenbach et al., 2015; Jersild et al., 1973; Naito et al., 1972; Werneck et al., 2018). Over the last few years, large cohort of patient samples became available and combined with advanced technology utilizing novel screening and/or detecting methods such as single nucleotide polymorphisms (SNPs) and

currently ongoing genome-wide association studies (GWAS) also shed light on to multiple possible genes linked to disease susceptibility (Gregory et al., 2007; International Multiple Sclerosis Genetics et al., 2013; International Multiple Sclerosis Genetics et al., 2011; Lill et al., 2013). Nonetheless, the list of possible genes involved in disease development is constantly expanding and further studies are needed to assess the complex genetic background of MS. Additionally, studies investigating a possible interplay between genetic and environmental factors also began in the last decade to identify epigenetic changes that may contribute to MS development (Ayuso et al., 2017; Koch et al., 2013; Marabita et al., 2017).

Clinically, MS is a heterogeneous disease and has a great diversity in the presentation of neurological symptoms across individuals. Depending on the affected CNS region- the brain and the spinal cord- the clinical manifestations may arise as visual disturbances, widespread dysfunctions of the motor and autonome system, sensory abnormalities or even emotional and cognitive changes. Notably, the combination and intensity of symptoms vary from individual to individual and across time (Capone et al., 2019; Coghe et al., 2019; Goldenberg, 2012; Hoff et al., 2019; McDonald et al., 2005; Motl et al., 2008; Noseworthy et al., 2000; Shin et al., 2019; Silveira et al., 2019; Sofologi et al., 2019). The disease does not necessarily follow a predictable progression from its onset, thus, the classification of the type of MS is often difficult. According to current literature, both features of disease evolution over time and well- specified diagnostic criteria should be considered for each individual (for the revised McDonald diagnostic criteria (Thompson, Banwell, et al., 2018) see Table 1.). MS is generally classified according to its clinical course into four main categories (Fig.1.): 1) relapsing- remitting (RRMS) is the most common clinical course among individuals (85%) diagnosed after disease onset. RRMS is characterised by periods of flare-ups of new or existing neurological symptoms ("attacks, relapses or exacerbations") and consequently followed by partial or complete recovery ("remission"). After long years or even decades most RRMS patients enter 2) the secondary progressive phase (SPMS), where the periodicity between relapses and remissions eventually turn into a gradual but constant deterioration of symptoms. Approximately 10% of patients are diagnosed with 3) a primary- progressive (PPMS) disease course, which is associated with gradual clinical worsening of symptoms without recovery after disease onset. In rare cases (<5%), patients follow 4) a progressive-relapsing (PRMS) course in which progressive accumulation of neurological disability is present from onset and also associated with acute relapses with or without remission (Goldenberg, 2012; Lublin et al., 2014; McKay et al., 2015; Thompson, Banwell, et al., 2018; Tullman et al., 2004). In view of the clinical spectrum, two other clinical entities- that do not fulfill the diagnostic criteria of dissemination in space and

time- should be also noted: 1) clinically isolated syndrome (CIS) where patients present novel neurological signs with or without a radiological proof and 2) radiologically isolated syndrome (RIS) in which incidental imaging findings are highly suggestive of demyelinating inflammatory lesions but patients lack clinical signs or symptoms (Lublin et al., 2014; Thompson, Banwell, et al., 2018). The complex nature of MS has been extensively studied throughout decades. Both genetic and environmental factors are well-established components of disease susceptibility. However, the exact pathomechanism of MS is still elusive and even separate pathological processes have been suggested to underlie the distinct clinical courses (Barnett et al., 2004; C. Lucchinetti et al., 2000).

Fig. 1: Clinical courses of MS

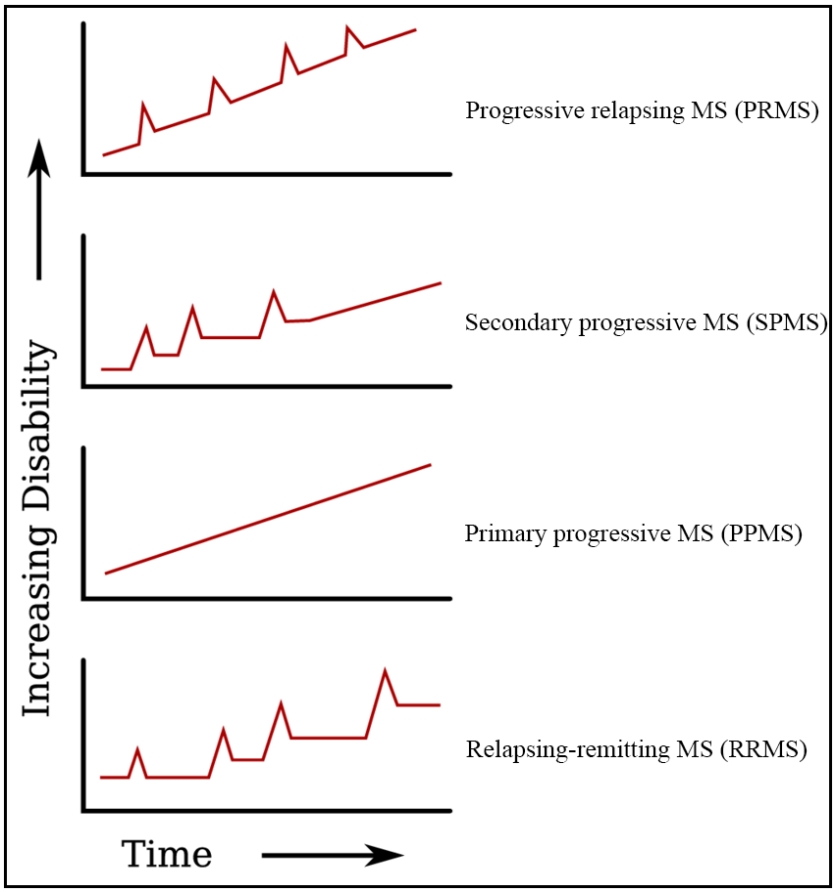

Modified image adapted from Brombin et al. 2016 (Brombin et al., 2016)

MS: Multiple Sclerosis

Table 1. Diagnostic criteria for MS

Clinical Presentation	Additional data needed to make MS diagnosis
Person with typical attack/CIS at onset	
• ≥2 attacks and objective clinical evidence of ≥2 lesions • ≥2 attacks and objective clinical evidence of ≥ 1 lesion with historical evidence of prior attack involving lesion in a different location	None. Dissemination in space (**DIS**) and dissemination in time (**DIT**) have been met.
• ≥2 attacks and objective clinical evidence of ≥ 1 lesion	**<u>One criteria from below:</u>** -**DIS**: additional clinical attack implicating different CNS sites. -**DIS**: ≥1 symptomatic or asymptomatic MS- typical T2 lesions in ≥2 areas of the CNS: periventricular, juxtacortical/cortical, infratentorial or spinal cord
• 1 attack and objective clinical evidence of ≥ 2 lesions	**<u>One criteria from below:</u>** -**DIS**: additional clinical attack -**DIS**: simultaneous presence of both enhancing and non-enhancing symptomatic or asymptomatic MS-typical MRI lesions -**DIT**: new T2 or enhancing MRI lesion compared to baseline scan (without regard to timing of baseline scan) -**CSF**: specific (not in serum) oligoclonal bands
• 1 attack and objective evidence of 1 lesion	**<u>One criteria from below:</u>** -**DIS**: additional clinical attack implicating different CNS site -**DIS**: ≥1 symptomatic or asymptomatic MS- typical T2 lesions in ≥2 areas of the CNS: periventricular, juxtacortical/cortical, infratentorial or spinal cord **AND <u>One criteria from below:</u>** -**DIT**: additional clinical attack -**DIT**: simultaneous presence of both enhancing and non-enhancing symptomatic or asymptomatic MS-typical MRI lesions -**DIT**: by new T2 or enhancing MRI lesion compared to baseline scan (without regard to timing of baseline scan) -**CSF**: specific (not in serum) oligoclonal bands

Clinical Presentation	Additional data needed to make MS diagnosis
Person with progression of disability form onset	
• Progression from onset	-1 year of disability progression (retrospective or prospective) **AND** **<u>Two criteria from below:</u>** -≥1 symptomatic or asymptomatic MS –typical T2 lesions (periventricular, juxtacortical/cortical or infratentorial) -≥2 spinal cord lesions -**CSF**: specific (not in serum) oligoclonal bands
Data adapted from Thompson et al. 2018 (Thompson, Banwell, et al., 2018) **CIS:** Clinically Isolated Syndrome; **CNS:** Central Nervous System; **CSF:** Cerebrospinal Fluid; **DIS:** Dissemination in Space; **DIT:** Dissemination in Time; **MRI:** Magnetic resonance imaging; **T2 MRI**: Lesions indicating evidence of MS on Magnetic Resonance Imaging	

1.1.2 Overview of the neuropathological features of Multiple Sclerosis

1.1.2.1 Pathogenesis and pathological spectrum of MS lesions

The neuropathological hallmark of MS is the presence of focal demyelinating plaque-like lesions associated with primary demyelination, OL destruction, inflammation, axonal injury and reactive gliosis (Kutzelnigg et al., 2014; Lassmann, 2018; Noseworthy et al., 2000). MS is traditionally regarded as a primary autoimmune disorder that affects the brain and the spinal cord. According to the classical hypothesis, lesion genesis is thought to occur on an autoimmune inflammatory background in which activated, myelin auto-reactive T lymphocytes (MHC Class I-II restricted $CD8^+$ and $CD4^+$ T cells) cross a disintegrated blood-brain-barrier (BBB), sequentially activate local, residential immune cells and propagate an inflammatory destruction of oligodendrocytes (OLs) and myelin (Kutzelnigg et al., 2014; Popescu et al., 2016). Topographically, plaques can randomly occur both in the white- and grey-matter (WM and GM) of the CNS, however, certain predilection sites such as the periventricular, subcortical, cerebellar WM, the optic nerves and the spinal cord, exist (Bo et al., 2003; Brownell et al., 1962; FOG, 1950; A. J. Green et al., 2010; Haider et al., 2014; Haider et al., 2016; Kutzelnigg et al., 2007; Kutzelnigg et al., 2005; Vercellino et al., 2009). Established demyelinating lesion are generally centred around small veins or postcapillary venules and accompanied by the presence of inflammatory infiltrates in the perivascular space, the meninges or within the brain parenchyma. The composition of inflammatory infiltrates varies between brain regions and lesion stages but most commonly involves T&B lymphocytes, plasma cells and macrophages (Frischer et al., 2009; Haider et al., 2016; Henderson et al., 2009; Kutzelnigg et al., 2005). Although it is still not understood in its details, the nature and extent of inflammatory response is thought to be amplified as well as modified by soluble factors (cytokines, pro- and anti-inflammatory molecules) secreted by the latter cell types (Carrieri et al., 1998; Göbel et al., 2018; Häusser-Kinzel et al., 2019; Kerschensteiner et al., 1999; Marik et al., 2007; Miyazaki et al., 2014; Stadelmann et al., 2002; Tzartos et al., 2011; Tzartos et al., 2008). Additionally, brain parenchyma resident cells namely, activated microglia and astrocytes are also key histological features within lesions in the MS brain (Henderson et al., 2009; Kutzelnigg et al., 2005; Noseworthy et al., 2000).

Pathologically, four main MS activity-related plaque-type can be distinguished, namely active (early and late), slowly expanding, inactive and remyelinating shadow plaques. Cellular traits of these lesions are generally suggestive of an ongoing form of the disease. For example, active plaques are most commonly found in patients with acute MS, RRMS or SPMS with relapses, while slowly expanding lesions are characteristic of progressive forms of the disease

(Frischer et al., 2009; Kutzelnigg et al., 2005; Popescu et al., 2016). However, plaques may start and evolve differently during and within each form of the disease (Kutzelnigg et al., 2014; Popescu et al., 2016). Recent observations revealed a profound heterogeneity of demyelination among MS patients and highlighted different immuno-histopathological patterns, which may represent distinct pathomechanisms underlying myelin destruction. A detailed histological study conducted by Lucchinetti et.al (C. Lucchinetti et al., 2000; C. F. Lucchinetti et al., 1996) distinguished four different patterns of active demyelinating MS plaques. Most of the examined lesions shared a common feature of infiltrating T cells and macrophages, but showed essential differences in aspects of demyelination, OL death and adaptive immune response. Pattern I-II are classified as macrophage and antibody mediated demyelinating processes, respectively. Lesions showed a typical perivenous distribution and had sharply demarcated edges. Active demyelination was accompanied by inflammatory infiltrates mainly composed of T cells and macrophages. Pattern II lesions showed pronounced immunoglobulin G (IgG) reactivity and complement deposition of C9neo antigen at sites of active plaque edge, whereas these distinctive features did not appear in Pattern I lesions. Loss of different myelin sheath proteins occurred in a similar manner in both Pattern I and II. In contrast, Pattern III is classified as primary OL injury-induced demyelinating event. In this pattern, profound OL apoptosis (reflected by nuclear condensation and fragmentation as well as DNA fragmentation) was the striking cellular trait at lesion edges but not in the centre. Additionally, OL death was associated with the substantial loss of myelin associated glycoprotein (MAG) compared to other myelin proteins in the injured tissue. Lesions appeared with ill-defined borders, did not follow a perivenous extension and thin layer of myelin was often still present around inflamed vessels. Similar to pattern I-II, inflammatory cells within lesions involved T lymphocytes, macrophages and activated microglia with no complement or Ig deposition. Pattern IV lesions were scarce to be found in biopsies/autopsies and only in a subgroup of patients with a variant of progressive course of MS. Lesions shared histological similarities with the characteristics of Pattern I lesions, involving plaque geography, the synchronous fashion of myelin protein loss as well as the cell types comprising inflammatory infiltrates. However, the strong resemblance of Pattern III lesions with the extensive loss of OLs in active and inactive plaques as well as the presence of DNA fragmentation in OLs in the periplaque WM; suggestive of a functional disturbance of OLs (dystrophy/apoptosis). In correlation with the different clinical courses of MS, Pattern II and III were the most frequent patterns followed by I and II in order of magnitude. Thus, the broad spectrum of MS histopathology challenged the classical immunological concept and raised the question whether a dysregulated inflammatory process or primary

neurodegeneration/ OL death may be the initial event starting new lesions. In subsequent studies by Barnett et. al, this novel initial neurodegenerative concept was further investigated. They performed a detailed histopathological analysis on samples from young patients with RRMS (Barnett et al., 2004). New symptomatic lesions were characterised by prominent and extensive OL loss. The early presence of apoptotic OLs was accompanied by a very early activation of microglia, while infiltration of T cells, macrophages and astrocytes were absent in the apoptotic zone. In line with OL death only slight demyelination was observed. Appearance of intramyelinic oedema and visible vacuolation were described after propagation of tissue injury where phagocytosis of degraded myelin took place by activated microglia/macrophages, which also seemed to promote the infiltration of T lymphocytes into the area. Based on these findings, it has been proposed that there is a temporal evolution of pathological processes in MS lesion formation (Barnett et al., 2004; Barnett et al., 2006). In the prephagocytic stage, OL apoptosis induced structural and molecular changes in myelin sheath triggers the activation of local microglia. Subsequently- as lesions evolve and tissue injury becomes apparent- it provokes a systemic immune response involving macrophages (innate immune system) to scavenge myelin debris and the recruitment of lymphocytes (adaptive immune system), which results in an amplified inflammatory process. Additionally, inflammatory cells involving T and B lymphocytes seen at recently demyelinated plaques are also thought to contribute regenerative processes of OLs (Henderson et al., 2009). These observations contradicted the general concept of a uniform T-lymphocyte mediated autoimmune mechanism underlying the formation of new plaques. Instead, the focus is shifted to apoptotic OL death that may not be only a dominant feature in type III MS lesion (C. Lucchinetti et al., 2000), but rather represent an initial point in lesions of MS exacerbations (Barnett et al., 2004). OL apoptosis and myelin damage unmask sequestered CNS antigens that activate local microglia and triggers a profound mononuclear cell recruitment into the brain. Consequently, a complex molecular interplay occurs between antigen presenting cells (expressing MHC II), subsets of T lymphocytes and other cell secreted factors (such as cytokines, chemokines, immunoglobulins), which are thought to play a key role in tissue injury (Barnett et al., 2006) and alternatively in remyelination (Henderson et al., 2009).

In summary, substantial effort have been invested in understating possible pathomechanisms and precise molecular changes underlying the heterogeneity of MS lesions in the last decade. In view of data gathered from the aforementioned pioneering human studies and different experimental conditions, it is clear that there is a systemic abnormality of immune self-tolerance and the inflammatory milieu is very complex. Experimental evidence suggests that peripherally activated auto-reactive $CD4^+$ Th1 and Th17 cell are key players mediating demyelination (Dendrou et al., 2015; Garg et al., 2015; Grigoriadis et al., 2015; Kebir et al., 2009; Lassmann et al., 2007; Legroux et al., 2015; van den Hoogen et al., 2017). Upon crossing the BBB, their reactivation by MHC class II restricted antigen presenting cells (APCs) is thought to propagate an inflammatory cascade involving pro-inflammatory cytokine production that triggers the recruitment and activation of other immune cells (T&B lymphocytes, macrophages and parenchyma resident microglia) to elicit myelin destruction. The extent of tissue injury is thought to be further augmented by the exposure of naturally hidden myelin-antigens, which broaden the spectrum of target points for infiltrating self-reactive T lymphocytes (termed as epitope spreading) (Ji et al., 2013; McMahon et al., 2005; Miller et al., 1997); ultimately creating a vicious cycle of inflammatory demyelination. Additionally, $CD8^+$ T lymphocytes, B cells and microglia/macrophages are also believed to contribute inflammatory destruction in a highly orchestrated and diverse manner (Häusser-Kinzel et al., 2019; Ji et al., 2013; Legroux et al., 2015; Ruiz et al., 2019; Schetters et al., 2017). This immunopathological process is also known as the "outside-in model" which reinforces the classical primary autoimmune theory regarding lesion development in MS (Stys et al., 2012; Tsunoda & Fujinami, 2002).

Another feasible explanation underlying heterogeneous lesion genesis has been attributed to the new concept of an immunological convolution (Stys et al., 2012). The theory is termed inside-out model, which postulates that MS might develop on a background of an "immunological convolution" between primary neurodegeneration and the host's variably primed immune system. According to the model, MS lesions start with an initial degenerative event of the OL-myelin complex and the subsequent release of highly antigenic substances in turn induce a secondary inflammatory autoimmune response. Importantly, the spectrum of diverse responses of the individual's predisposed immune system defines the extent of secondary inflammation and governs the clinical course of the disease.

Regardless of these observations there has been no MS specific trigger identified yet to induce either a robust autoimmune response or a progressive cytodegenerative process. However, it is

undisputable that both processes play a key role in the temporal and inter-individual heterogeneity of MS lesion pathology and in the broad spectrum of disease courses.

1.1.2.2 Pathological substrate of MS progression

Axonal injury and axonal transection is another prominent feature of acute and chronic MS lesions. The extent of axonal degeneration correlates with the progressive and permanent neurological disability in MS patients. In the progressive stage, both axonal and neuronal degeneration is seen with secondary changes in their ultrastructure (Evangelou et al., 2000; Fischer et al., 2013; Haider et al., 2016; Trapp et al., 1998). Inflammatory cells play a key role in the process, T lymphocyte secreted molecules and microglia/macrophages are thought to contribute to damage (Bitsch et al., 2000; Fischer et al., 2012; Marik et al., 2007). By transition of the disease course into secondary progressive stage, demyelinated lesions are slowly expanding into the surrounding WM in parallel with the dispersion of inflammatory cells and activated microglia into the parenchyma. Cortical GM pathology becomes more prominent in alignment with changes of the normal appearing white matter (NAWM). Denuded axons are in close proximity with reactive astrocytes and often embedded in a glial scar. Inflammation is more pronounced in the perivascular spaces and meninges where cells form follicle-like inflammatory aggregates; and seems to be trapped behind the repaired BBB in the CNS. In contrast, PPMS lesions are characterised by a relative hypocellular centre, low degree of ongoing inflammation without lymphocytic aggregates. (Frischer et al., 2009; Holley et al., 2003; Kutzelnigg et al., 2014; Kutzelnigg et al., 2005; Magliozzi et al., 2007; Serafini et al., 2004; Tanuma et al., 2006). Demyelinated lesions can be repaired by remyelination in the MS brain, but with variable extent. Complete remyelination occurs as shadow plaques with sharply demarcated edges and appear to have uniformly thin myelin sheaths (Prineas et al., 1993). Remyelinating process is accomplished by newly formed OLs recruited to the site of demyelination. Extensive remyelination is frequently seen in association with active inflammation and ongoing phagocytic activity to clear myelin remnants. In turn, oligodendrocyte precursor cells (OPC) are recruited to the demyelinated region to remyelinate the denuded axons. Although tissue repair can be robust and effective in early lesions, the remyelinating capacity becomes impaired and the reparative process may completely fail at later stages of the disease (Bramow et al., 2010; A. Chang et al., 2002; Kuhlmann et al., 2008; Patrikios et al., 2006; Prineas et al., 1993; E. G. Rodriguez et al., 2014).

Considering the above mentioned complexity of tissue injury it is clear that all cellular components are affected to a certain extent at all stages of the disease. Setting a mutual ground

for cellular changes, recent data identified oxidative stress induced mitochondrial injury in the centre of a pathogenic cascade that leads to a state of "virtual hypoxia" and subsequent energy deficiency. The lack of energy results in ionic imbalance in the cells (OLs, axons, neurons) and triggers degenerative events via Ca^{2+} dependent signalling pathways (Trapp et al., 2008; Trapp et al., 2009). The process is thought to be propagated by the oxidative burst of microglia (Fischer et al., 2012) and the ongoing mitochondrial dysfunction (DNA deletions, liberation of pro-apoptotic factor and reactive oxygen species) (Campbell et al., 2011; Fischer et al., 2013; Veto et al., 2010) becomes a vicious cycle, which is further amplified by aging-related lesion burden (Mahad et al., 2015). Overall, mitochondrial injury-linked virtual hypoxia has been suggested to be a possible driving force underlying demyelination, neurodegeneration and cellular dysfunctions. Nonetheless, details of molecular neuropathology of tissue injury are the main sources of the management of MS therapy.

1.1.3 Road to MS therapy via animal models

The clinical management of MS is a complex task. Up until now, there is no curative treatment available for MS. However, it has become more manageable in the last decade due to a constantly expanding list of new therapeutic compounds being developed, used and tested. Importantly, current European and American guidelines (Ghezzi, 2018; Montalban et al., 2018; Rae-Grant et al., 2018) lay out a framework of evidence-based therapeutic options depending on the course and associated neurological complications of the disease. It is beyond the scope of the thesis to review all diagnostics-linked therapeutic algorithms in details. Instead, we intend to highlight three main clinical categories that require different approaches, type and duration of treatment: 1) Short-term, series of high-dose corticosteroids is still one of the most common treatment of acute, disabling relapses (ACTH injections or plasma exchange are additional alternatives) (Burton et al., 2009; Citterio et al., 2000; Lipphardt et al., 2019; Perrin Ross et al., 2013). Although the exact mechanism is still unclear, corticosteroids have been postulated to reduce oedema, inflammation and apoptotic cell death as well as stabilize BBB integrity resulting a faster recovery (Burton et al., 2009; Gold et al., 2001; Perrin Ross et al., 2013). 2) Long-term administration of disease-modifying treatments (DMTs) have a well-established role in relapsing MS. These drugs primarily target the dysregulated immune system to limit CNS inflammation and reduce the frequency of relapses. Their immunosuppressive and immunomodulatory effects are mediated by various mechanisms (De Angelis et al., 2018; S. Faissner et al., 2018; Rommer, Milo, et al., 2019). As of January 2020, more than a dozen DMTs have become available and approved medications of the disease (Rommer, Milo, et al.,

2019; Thompson, Baranzini, et al., 2018). However, so far, only a few of them seem to be beneficial during progressive MS stages (Simon Faissner et al., 2019). Last but not least, 3) symptoms and complications associated with MS sometimes also require targeted pharmacological intervention. For instance, the presence of severe spasticity, neuropathic/chronic pain or voiding dysfunctions have a major impact on the quality of life of patients (Henze et al., 2006; Rommer, Eichstadt, et al., 2019).

Overall, the expansive list of available drugs provides a broad spectrum of opportunities for MS management. The administration of corticosteroids and types of DMTs, however, should be carefully chosen. In particular, DMTs have a different spectrum of safety and efficacy profile (for reviews see: (De Angelis et al., 2018; S. Faissner et al., 2018; Rommer, Milo, et al., 2019)). Depending on the existing co-morbidities of patients DMTs may trigger different and serious side effects (progressive multifocal leukoencephalopathy, cardiac arrhythmias, hepatotoxicity, secondary autoimmunity or even malignancies). Additionally, personal factors (age, lifestyle, compliance), individual pharmacokinetic- pharmacodynamic properties as well as the formulation and tolerability of a selected medication also influence the choice of treatment. Thus, a comprehensive approach is necessary in MS care and individualized decisions are the most imperative.

As previously discussed, neuropathological observations indicated that demyelinating lesions are not uniform. Some MS lesion subtypes are characterised by a predominant autoimmune reaction (C. Lucchinetti et al., 2000), while other subtypes are associated with primary oligodendrocyte apoptosis, suggestive of an initial degenerative pathomechanism (Barnett et al., 2004; Barnett et al., 2006). Cellular events such as axonal injury, microglia/macrophage invasion and reactive astrogliosis are also profound features of demyelinating plaques throughout the entire course of the disease. Additionally, tissue injury and abnormality can occur virtually anywhere in the CNS including the WM, GM and NAWM (Kutzelnigg et al., 2005). Currently, immunomodulatory therapies aim to modulate the immune-inflammatory processes that are most effective in relapsing course of MS but do not provide a complete solution to influence primary degenerative mechanisms or halt the progression of the disease. Thus, novel pharmaceutical targets are increasingly needed for the adequate management of MS therapy. Experimental animal models provide an excellent tool to study details of molecular neuropathology of tissue injury. It is important to emphasize that MS is – as far as we know - solely a human disease. There is no single animal model which can recapitulate the entire spectrum of heterogeneity of MS lesions and clinical courses. However,

each of the models reflect specific aspects of disease pathology and mechanisms which might cause or influence MS.

1.1.3.1 Virus-induced experimental demyelination models

Based on previous epidemiological observations as well as the histopathological similarities between MS lesions and virus- induced demyelinating disorders, an infectious aetiology has been long hypothesized in the pathogenesis of MS. Until now, however, no-MS specific virus has been identified as an active trigger of demyelination or a direct cause to the disease. It has been suggested that Ebstein-Barr virus (EBV) infection might be a critical environmental susceptibility factor (Ascherio et al., 2016; Levin et al., 2010). Due to the profound complexity of MS pathogenesis, virus-induced experimental animal models are most frequently utilized to gain insight how such pathology can be propagated and what are the basic and/or additional molecular mechanisms which are related to inflammation, demyelination and neurodegeneration. Infection-induced experimental demyelination in the mouse brain are best studied by two main viruses namely, Theiler's murine encephalomyelitis virus (TMEV) and Mouse hepatitis virus (MHV).

1.1.3.1.1 Theiler's murine encephalomyelitis

TMEV is a single-stranded RNA virus, which belongs to the Picornaviridae family and it is an enteric pathogen in mice. After the direct intracerebral injection of the virus the course of the disease and mortality are strongly defined by two factors: 1) the neurovirulence of the virus strain (highly virulent and lethal GDVII strains or low virulent Daniel's and BeAn8386 strains) and 2) the genetic ability of the host animal to efficiently escalate a T-cell mediated anti-viral response. By using Daniel's (DA) and BeAn8386 (BeAn) strain in mice with specific major histocompatibility complex class I (MHC I) haplotypes, the virus leads to either a monophasic or a biphasic disease (Denic et al., 2011; M. Rodriguez et al., 1985; Tsunoda et al., 2010). In the latter case, mice develop encephalomyelitis in the acute phase followed by a chronic demyelinating disease predominantly affecting the spinal cord (Denic et al., 2011). On a molecular level, while virus antigen is cleared from the brain, the virus persists in the spinal cord in oligodendrocytes and macrophages (Lipton et al., 1995; M. Rodriguez et al., 1983). Notably, lesions are characterized by confluent plaques of primary demyelination, microglia/macrophage activation, axonal damage and chronic inflammatory infiltrates including CD4+ and CD8+ T cells, B and plasma cells (Bieber et al., 2005; Pachner et al., 2011;

Tsunoda, Kuang, et al., 2002). Based on these histological features and other additional observations, the possible pathomechanism has been suggested to involve numerous different complex pathological steps. However, it became evident that the process is more likely to be mediated by the activation of the immune system rather than a direct, virus-induced toxic effect on the target cells (Denic et al., 2011; Procaccini et al., 2015). Despite of the complexity of TMEV, the model is a valuable tool to study viral clearance from the CNS, the neuropathology of immune activation, the role of different T-cell lines and clinical courses.

1.1.3.1.2 Mouse hepatitis virus

In contrast to TMEV, MHV is a positive-stranded RNA virus of the Coronoviridae family. It is also a natural enteric pathogen in mice, which can induce neurological, hepatic, enteric and respiratory disorders. Similar to TMEV, the susceptibility to MHV depends on the virus strain, genetic background of the experimental animal and the route of administration. Neurological disease occurs via intracerebral or nasal infection with the neurovirulent strain MHV-A59 (Bleau et al., 2015; Cowley et al., 2010). Infection leads to a biphasic disease course in which mice develop an initial panencephalitis within days followed by a short recovery period then a progressive neuroparalysis occurs with chronic inflammatory demyelinating lesions in 4 weeks postinjection (Bender et al., 2010). Although the virus is cleared in the acute phase, viral RNA can be detected in the brain, spinal cord and optic nerve in the infected cells (oligodendrocytes, neurons, astrocytes and microglia/macrophages) at different time points in the disease (Cowley et al., 2010; Shindler et al., 2008). Chronic lesions are characterised by primary demyelination with variable extent of axonal damage and inflammatory infiltrates involving T lymphocytes, microglia/macrophages as well as additional immune cells (Dandekar et al., 2001; Das Sarma et al., 2009; Shindler et al., 2008). Numerous different immune mechanisms have been suggested to contribute to tissue injury (Cowley et al., 2010; Dandekar et al., 2001; Das Sarma et al., 2009). Previous studies have revealed that MHV infection triggers an increased immune response of the innate immune system (such as NK cells and interferons) which contributes to tissue damage. Moreover, studies with immune-deficient animal models showed that CD4+ and CD8+ T cells along with anti-viral antibodies targeting infected cells also play a crucial role in different stages of viral clearance as well as the process of inflammatory demyelination (Bleau et al., 2015; Dandekar et al., 2004; Dandekar et al., 2001; T. S. Kim et al., 2005; Williamson et al., 1991; Zuo et al., 2006). Based on these data, researchers are in support of the general view

that different immune mechanisms are triggered upon viral infection and during inflammation associated myelin destruction.

In summary, virus-induced experimental demyelination models such as TMEV and MHV are useful to study acut and/or chronic/ progressive phases of MS. Moreover, these models are also excellent to investigate processes of direct CNS infection related autoimmunity and consequent demyelination. However, one major limitation of the models is that the key aspects of the complex molecular changes are difficult to distinguish. Thus, additional studies are needed to reveal the precise molecular disease mechanisms underlying virus-induced immune responses and primary demyelination.

1.1.3.2 Experimental Autoimmune Encephalomyelitis (EAE)

Immunization of experimental animals with brain tissue-based specific CNS antigens gives rise to a spectrum of disorders, collectively termed Experimental autoimmune encephalomyelitis (EAE). EAE is the most commonly used in vivo model that reflects many clinico-pathophysiological features of MS. The pathomechanism of EAE is based on the general concept that immunization of host animals with CNS antigens in combination with a strong adjuvant triggers a profound activation of their immune system, which results in inflammation and the destruction of antigen positive structures mediated by mainly MHC Class II type CD4+ T lymphocytes (Fletcher et al., 2010). Although EAE can be induced in almost all vertebrates, the genetic susceptibility of the animal strain, the immunisation protocol and CNS antigens applied strongly determine the degree of efficacy (Pierson et al., 2012; Procaccini et al., 2015). Based on the existing protocols four types of approaches can be distinguished (for review see: (Lassmann et al., 2017): 1) actively-induced EAE (aEAE) in which experimental animals are immunised with a CNS antigen together with a strong adjuvant (Berard et al., 2010; Mendel et al., 1995), 2) passive or adoptive transfer- induced EAE (pEAE), where encephalitogenic cells such as lymph node cells, or specific T cell lines or clones of an immunised animal are transferred to a naïve recipients (Bartholomaus et al., 2009; Flugel et al., 2001; Linington et al., 1988), 3) spontaneous EAE (sEAE) where autoimmune mechanisms can be studied without exogenous manipulation such as utilizing single or even double transgenic animals. For example mice transgenically expressing a T-cell receptor of encephalitogenic T-cells and/or B-cell receptors that induce myelin auto-reactive antibody response (Bettelli et al., 2006; Bettelli et al., 2003; Krishnamoorthy et al., 2006). More recently, 4) humanized EAE (hEAE) has been added to the experimental approaches, which allows us to investigate the encephaliltogenic properties of peptides in transgenic animals expressing human MHC class I or II (Ellmerich et

al., 2004). Although it is beyond the scope of this thesis to describe all above mentioned experimental conditions in details, we focus on aEAE and the most commonly used combination of peptides (e.g.: myelin-oligondendrocyte glycoprotein (MOG), myelin basic protein (MBP), myelin proteolipid protein (PLP) and mouse strains (e.g.: C57BL/6, SJL/J, Biozzi ABH, NOD) in which different disease courses (acute monophasic, chronic/progressive and relapsing-remitting) occur.

For aEAE induction, mice receive a subcutaneous injection of an immune-response triggering mixture consisting a myelin-specific antigen or epitope solubilized in an adjuvant, such as complete Freud's adjuvant (CFA) (Bittner et al., 2014). CFA is assumed to provide a prolonged liberation of the active immunising peptide by partly promoting its phagocytic uptake and its transport via the lymphatic system (Billiau et al., 2001). To further facilitate the process, the addition of an intraperitoneal injection of Bordatella pertussis toxin (PT) has been suggested to increase susceptibility to induce EAE, modulate blood-brain barrier (BBB) (C. Lu et al., 2008) and immunological responsiveness (X. Chen et al., 2006; Dumas et al., 2014; Kamradt et al., 1991). The pathogenetic principle of aEAE is that following inoculation, the antigen is phagocytized by local peripheral antigen presenting cells (pAPC; such as dendritic cells) and by the tracking the lymphatic network these cells reach the intersecting lymphoid organs (lymph nodes, spleen). Consequently, an interplay between pAPC and T lymphocytes occurs, which triggers the formation of encephalitogenic T-cells (Th1 and Th17). Activated myelin-specific T-cells migrate to the CNS across the BBB and induce inflammatory cascades with a profound inflammation (Fletcher et al., 2010; Pierson et al., 2012). Importantly, the pathology of lesions is different from what that seen in MS, aEAE chronic lesions are generally characterised by primary axonal injury with secondary demyelination driven by MHC class II restricted CD4+ T cells (Nikic et al., 2011; Procaccini et al., 2015; Soulika et al., 2009). Additionally, myelin destruction and axonal damage is largely confined to the spinal cord, the cerebellum and the optic nerve can be also affected by a certain extent (Storch et al., 2006). As mentioned above, the histopathology of lesions and disease course are not uniform due to different genetic factors and the type of epitope used. For example, immunization of SJL/J mice with the immunodominant $PLP^{131-151}$peptide results in a relapsing-remitting course (Basso et al., 2008; McRae et al., 1995). In contrast, EAE induced by MOG^{35-55} in C57BL/6 or NOD mice strains follows a chronic course (Berard et al., 2010; Hjelmstrom et al., 1998; Mendel et al., 1995). Interestingly, Biozzi ABH mice are less sensitive to EAE induced by encephalitogenic epitopes of MBP (Amor et al., 1996), whereas the administration of specific MOG epitopes leads to a chronic relapsing-remitting form of EAE (Smith et al., 2005). Considering the heterogeneity of

MS lesions, EAE animal models provide an extensive range of possibilities to investigate the pathological mechanisms of disease progression, neurodenegeneration or protection.

1.1.3.3 Toxin-induced experimental demyelination models

Although EAE is the most common model to study autoimmune mechanisms underlying MS, the use of toxin-induced experimental demyelination models are also well-established to investigate primary demyelination and the molecular mechanisms of de- and remyelination processes. Ethidium bromide (EB), lysophosphatidylcholin (lysolecithin/LPC) and cuprizone are the most common toxins for the induction of demyelination in the rodent CNS. All agents have been long known to induce primary demyelination in well-defined regions of the rodent brain, however, their mechanism of action are essentially different.

1.1.3.3.1 Ethidium bromide (EB) and lysophosphatidylcholin (lysolecithin/LPC)-induced focal demyelination

LPC is an endogeneous lysophospholipid of the phospholipase A2 superfamily. It is generally accepted that exogenous injection of LPC to specific WM tracts leads to focal plaques of demyelination via its direct detergent action targeting the lipid rich myelin sheath (Hall, 1972; Jeffery et al., 1995). LPC induced lesions are characterised by demyelination, macrophage/microglia infiltration, reactive astrocytosis, axonal injury and OPC proliferation. Lesions evolve over a period of few weeks in line with spontaneous remyelination (Jean et al., 2002; Kotter et al., 2001; Lau et al., 2012; Miron et al., 2013; Schulz et al., 2012). While the model is most frequently used to study processes linked to OL damage and remyelination, the mechanism of the agent's toxicity on OLs has been only speculated. However, a recent study by Plemel et al. elegantly mapped the histopathology of lesions and thoroughly investigated the lipid disrupting properties of LPC toxicity upon injection into the mouse ventral spinal cord. They postulated that injection of the agent initiates toxicity by integrating into cellular membranes and by reaching a threshold concentration in myelin it further triggers cell membrane permeability subsequently causing cell death and myelin damage. Moreover, the study revealed that LPC injection may exert non-specific toxicity affecting the main glial cell types (astrocytes, microglia/macrophages, oligodendroglial lineage cells) *in vivo* and *in vitro* conditions, which could also have a major impact on remyelination and secondary inflammatory processes (Plemel et al., 2018).

In contrast to LPC, injection of EB into white matter tracts leads to both oligodendrocyte damage and astrocyte loss. It is generally established that EB exerts cellular toxicity through DNA intercalation (Blakemore, 1982). The mechanism of preferential gliotoxicity has been suggested to arise from its intercalation into the mitochondrial DNA (mtDNA) (Desjardins et al., 1985; Hayashi et al., 1990). Similarly to LPC, the histopathology of lesions are also not uniform. Based on previous studies, the applied protocol, the anatomical location of injection as well as the animal species used greatly define lesion formation (such as extent of demyelination and axonal injury) and additional inflammatory immune responses (Kuypers et al., 2013). Notably, this model led to the discovery that the presence of astrocytes are necessary to promote remyelination and in their absence lesions are repaired by Schwann cells (Blakemore, 1982; Woodruff et al., 1999).

In view of the countless possibilities listed above, toxin- induced focal demyelination models are highly reproducible and are excellent tools to gain insight into the spatio-temporal regulation of cellular processes underlying de- and remyelination.

1.1.3.3.2 Cuprizone-induced experimental demyelination model

Another model to investigate MS related pathology is the cuprizone-induced experimental demyelination. It is one of the most commonly applied model to study the mechanism of demyelination and remyelination with a relatively intact blood-brain barrier (BBB) and no signs of an adaptive immune response (Berghoff et al., 2017; Ruther et al., 2017). Cuprizone [Bis(cyclohexanone)oxaldihydrazone] is a copper-chelating reagent originally discovered in the late 1960's (Blakemore, 1972; Suzuki et al., 1969). Pioneering studies have revealed that systemic administration of the compound- by feeding mice with 0,2% cuprizone mixed into powdered rodent chow- induces a highly reproducible demyelinating brain pathology in a well-defined spatio-temporal fashion (Hiremath et al., 1998). More importantly, the main histological features of cuprizone lesions seem to mimic fundamental aspects of the type III. lesions observed in MS (Acs & Kalman, 2012; Kipp et al., 2009; Torkildsen et al., 2008).

In cuprizone-induced lesions the main pathological event is the selective apoptotic death of mature oligodendrocytes (OL) in particular brain regions, which subsequently results in primary demyelination of the affected areas (Blakemore, 1972; Komoly et al., 1992; Komoly et al., 1987). The exact mechanism initiating or propagating selective OL death is still unclear, however, it is preceded by the appearance of enlarged mitochondria (Acs & Komoly, 2012; Blakemore, 1972). Recent studies propose a hypothesis that OLs undergo apoptosis partly

through mechanisms involving a mitochondria-linked metabolic failure and increased oxidative stress due to the copper-chelating properties of the agent (Acs et al., 2013; Gudi et al., 2014; Praet et al., 2014). Subsequent to cuprizone exposure, OL apoptosis is followed by demyelination but with variable extent. For long, cuprizone was thought cause massive demyelination of only the white matter tracts such as the corpus callosum, anterior commissure or the superior cerebellar peduncules. However, series of studies showed that other areas (i.e.: hippocampal formation, cerebellum, caudate putamen, ventral part of the caudate nucleus) or even distinct gray matter regions (i.e.: striatal complex) and the cortex are also affected, but largely spares the spinal cord (Acs et al., 2013; Koutsoudaki et al., 2009; Matsushima et al., 2001; Norkute et al., 2009; Pott et al., 2009; Skripuletz et al., 2010; Skripuletz et al., 2008). Besides the well-established selective vulnerability of brain regions, the length of exposure also alters remyelination capacity. After 6 weeks of cuprizone treatment the peak demyelination is reached within the GM and WM, a process termed acute demyelination. When cuprizone challenge is ceased after 6 weeks and animals return to normal chow, acute demyelination is shortly followed by almost complete spontaneous remyelination driven by the repopulating and maturating oligodendrocyte progenitor cells (OPC). In contrast, prolonged cuprizone administration for 12 weeks or longer induces chronic demyelination, in which spontaneous remyelination is impaired or even fails to occur (Matsushima et al., 2001).

Beyond OL apoptosis the pathology of cuprizone lesion is also associated with a profound astrocytic activation and microglia/macrophage invasion. These cellular events are rather considered secondary responses to demyelination (Praet et al., 2014). Although astrocytes and microglia/macrophages are known to fulfil a multitude of different functions, the precise roles of these cells are controversial and the complex interplay between them are still not understood in details. Indeed, both activated astrocytes and microglia have been proven to exert beneficial as well as detrimental functions during de-, remyelination processes under different experimental conditions (Kang et al., 2012; Pasquini et al., 2007; Skripuletz et al., 2013; Voss et al., 2012). For example, both of these cell types produce different growth factors (GFs) during cuprizone-induced demyelination, thereby promoting OPC proliferation or regulating OL differentiation and survival. Moreover, the dynamics and density of astrogliosis as well as microgliosis/macrophage invasion appear with a temporal correlation of changes in myelin protein gene expression (MBP, PLP, MAG), indicating their key role influencing the damaged microenvironment (Gudi et al., 2011; Morell et al., 1998).

The precise mechanism or trigger underlying the development of demyelinating lesion in MS is still unknown. Besides the well-established autoimmune concept involving

autoreactive T-cells targeting the myelin sheath components, some MS lesions predominantly exhibit primary OL death suggesting that primary neurodegenerative events are the initial steps in their genesis (Barnett et al., 2004; C. Lucchinetti et al., 2000). Considering the latter, the histopathology of cuprizone lesions represent significant similarities of the human type III MS lesions (Acs & Kalman, 2012; Torkildsen et al., 2008). Cuprizone-induced primary OL death is preceded by very early downregulation of MAG compared to other OL/myelin specific mRNA levels. Soon after visible OL apoptosis is followed by demyelination, microglia/macrophage invasion to clean myelin debris and axonal damage (Gudi et al., 2011; Mason et al., 2001; Morell et al., 1998). However, one notable difference is that it lacks the significant lymphocyte infiltration which is present in human lesions (Hiremath et al., 2008).
Recently, the process of inflammatory lesion development gained a new concept, which proposes that two triggers have to occur concurrently in the CNS. The study by Scheld et al. and Ruther et al. investigated this "two-hit" hypothesis by utilizing the cuprizone model to induce intracerebral OL death/significant myelin damage. Subsequently, they applied active immunization with MOG^{35-55}, which triggered a massive peripheral immune response and ultimately led to a prominent immune cell recruitment to the mouse brain. Inflammatory lesions were characterized by profound lymphocyte invasion in perivascular spaces as well as at predilection sites of cuprizone-induced demyelination and also showed transient loss of vascular impermeability. Their findings signify the relevance of brain-intrinsic degenerative cascades to orchestrate a secondary peripheral immune response and a possible initial process of early MS lesions formation (Ruther et al., 2017; Scheld et al., 2016).

In summary, the cuprizone-induced experimental demyelination model is indispensable for examining the initial neurodegenerative cascades mimicking MS lesion genesis and remyelination. Additionally, its complementary use with other immune-mediated animal models also harbour numerous possibilities to study the inflammatory aspects of MS ultimately paving the way for novel treatment strategies.

1.2 General overview of primary cilia and their function in the brain

Primary cilia are solitaire, non-motile organelles on the surface of most mammalian cell types. As opposed to motile cilia, mature primary cilia do not propagate movement reflected by their unique structure involving a ciliary axoneme (nine-fold microtubule doublets, 9+0 constellation) that is connected to the cell through a modified mother centriole (basal body) (Fig.2A-B). Although the core structure is surrounded by a bilayer phospholipid membrane continuous with the cellular plasma membrane, it is highly compartmentalised. Importantly, the ciliary membrane is enriched in cell type/organ specific receptors and signalling molecules which enable these tiny organelles to serve as cellular antennas to coordinate numerous developmental and physiological signalling pathways (Fabbri et al., 2019; Gerdes et al., 2009; Marshall et al., 2006; Singla et al., 2006; Wheway et al., 2018). Assembly and maintenance of primary cilia utilize highly organised and sophisticated systems that allow selective trafficking within the organelle. The composition of the ciliary membrane relies on distinct molecular machineries (Fig.2C). Selective access of molecules into and out from the compartment are gated by a diffusion/permeability barrier at the cilia base, called the transition zone (TZ) and a trafficking adaptor system that strictly controls protein localisation towards as well as within cilia, termed the Bardet-Biedl syndrome protein complex (BBSome). Once proteins gain entry from the cell into the compartment, the intraflagellar transport (IFT) system (involving IFT-A, IFT-B complexes, kinesin, dynein motor proteins coupled to specific BBsome proteins) delivers cargo-complex proteins to their designated destination by operating bi-directionally along the microtubule based axoneme (Avidor-Reiss et al., 2015; Garcia et al., 2018; Goncalves et al., 2017; J. Lee et al., 2015; Nachury, 2018; Nakayama et al., 2017; Ye et al., 2018). Thus, the TZ, the BBSome, the IFT system and the specific signalling proteins expressed in the ciliary compartment grant each primary cilium an organ/cell type specific signalling capacity. Additionally, the coordinated work of these systems also provide primary cilia an extraordinary sensory ability by dynamically maintaining or altering their composition in response to changes in the tissue environment.

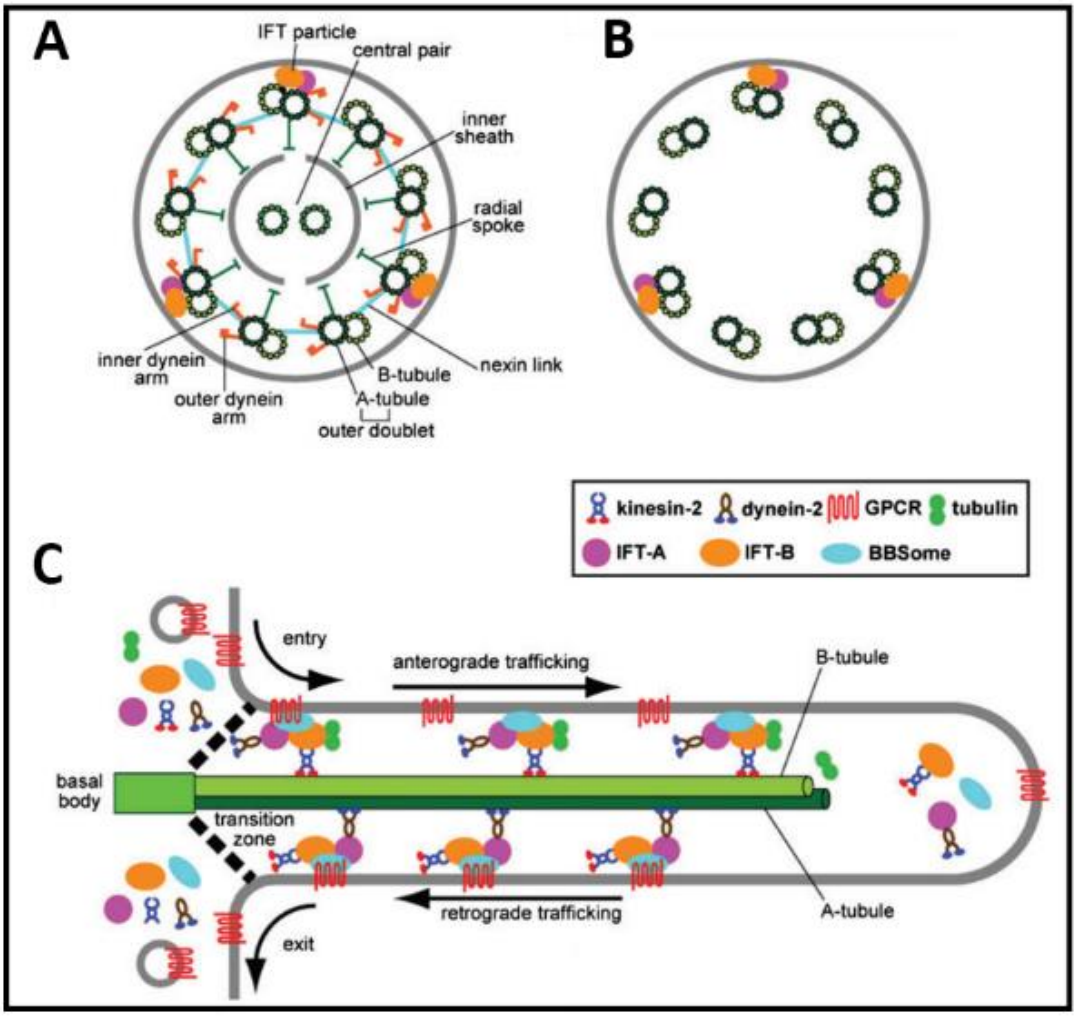

Modified picture adapted from (Nakayama et al., 2017)

Fig.2: Schematic illustration of ciliary structures and intraflagellar transport (IFT) system. Cross-sectional representation of the typical microtubule based structure of motile cilia/flagella with a 9+2 axoneme (A) and primary cilia with a 9+0 axoneme (B). Note that primary cilia lack the central pair of microtubules and motor components (radial spokes and inner-outer dynein arms) that would generate bending movements. (C) Longitudinal section of primary cilia structure and IFT system. At the base of the primary cilium, IFT-A and IFT-B proteins assemble with trafficking proteins (kinesin-2 or dynein-2) to form cargo particles. Cilia targeted cargo proteins- such as GPCRs- are loaded onto and connected to the assembled IFT protein complexes via the BBSome. Upon entry to the compartment, cargo-protein complexes cross the transition zone (TZ) and travel along the axonemal tracts (anterograde trafficking) powered by the constituent trafficking proteins. At the tip of the cilia, IFT particles are thought to disassemble and release cargo proteins to reach their designated destination. In return, IFT complexes reassemble again within the cilia and cargo loaded particles move in the opposite direction (retrograde trafficking) to leave the compartment through the TZ.

The functional importance of primary cilia-mediated signalling in organogenesis and postnatal physiology has become one major focus of interest in the last decade. Studies revealed that cellular loss of primary cilia or impaired function of ciliary proteins results in abnormal signal transduction towards the cells, which is thought to underlie a wide range of human genetic disorders, collectively termed ciliopathies (Badano et al., 2006; Grochowsky et al., 2019; Y. J. Kim et al., 2019; Reiter et al., 2017). Some human ciliopathies such as Bardet-Biedl Syndrome (Forsythe et al., 2013; Forsythe et al., 2018; Kenny et al., 2017), Joubert Syndrome (Melissa A. Parisi, 2009; M. A. Parisi, 2019; Sattar et al., 2011), Alström Syndrome (Alvarez-Satta et al., 2015; Hearn, 2019; Jan et al., 2011), or Meckel-Grüber Syndrome (Barker et al., 2014; Hartill et al., 2017) comprise severe central nervous system (CNS) involvement including cognitive deficits, mental retardation, and brain malformations. Therefore, the series of experimental findings highlighted that proper primary cilia transduced signalling plays a key role in brain development and postnatal homeostasis (tissue patterning during embryonic stages as well as regulating migration, differentiation and maintenance of stem/progenitor niche) (Alvarez-Satta et al., 2019; Amador-Arjona et al., 2011; Breunig et al., 2008; Y. G. Han et al., 2010; Y. G. Han et al., 2008; Khatri et al., 2014; Tong et al., 2014); and their dysfunction might be the underlying cause of a broad spectrum of congenital human syndromes. Although most CNS cell types (neural stem cells, neurons and astrocytes) harbour a single primary cilium, their precise physiological functions in the adult brain are still vaguely known.

In the CNS, primary cilia on neurons are known to be enriched for specific G protein-coupled receptors (GPCRs) including somatostatin 3 receptor (Sstr3) (Händel et al., 1999), melanin-concentrating hormone receptor subtype 1 (Mch1r) (Berbari, Johnson, et al., 2008; Berbari, Lewis, et al., 2008), serotonin receptor 6 ($5HT_6$) (Brailov et al., 2000; Hamon et al., 1999), dopamine receptor 1 (D1r) (Domire et al., 2011), kisspeptin receptor 1 (Kiss1r) (Koemeter-Cox et al., 2014), neuropeptide Y 2 and 5 receptor (NPY2r and NPY5r) (Loktev et al., 2013), as well as downstream signalling molecules such as type 3 adenylyl cyclase (AC3) (Bishop et al., 2007). Notably, ciliary expression of these signalling proteins are known to be restricted to different subsets of neurons in the brain. Primary cilia have been implicated in the regulation of the hypothalamus, the main controlling centre of feeding behaviour. Many concise studies have highlighted that specific molecules concentrated in cilia of hypothalamic neurons—such as Mch1r, AC3 and Bardet-Biedl Syndrome proteins (BBS)—contribute to the complex signalling pathways coordinating appetite (Berbari, Johnson, et al., 2008; Berbari, Lewis, et al., 2008; Einstein et al., 2010; Pissios et al., 2006; Schou et al., 2015). In particular, genetic loss

of ciliary structure or certain proteins have been shown to profoundly compromise signalling cascades and cause hyperphagia-induced obesity in mice under different experimental conditions (Davenport et al., 2007; Wang et al., 2009). Besides the hypothalamus, the hippocampus is also a region where disruption of neuronal primary cilia (NPC) have been proven to have a significant influence on neuronal connections and adversely affect learning, memory, as well as novel object recognition in mice (Einstein et al., 2010; Wang et al., 2011). Possible functions of primary cilia are also reflected by changes in ciliary morphology and length. Adaptation of cilium length—such as elongation—has been proposed to fine-tune the signalling activity of the organelle in response to changes in extracellular environment (Dummer et al., 2016; Hilgendorf et al., 2016). Moreover, abnormal signalling indicated by either altered morphology or the loss of ability to adjust might be pathological hallmarks of NPC related diseases. Similarly to GPCRs, ADP ribosylation factor-like protein 13B (Arl13b) also localizes to primary cilia and plays a direct role in the initiation, differentiation, and elongation of the organelle (Cevik et al., 2010; Kasahara et al., 2014; Larkins et al., 2011; H. Lu et al., 2015). Arl13b belongs to the Ras superfamily of small GTPases that has a dedicated role in wide range of different cellular processes (for review see: (D'Souza-Schorey et al., 2006; Gillingham et al., 2007)). Cells lacking functional Arl13b exhibit significantly shortened and structurally altered cilia, whereas overexpression of Arl13b increases ciliary length on the cells (Caspary et al., 2007; Larkins et al., 2011; H. Lu et al., 2015). In line with this, studies have also reported that pharmacological activation, inhibition or genetic absence of other ciliary signalling components can also influence cilium length and morphology under different experimental conditions (Miyoshi et al., 2009; Miyoshi et al., 2014; Ou et al., 2009). Taken all data together, it is undisputable that primary cilia can dynamically adapt to environmental cues by altering its molecular components and morphology. Besides their well-established role in CNS development, neurogenesis and homeostasis (Alvarez-Satta et al., 2019; Breunig et al., 2008; Khatri et al., 2014), primary cilia exerted signal transduction is also critical in cell-cycle control during perinatal and postnatal life (for review see: (Fabbri et al., 2019; Izawa et al., 2015). Emerging experimental evidence implicated their dysfunction in different types of cancers such as glioma and medulloblastoma (Basten et al., 2013; Di Pietro et al., 2017; Y.-G. Han et al., 2009; H. Liu et al., 2018; Sarkisian et al., 2019). Additionally, recent experimental data drawn from rodent models suggest that impaired functions of primary cilia (reflected by altered morphology, signalling protein localisation or its absence) might contribute to the pathogenesis of other neurological disorders such as Amyotrophic lateral sclerosis- (Ma et al., 2011), Alzheimer's- (Armato et al., 2013; Chakravarthy et al., 2010; Chakravarthy et al., 2012;

Hu et al., 2017), Hungtinton's- (Kaliszewski et al., 2015; Keryer et al., 2011; Mustafa et al., 2019), Parkinson's disease (Bae et al., 2019; Dhekne et al., 2018), Niemann Pick type-C lysosomal storage disorder (Canterini et al., 2017; Lucarelli et al., 2019) or certain brain tissue injury (seizures and cerebral ischaemia) (Kirschen et al., 2017; Parker et al., 2016).

Despite all of these observations, our knowledge about the precise, physiological roles of primary cilia in the adult CNS are scarce and still not fully understood. Moreover, currently available information about primary cilia in human tissues are mostly limited to human *in vitro* cell lines due to the species and organ specific signalling complexity of the organelle. Nonetheless, detailed neuropathological and cellular characterization of primary ciliary traits in the mature rodent CNS provide an essential tool to investigate their pivotal role in the brain, which might also propagate a better understanding of their clinical relevance and promote novel identification methods for the analysis of post-mortem human tissues in the future.

2. PURPOSE, HYPOTHESIS AND BACKGROUND OF THE STUDIES

2.1 Study 1: TRPA1 deficiency is protective in cuprizone-induced demyelination—A new target against oligodendrocyte apoptosis

2.1.1 Theoretical background of the study

MS is a chronic, demyelinating and degenerative disease of the CNS. The formation of demyelinating lesions is pathologically a heterogeneous scenario (C. Lucchinetti et al., 2000) and recent data indicate a primary degenerative process in the initial disease phase (Barnett et al., 2004; Barnett et al., 2006). Primary apoptosis of OLs has been suggested to be an earliest point in lesion evolution, which results in the exposure of naturally hidden CNS antigens that trigger a subsequent autoimmune inflammatory process. Additionally, OL loss becomes even more prominent by the progression of the disease course (SPMS, PPMS) (Kutzelnigg et al., 2005). Currently available immunomodulatory therapies are effective to modify the inflammatory nature of the disease, but have mild efficacy on long term clinical course. Thus, there is an increasing need of new pharmacological targets to extend the management of MS therapy for progressive stages. Cuprizone-induced experimental demyelination model is frequently used to recapitulate primary OL pathology and cellular environment of pattern III-IV MS lesion (Acs et al., 2013; Torkildsen et al., 2008). It is a highly reproducible and reliable model, which also allows the dissection of the primary degenerative and reparative processes on a molecular level.

Transient Receptor Potential Ankyrin 1 (TRPA1) receptor is a member of the TRP channel superfamily, which contains 28 mammalian members and is subdivided into six subfamilies (Clapham et al., 2001). TRPA1 is a non-selective cation channel with relatively high Ca^{2+} permeability. Activators of TRPA1 receptor are exogenous electrophilic compounds such as allyl-isothiocyanate (AITC, also known as “mustard oil”), cinnamaldehyde , and allicin (aroma of fresh garlic) (Bandell et al., 2004; Bautista et al., 2005). Additionally, TRPA1 can be activated by endogenous substances such as 4-hydroxy-2-nonenal (4-HNE), 4-oxo-nonenal, 5,6-eposyeicosatrienoic acid (5-6-EET), 15-deoxy-D12,14-prostaglandin J2, 8-iso-prostaglandin A2, nitrooleic acid (9-OA-NO2), general long-chain polyunsaturated fatty acids, formaldehyde, a cytotoxic metabolite methylglyoxal and small endogenous reactive molecules (H2O2) (Andersson et al., 2008; Cruz-Orengo et al., 2008; Motter et al., 2012; Sisignano et al., 2012; Taylor-Clark, McAlexander, et al., 2008; Taylor-Clark et al., 2009; Taylor-Clark, Undem, et al., 2008; Trevisan et al., 2014). These mediators are released during inflammation, oxidative stress or tissue damage, therefore, TRPA1 could be a sensor for oxidative stress. Cold and mechanical stimuli also gate the TRPA1 (Andersson et al., 2008; Story et al., 2003), which

is predominantly expressed in peptidergic primary afferent somatosensory neurons in dorsal root (DRG), trigeminal (TRG), and nodose ganglia (NG) (Nagata et al., 2005). It has a well-known function in pain sensation (Bautista et al., 2006). TRPA1 has also been detected in several nonneuronal cell types (keratinocytes, lung fibroblasts, vascular endothelial cells) (Nilius et al., 2012) and has been suggested to have a functional role in other inflammatory human diseases (asthma, migraine, colitis, itch, cystitis) (DeBerry et al., 2014; Engel et al., 2011; Grace et al., 2014; Oxford et al., 2013; Wilson et al., 2011). Regarding the CNS, TRPA1 has been implicated in the functional role of astrocytes. In cultured astrocytes near-membrane local spontaneous $[Ca^{2+}]_i$ transients were inhibited by the TRP channel antagonist HC-030031 or anti-TRP silencing RNA; and AITC also activated currents in voltage-clamped in these cells (Shigetomi et al., 2011). Moreover, TRPA1 channels were associated with regulation of functional expression of GABA transporters in astrocytes (Shigetomi et al., 2011). TRPA1 channels were also detected in GFAP positive astrocytes of the superficial laminae of the rat trigeminal caudal nucleus using electronmicroscopy combined with immuno-silver-gold labelling (S. M. Lee et al., 2012). A recent study showed that rat and mouse cerebellar OLs also express TRPA1 by in situ hybridization (Hamilton et al., 2016). Although the latter study suggests that a TRPA1 antagonist reduces myelin damage in ischaemia in *in vitro* circumstances (Hamilton et al., 2016), there are no *in vivo* data to indicate the function of TRPA1 in the CNS.

2.1.2 Hypothesis and aim of the study

In this study we aimed to investigate 1) whether TRPA1 is expressed in the mouse CNS, 2) whether TRPA1 expression is restricted to specific cell types, 3) whether the genetic deficiency of TRPA1 has a functional role in cuprizone-induced demyelination. In order to assess these possibilities we applied the cuprizone model on wild-type (WT) and TRPA1 deficient mice bred on a common C57BL/6 background. Our set of experiments included a detailed comparative histopathological analysis with the primary focus on cellular reactions, myelin loss and OL apoptosis. Besides the determination of markers and extent characterising cuprizone-induced demyelinating lesions, we conducted a different set of *in vitro* molecular biological experiments to determine the expression of genes or proteins linked to OL apoptosis and survival.

2.2 Study 2: Quantitative comparison of primary cilia marker expression and length in the mouse brain

2.2.1 Theoretical background of the study

Primary cilia are small, special cellular organelles that provide important sensory and signalling functions during the development of mammalian organs as well as in the coordination of postnatal cellular processes (Fabbri et al., 2019; Gerdes et al., 2009; Izawa et al., 2015; Marshall et al., 2006; Schou et al., 2015; Singla et al., 2006; Wheway et al., 2018). Dysfunction of primary cilia are thought to be the main cause of ciliopathies, a group of pleiotropic human genetic disorders characterized by overlapping developmental defects and prominent neurodevelopmental features (Badano et al., 2006; Grochowsky et al., 2019; Y. J. Kim et al., 2019; Reiter et al., 2017). Besides congenital anomalies in the brain, disrupted cilia-linked signalling pathways have been implicated in the regulation of numerous neuronal functions (Berbari et al., 2013; Xuanmao Chen et al., 2016; Davenport et al., 2007; Einstein et al., 2010; Koemeter-Cox et al., 2014; Mukhopadhyay et al., 2013; Wang et al., 2009; Wang et al., 2011). Importantly, studies of recent years have highlighted that different functions of primary cilia are reflected by their diverse morphology and unique signalling components localized in the ciliary membrane. In the CNS, primary cilia on neurons (neuronal primary cilia/NPC) are known to be enriched for a specific subset of G protein-coupled receptors (GPCRs) and signalling proteins- such as somatostatin 3 receptor (Sstr3) (Händel et al., 1999), downstream signalling molecule type 3 adenylyl cyclase (AC3) (Bishop et al., 2007) and ADP ribosylation factor-like protein 13B (Arl13b) (Cevik et al., 2010; Kasahara et al., 2014; Larkins et al., 2011; H. Lu et al., 2015)- that selectively localize to NPC. Despite of these observations, our knowledge about the precise roles of these organelles in the adult brain are still elusive and are just beginning to be understood.

2.2.2 Hypothesis and aim of the study

To further investigate the relationship between primary cilia and brain pathology, the current study was designed to serve as a foundation for future studies in the cuprizone-induced experimental demyelination model. To understand the possible histological and cellular changes of primary cilia under such pathological condition first, we intended to examine these organelles within well-characterised physiological circumstances. Thus, we conducted a comparative histopathological analysis of primary ciliary traits within the CNS. Regarding the aforementioned specific histological features of the cuprizone model, we aimed to characterise 1) the regional distribution, 2) the length and 3) cellular localization of AC3, Sstr3 and Arl13b

expressing primary cilia in the adult mouse brain under physiological conditions. Quantitative comparison of cilia traits were investigated by immunohistochemical studies in 19 different brain regions (Fig.3).

2.3 MATERIALS AND METHODS

2.3.1 Ethics statement

Animal experiments were conducted in accordance with European legislation on animal experimentation [Directives of the European Community (DIRECTIVE 2010/63/EU) and Hungarian regulations (40/2013, II.14)] in our laboratories at the University of Pecs. The project was approved by local and national ethical boards and licence was issued by government authorities (License number: BA02/2000-17/2016 and BA02/2000-44/2016 (KA-2068)).

2.3.2 Experimental animals and the generation of TRPA1 gene-deficient mice

The thesis involves two independent set of animal experiments. For the first study, experiments were carried out using TRPA1 receptor gene-deficient mice ($TRPA1^{-/-}$, TRPA1 KO) and their wild-type counterparts ($TRPA1^{+/+}$, TRPA1 WT). All animals were bred and kept in the Animal House of the Department of Pharmacology and Pharmacotherapy of the University of Pécs at 24 °C and provided with standard chow food and water *ad libitum*. $TRPA1^{-/-}$ and $TRPA^{+/+}$ mice were generated from an original pair of heterozygous mice received as a gift from Prof. P. Gepetti (University of Florence, Italy). Offspring were genotyped and homozygous mice were selected for further breeding. After 4 generations, stable homozygous lines of $TRPA1^{-/-}$ and $TRPA1^{+/+}$ were successfully generated.

For the second study 8-week-old male C57/Bl6 mice were used (Charles River Laboratories Magyarország Kft, Isaszeg, Hungary). Animals were housed in groups 3–4 and kept in standard conditions at 24 °C (12-h light dark cycle and were provided standard rodent chow and water *ad libitum*). Their general appearance as well as health status was observed daily and their weight was monitored three times a week until the day of experiment.

2.3.3 Experimental design and groups for the cuprizone model

For all experiments 8 week old male TRPA1 WT and TRPA1 KO mice were used. They were housed in groups of 3-5 in polycarbonate cages (530 cm^3 floor space, 14 cm height) on wood shavings bedding. Treatment consisted of feeding mice a diet containing 0.2% cuprizone mixed into standard rodent chow ground into a fine powder for six weeks, except for the gene expression studies where treatment lasted only for four weeks. The powder was served in small ceramic bowls placed into the cages which were cleaned daily. In each experimental series, untreated littermates served as controls for both the TRPA1 WT and TRPA1 KO groups which were kept under identical conditions and fed the same powdered chow. Littermates were randomly allocated into the treated or untreated group. The health status of mice was monitored

daily by observation and also by measuring body weights every second day throughout the treatment. A total number of 95 animals were used for the present study. 44 mice were used for immunohistochemistry (n=10-12), 30 mice for immunoblot analysis (n=6-9) and 21 for quantitative real-time PCR (n=5-6) in two independent experiments. Tissue samples were coded by study number and animal number and evaluation were performed by independent investigators who were not aware of the group allocations.

Each experiment consisted of four animal groups, stated as untreated wild-type (WT CTRL), cuprizone-treated wild-type (WT CPZ), untreated TRPA1 knockout (KO CTRL) and cuprizone-treated TRPA1 knockout (KO CPZ) group.

2.3.4 Tissue preparation

For histological and immunohistochemical studies mice were deeply anesthetized with 70 mg/kg i.p. sodium pentobarbital (Euthasol) and perfused transcardially with phosphate buffered saline (pH. 7.4; PBS) followed by 4% paraformaldehyde in 0.1M phosphate buffer (PB). Brains were dissected and post-fixed in the same fixative overnight at 4 °C. For cuprizone experiments paraffin-embedded brains were coronally sectioned 8 µm thickness and mounted onto gelatin and silane-coated slides (Acs et al., 2009; Veto et al., 2010). For immunoblot and qRT-PCR analysis, anesthetized animals were sacrificed by rapid decapitation. Brains were quickly removed and the corpus callosum was carefully dissected under stereomicroscopic control. Tissues were placed in RNAlater or immediately frozen on dry ice and kept at -80 °C until used. For the immunohistochemical analysis of primary cilia brains were cryoprotected in 30% sucrose in PB overnight and coronally sectioned with a freezing microtome. Then, 30-µm-thick, free-floating sections were collected and stored in 1% sodium-azide solution at 4 °C for a maximum of 3–14 days until further processing. For immunofluorescence studies, 8-µm-thick brain sections were mounted onto gelatine-coated slides and kept at − 80 °C until used.

2.3.5 Immunohistochemical studies

Study 1: For immunohistochemistry (IHC), 8 µm-thick, gelatine-coated slides were rehydrated and heat-unmasked in 10 mM citrate buffer (pH 6.0). Sections were treated with 3% hydrogen peroxide in 0.1 M phosphate buffered saline (pH. 7.6; PBS), blocked in Power Block solution (Biogenex Life Sciences,) and incubated overnight with the primary antibody diluted in a solution containing 1% normal horse serum and 0.1M PBS at 4°C. Primary antibody against TRPA1 (1:1000, rabbit IgG, Abcam) was used to identify TRPA1 receptor, anti-myelin basic

protein (MBP) (1:100, mouse IgG, Novocastra Laboratories Ltd) to detect myelin, anti-glial fibrillary acidic protein (GFAP) (1:500, rabbit IgG, Dako) to visualize astrocytes, anti-adenomatus polyposis coli (APC) (1:000, mouse IgG,Calbiochem) to detect mature oligodendrocytes, anti-oligodendrocyte lineage marker-2 (Olig-2) (1:200, rabbit polyclonal, Chemicon) to recognize cells from oligodendroglial lineage and anti-Ionized calcium-binding adaptor molecule 1 (Iba-1) (1:500, rabbit IgG, Abcam) was used as a marker for microglia/macrophages (panmacrophage). For visualization, avidin-biotin complex (Vectastain kit, Vector) or appropriate HRP-conjugated secondary antibodies (Super Picture kit, Invitrogen) were applied according to the manufacturer's manual and 3,3′-diaminobenzidine (DAB) reaction was used.

Study 2: Free-floating brain sections were treated with 3% hydrogen peroxide in 0.1MPB (pH 7.2), were rinsed in PB three times, and were permeabilized with 0.5% Tx100 in PB, 0.1% sodium-azide (NaN_3), and 30 mg/ml bovine serum albumin (BSA). Thereafter, sections were washed again three times and incubated with primary antibody diluted in Tx100/PB/NaN_3/BSA overnight at 4 °C. The following antibodies were used: rabbit polyclonal anti-adenylyl cyclase subtype 3 (AC3) (1:1000, Santa Cruz, Cat.No.: sc-588), rabbit polyclonal anti-somatostatin receptor 3 (Sstr3) (1:2000, Thermo scientific, Cat.No.: PA3-207) and rabbit polyclonal anti-ADP rybosylation factor-like protein 13 B (Arl13b) (1:2000, Protein Tech, Cat.No.: 17711-1-AP). For visualization, appropriate anti-rabbit biotin-conjugated secondary antibody (1:1000) and avidin-biotin complex (1:500) (ABC, Vectastain kit, Vector Laboratories) was applied according to the manufacturer's manual. Following rinses in PB and once in 0.05M Tris buffer (pH 8.2, TRIS), the reaction product was generated by 3'3'-diamimobenzidine-nickel-sulfate (DAB-nickel) solution. Tissue was mounted onto gelatine-coated slides and counterstained with 1% neutral red to detect neuronal cell bodies.

All sections were viewed with an Olympus BX-50 microscope and photographed with an Olympus C-7070 colour digital camera. Slides were also digitized with an automated whole slide scanner (Pannoramic 250 Flash II scanner, 3DHistech Ltd, Budapest, Hungary) attached to a three-CCD (charge-coupled device) digital camera (CIS 3CCD, 2 megapixel, CIS Corporation, Tokyo, Japan). High-resolution images were captured by using Pannoramic Viewer software.

2.3.6 Immunfluorescent co-localization studies

For both studies 8-µm-thick, gelatine-coated slides were used. Frozen sections were first brought to room temperature. Then, all sections (either paraffin or frozen) rehydrated in 0.1 M phosphate buffered saline (pH 7.6; PBS) and heat-unmasked in 10 mM citrate buffer (pH 6.0). Sections were blocked in Power Block solution (Biogenex Life Sciences) and incubated overnight with primary antibodies diluted in 1% normal horse serum (Vector Laboratories). TRPA1 and primary cilia were labelled with the same primary antibodies applied in IHC, namely rabbit polyclonal anti-TRPA1 (1:1000, rabbit IgG, Abcam), rabbit polyclonal anti-adenylyl cylase subtype 3 (AC3) (1:500, Santa Cruz), rabbit polyclonal anti-somatostatin receptor subtype 3 (Sstr3) (1:1000, Thermo Scientific), and rabbit polyclonal anti-ADP rybosylation factor-like protein 13 B (Arl13b) (1:1000, Protein Tech). For the detection of CNS cell types, rabbit polyclonal anti-RBFOX3/NeuN (NeuN) (1:200, Novus Biologicals) was applied to identify neurons, rabbit polyclonal anti-glial fibrillary acidic protein (GFAP) (1:500, Dako) to visualize astrocytes, mouse monoclonal anti-adenomatosus polyposis coli (APC) (1:500, Calbiochem) to detect mature oligodendrocytes, and rabbit polyclonal anti-ionized calcium binding adaptor molecule 1 (Iba-1) (1:500, Abcam) was used as a marker of microglia/macrophages (panmacrophage). For double immunofluorescence analysis, sections were incubated with appropriate Alexa fluor 594/488-conjugated secondary antibodies (1:200 Invitrogen) or with appropriate HRP-conjugated secondary antibodies (Biogenex) followed by signal amplification with Alexa labelled 594 or 488 tyramide (1:100 or 1:500, Tyramide Amplification kit, Invitrogen) according to the manufacturer's protocol. All sections were labelled with 4′6-diaminidino-2-phenylindol (DAPI) (Invitrogen) for visualizing cell nuclei. All fluorescent images were captured using Axio Scope A1 imaging system (Zeiss, Germany) equipped with a Canon Powershot A620 digital camera and ISIS software (Metasystems, Germany) for image acquisition and processing.

2.3.7 Histopathology and scoring of demyelination in cuprizone lesions

2.3.7.1 Luxol fast blue staining and scoring of demyelination

Demyelination was evaluated in 8 µm paraffin sections using Luxol fast blue-cresyl-violet (LFB/CV) staining. Sections were mounted onto silane-coated slides, deparaffinised, rehydrated to 95% alcohol and incubated in LFB solution (0.01%) overnight at 60 °C. Afterwards, sections were differentiated in lithium carbonate solution (0,05%) and counterstained with cresyl-violet. For the assessment of myelin loss in the corpus callosum a four-tiered scoring system (from 0 to 3) was used and assessment was carried out in a double-

blind manner by three independent investigators. A score of 0 was used when myelin was entirely intact, whereas score 3 was given when the corpus callosum was totally demyelinated. A score of 1 or 2 was given when one-third or two-thirds of the fibres of the corpus callosum were demyelinated. Assessment was carried out in four different regions corresponding to bregma levels 0.14, -0.22, -1.06 and -1.94mm, *i.e.* Figs. 30, 33, 40 and 47 in the atlas of Paxinos and Franklin (Paxinos et al., 2001). Using the scores generated by the assessment of the four regions, for each animal a mean score was calculated and used for subsequent statistical analysis (Acs et al., 2009; Hiremath et al., 1998; Veto et al., 2010).

2.3.7.2 Quantification of mature oligodendrocytes

Quantification of oligodendrocytes was achieved by manual counting the number of APC-immunopositive cells in the corpus callosum. APC immuno-labelled sections were investigated in the same four different regions according to the atlas of Paxinos and Franklin (Paxinos et al., 2001) as described above under LFB/CV staining. Cell numbers were calculated, the mean scores from the four different regions were generated and the mean scores were used for statistical analysis. Cell counting was performed with an Olympus BX-50 microscope with a x 40 objective.

2.3.8 Molecular biological studies

2.3.8.1 Quantitative real-time polymerase chain reaction (qPCR) in the mouse CNS

Frozen TRPA1 WT and KO mouse brain nuclei were homogenized and total RNA content was isolated using Direkt-zoll RNA MiniPrep kit, according to the instruction of the manufacturer. Samples were diluted to equal RNA content and cDNA generated by reverse transcription using Maxima First Strand cDNA Synthesis kit. The expression level of TRPA1 receptor mRNA was determined with Stratagene Mx3000 qPCR instrument using primers and probes designed by our group (primer 1: atgccttcagcaccccattg, primer 2: gacctcagcaatgtccccaa, probe: 56FAMtgggcagctZENtattgccttcacaat3IABkFQ; (Bautista et al., 2006). Primers and probe were obtained from IDT-Integrated DNA Technologies, Leuven, Belgium. Protocol of the polymerase chain reaction was: 5 min denaturation on 95 °C, 30 sec annealing on 62 °C and 1 min synthesis on 72 °C. TRPA1 expression level was compared to the Hprt-1 (hypoxanthine phosphoribosyltransferase 1), primers: IDT – Integrated DNA Technologies, Mm.PT.39a.22214828) housekeeping gene.

2.3.8.2 RNA extraction and quantitative real-time PCR (qPCR) in the corpus callosum of experimental animals

Total RNA from mouse corpus callosum was extracted using TRI Reagent (Molecular research Centre Inc, Cincinatti, OH, USA) and Direct-Zol RNA isolation kit following the manufacturer's instructions. RNA then treated with DNase I (both supplied by Zymo Research, Irvine, CA, USA) and the concentration of purified RNA was quantified by spectrophotometer (NanoDrop ND-1000, NanoDrop Technologies Inc., Wilmington DE, USA). First strand cDNA synthesis was carried out with 1μg of total RNA/sample using Maxima™ First Strand cDNA Synthesis Kit for RT-qPCR (Thermo Scientific, Waltham, MA, USA). Relative gene expression analysis was performed to determine levels of transcriptional activity for *Bak, NG2, IGF-1, FGF-2, PDGFRα* and *TRPA1* in tissue samples. The reaction was conducted in triplicates, with Stratagene Mx3000P QPCR System (Agilent Technologies, Santa Clara, CA, USA), and mouse β-actin expression was used as a reference gene. Each reaction contained 20 ng cDNA, 1x Luminaris HiGreen Low ROX qPCR Master Mix (Thermo Scientific), 0.3 μM primer from each primer. qPCR cycle conditions were as follows: 95°C 10 min, followed by 40 cycles of 95°C 15 sec, 60 °C 45 sec, 72°C 45 sec. Measurements included a dissociation curve analysis to verify amplification specificity. Primer efficiencies were taken into account when the gene expression ratios were calculated using MxPro QPCR Software (Agilent Technologies), WT CTRL samples served as a calibrator. Primers and product lengths for each gene are listed in **Table 2** according to the HUGO Gene Nomenclature Committee.

Table 2: Oligonucleotide primer sequences for qPCR

Gene	Primer sequence	Product length (bp)	GenBank reference number
Bak	Forward: ACAGTCCTCTCCTTCCTCCC Reverse: GGTATTGATGACCCCTGGGC	90	NM_007523.2
NG2	Forward: ACCCTCATCAGGAGACCCTC Reverse: CAGGAGGTTGCCTCTTCTGG	131	NM_139001.2
IGF-1	Forward: AGCTGCATTAGACACACCCT Reverse: ATGCCACAGATGGAGTCAGG	125	NM_001111274.1
FGF-2	Forward: TCCAGTTGGTATGTGGCACT Reverse: CTTCTGTCCAGGTCCCGTTT	72	NM_008006.2
PDGFRα	Forward: AGTGTTGGTGCTGTTGGTGA Reverse: GACTCGATAACCCTCCAGCG	102	NM_001083316.1
TRPA1	Forward: TCCAAATAGACCCAGGCACG Reverse: CAAGCATGTGTCAATGTTTGGTACT	101	NM_177781.4
GAPDH	Forward: TTCACCACCATGGAGAAGGC Reverse: GGCATGGACTGTGGTCATGA	87	NM_002046

Abbreviations: Bak—Proapoptotic protein Bak, NG2—chondroitin sulfate proteoglycan 4 (Cspg4), IGF-1—insulin-like growth factor 1, FGF-2—fibroblast growth factor 2, PDGFRα—platelet-derived growth factor receptor α, TRPA1—Transient Receptor Potential Ankyrin 1.

2.3.8.3 Immunoblot analysis

Tissue samples were collected from animals sacrificed after 6 weeks of treatment in two separate experiments and each immunoblot analysis was repeated three times. The corpus callosum of each animal was homogenized in ice-cold 0.5M Tris buffer, pH 7.4 (containing 5M sodium chloride, 50% glycerol, 100mM *ethylene glycol tetraacetic acid,* 10 mM sodium orthovanadate, 1 mM zinc chloride, 0.5 mM sodium fluoride, aprotinin, 200 mM phenylmethylsulfonyl fluoride, 10% *Triton X-100* and distilled water; (all purchased from Sigma-Aldrich, Steinheim, Germany). Homogenates (10 µg each) were loaded onto 10 % sodium dodecyl sulphate polyacrylamide gels, electrophoresed and transferred to polyvinylidene fluoride (PVDF) membranes (Amersham Hybond P, Sigma-Aldrich, Steinheim, Germany). The membranes were blocked in 5% nonfat dry milk or 3% bovine serum albumin

in TBST and then incubated overnight with each specific antibody. The following antibodies were used at a *dilution* of 1:1000 *unless otherwise stated:* anti-myelin-associated glycoprotein (MAG) (Santa Cruz Biotechnology, Santa Cruz, CA, USA), anti-phospho-p38 ($pThr^{180}/pTyr^{182}$) (Sigma-Aldrich, Steinheim, Germany), anti-p44/42 MAPK (Erk1/2), anti-phospho-p44/42 MAPK (ERK1/2) (Thr^{202}/Tyr^{204}), anti-phospho-SAPK/JNK (Thr^{183}/Tyr^{185}), anti-phospho-c-Jun (Ser^{73}), anti-β actin (all from Cell Signalling Technology, Beverly, MA, USA) and anti-Hsp90 (1:2000, Santa Cruz Biotechnology, Santa Cruz, CA, USA) (Delgado et al., 2014; Gomez et al., 2011; Hao et al., 2007; J. Y. Kim et al., 2015; Y. P. Liu et al., 2014; Petrov et al., 2015; Watanabe et al., 2015). Appropriate horseradish peroxidase-conjugated secondary antibody was used at a 1:10000 dilution (anti-rabbit IgGs; Cell Signalling Technology, Beverly, MA, USA) and labelled proteins were visualized by enhanced chemiluminescence (Immobilon, Merck Millipore, Darmstadt, Germany). Chemiluminescence signal was detected with a cooled charge-coupled device (CCD) camera attached to an imaging capturing system (Gene-Gnome, Syngene). Quantification of band intensities was performed using National Institutes of Health Image J software (Bethesda, MD, USA). Relative densities of the bands were normalized to the corresponding total non-phosphorylated proteins (ERK), β- actin (c-Jun, p38, JNK) or Hsp90 (MAG) as internal controls. Image processing, analysis, and measurements were carried out using NIH Image J software.

2.3.9 Quantification and length measurement of primary cilia

Assessment of primary cilia distribution and length were carried out in 19 different regions of the brain according to the mouse brain atlas of Paxinos and Franklin (Franklin et al., 2008). Regions of interests were summarized in Fig.3. Sections were photographed at ×20, ×40, and ×60 magnification by using the Pannoramic Viewer or ISIS software. All raw images were processed and analysed by using Fiji-ImageJ software. Quantification of primary cilia was achieved by counting the number of immunopositive structures on neurons and astrocytes in the different regions of the brain. The length of each primary cilia was determined for 150–200 co-labelled cells per region utilizing the double immunofluorescent labelled sections. To obtain accurate measurements, primary cilia length assessment involved only those cilia which aligned longitudinal in plane and sharpness was observed from base to the tip. Measurements were repeated three times for each ciliary marker per brain region and animal. All data from primary cilia measurements were collected, a mean value was generated and used for statistical analysis.

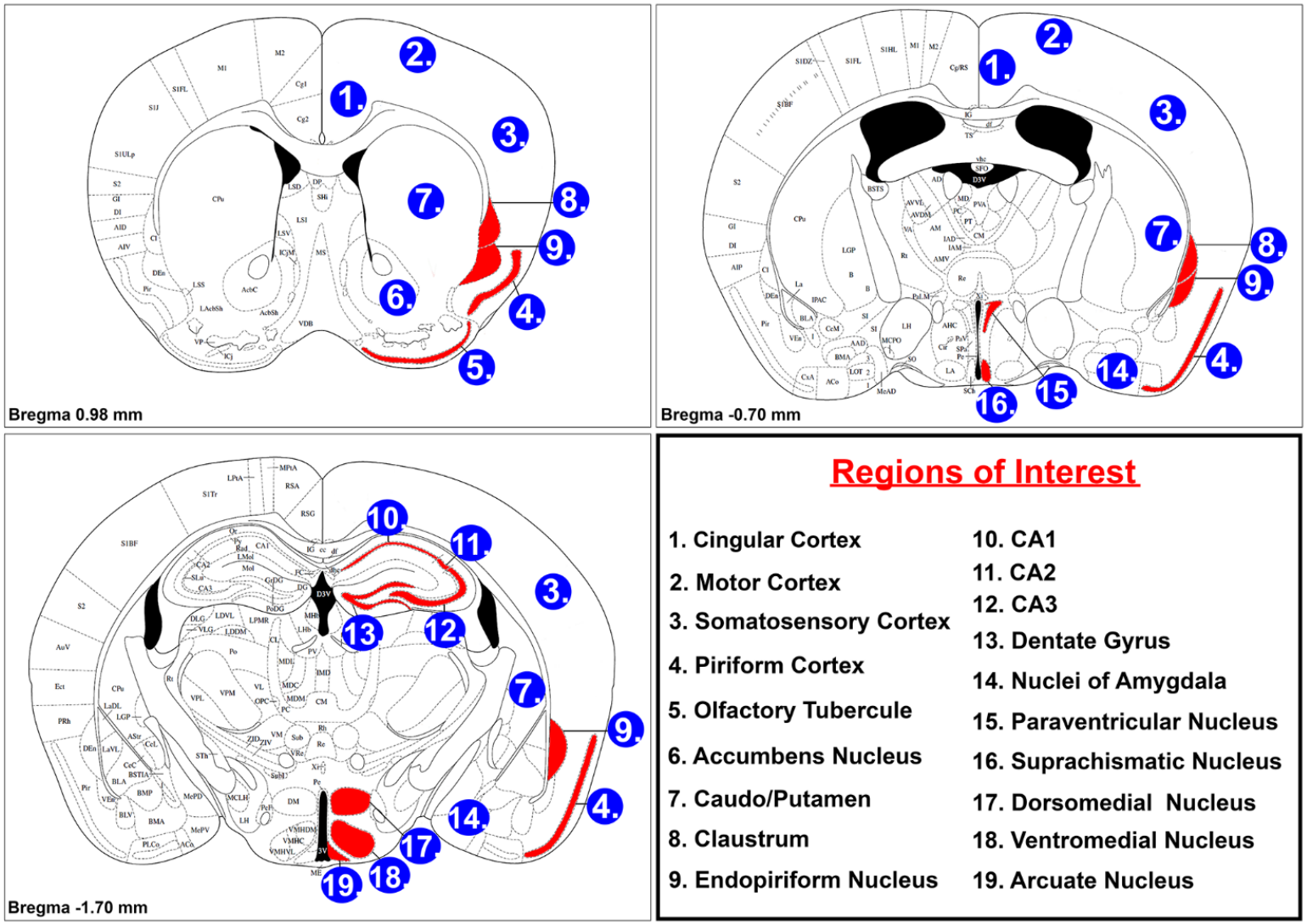

Fig.3

Coronal brain sections representing regions of interest for the assessment of primary cilia distribution and length in the mouse brain. Schematic diagrams were adapted from the mouse brain atlas of Paxinos and Franklin (Franklin et al., 2008) showing the topography of regions of interest (ROI) at different Bregma levels. Smaller areas are outlined according to their shape (piriform cortex, olfactory tubercule, endopiriform nucleus, claustrum, hippocampal subregions and hypothalamic subnuclei) and circles are centred within the other ROIs.

2.3.10 Statistical analysis

The statistical calculations and graphs were made using GraphPad Prism version 5 and 6 (GraphPad Software, San Diego, CA). Statistics were performed using absolute data. For the quantitative analysis of mature oligodendrocytes, APC-immunopositive cells were counted manually and statistical difference between groups was determined with Kruskal-Wallis test followed by Dunn's *post hoc* analysis. The histological degrees of corpus callosum myelination were compared pairwise using the non-parametric Mann–Whitney test. The immunoblot band intensities in the four experimental groups were normalized to the loading control and intergroup differences were tested by one-way ANOVA followed by Bonferroni's multiple comparison *post hoc* test. Gene expression ratios were normalized to GAPDH as a reference gene and the statistical analysis was performed using one-way ANOVA followed by Bonferroni's multiple comparison *post hoc* test.

The comparative distribution of ciliary markers was determined by the fraction of total analysis, in which all three ciliary markers co-labelled with NeuN or GFAP were separately counted and were divided by the total number of primary cilia calculated in each brain region. The length of AC3-, Sstr3-, or Arl13b-positive primary cilia on neurons and astrocytes was also measured individually. After all measurements were collected, a mean value was separately generated for each marker in each investigated brain area. Then, comparison of cilia length was conducted, in which a marker's average length was statistically compared to the value of the other marker or markers present in each region, respectively (unless stated otherwise, shorter or longer terms are used in the following sections to refer to the statistical comparison of the length of labelled cilia on neurons and astrocytes within a brain region). Statistical differences within distinct regions were tested with unpaired t tests or with one-way ANOVA followed by Tukey's multiple comparison *post hoc* test.

Differences were considered significant at values of $P<0.05$ (P values are indicated as *$P<0.05$; **$P<0.01$; ***$P<0.001$). Unless noted otherwise, all data represent the mean ± SEM.

3. RESULTS

3.1 TRPA1 deficiency is protective in cuprizone-induced demyelination- A new target against oligodendrocyte apoptosis

3.1.1 Body weight monitoring during cuprizone treatment

Body weights at the beginning and at week 6 or week 4 of cuprizone treatment are summarized in Table 3. Cuprizone treatment led to significant body weight loss in the first 2 weeks of treatment in both TRPA1 WT and KO mice compared to their untreated counterparts but there was no significant difference between the extent of body weight changes between the two genotypes.

Table 3: Body weights of animals at the beginning and end of cuprizone treatment

Study duration	Genotype and treatment (n)	Baseline body weight (g)	Body weight at the end of treatment (g)
6 weeks	TRPA1 WT control (19)	20.5±0.5	26.1±0.7
	TRPA1 KO control (17)	20.9±0.6	25.9±0.5
	TRPA1 WT CPZ (21)	21.3±0.6	23.9±0.7
	TRPA1 KO CPZ (17)	21.3±0.6	23.6±0.5
4 weeks	TRPA1 WT control (5)	19.6±0.7	22.4±1.0
	TRPA1 KO control (6)	20.6±0.9	25.8±0.7
	TRPA1 WT CPZ (5)	21.5±0.2	20.8±0.6
	TRPA1 KO CPZ (5)	21.0±0.3	20.0±1.3

Data are means ± SEM. Number of animals included in each treatment group is shown in brackets. Abbreviations: TRPA1 WT CTRL— untreated Transient Receptor Potential Ankyrin 1 wild-type mice, TRPA1 KO CTRL—untreated Transient Receptor Potential Ankyrin 1knockout mice, TRPA1 KO CPZ—cuprizone-treated Transient Receptor Potential Ankyrin 1 knockout mice, TRPA1 WT CPZ— cuprizone-treated Transient Receptor Potential Ankyrin 1 wild-type mice.

3.1.2 TRPA1 expression in the CNS

Supporting the functional importance of TRPA1 in the CNS, we detected TRPA1 mRNA expression in different brain regions (CC, hippocampus, substantia nigra, basal forebrain, and hypothalamus) of wild-type mice by RT-qPCR (data not shown). Immunostaining of TRPA1 receptor protein showed intensive positivity in the CC and the adjacent white matter areas (Fig.4A-B). In addition, double fluorescence labelling revealed a broad overlap in TRPA1 and GFAP expressing cells both in cuprizone naive and treated mice (Fig.4A-B).

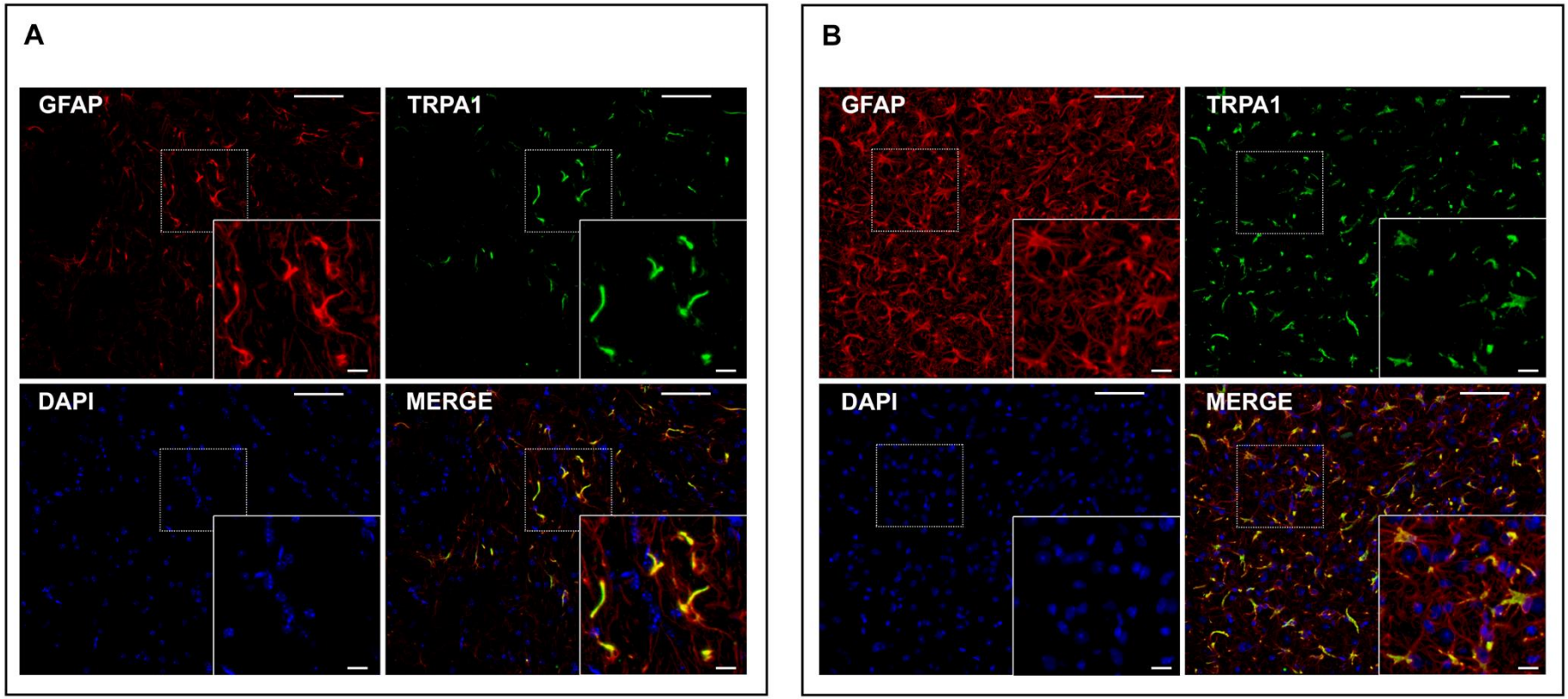

Fig.4: TRPA1 expression in the CC of control and cuprizone-treated WT mice. Representative double fluorescent images of TRPA1 expressing astrocytes: (A) untreated WT and (B) cuprizone-treated WT mice. Anti-GFAP immunoreactivity (red), anti-TRPA1 immunoreactivity (green), DAPI nuclear staining (blue) and a corresponding overlay (scale bar 100 μm). Note that GFAP and TRPA1 immunoreactivities significantly overlap (yellow) as shown in merged images. The inserts in A and B panel indicate expression of the markers at higher magnification (scale bar 20 μm).

3.1.3 Cuprizone-induced demyelination is attenuated in TRPA1 deficient mice

LFB/CV-stained sections from untreated WT and TRPA1 KO mice showed intact myelination (myelination score 0.2) (Fig.5A). Semiquantitative histological analysis revealed significantly elevated scores indicating profound demyelination in the CC of both cuprizone-treated WT (myelination score: 2.6) (Fig.5B) and TRPA1 KO mice (myelination score: 1.7), however in the latter group demyelination was significantly less severe compared to treated WT mice (***$P<0.001$) (Fig.5C and H). In line with LFB/CV findings, IHC also demonstrated that cuprizone feeding induced a prominent reduction in myelin-basic protein (MBP) expression in the CC of WT animals (Fig.5E). Importantly, MBP loss was diminished in cuprizone-fed TRPA1 KO mice (Fig.5F). Immunoblotting analysis of myelin-associated glycoprotein (MAG) expression levels were consistent with the differences observed in LFB/CV and MBP labelling (Fig.5G).

Fig.5: Effect of cuprizone administration on myelination in the CC of TRPA1 KO and WT mice. Representative histopathology images of myelin status in the CC demonstrated by LFB-cresyl violet staining (A–C) and MBP-IHC (D–F). Black arrow heads in (A–C) delineate the CC region. Asterisk labels the lateral ventricle. Blue staining with LFB indicates intact myelin sheath. Note the strong CC demyelination after cuprizone treatment and appearance of hydrocephalus in WT mice which are diminished in the brains of KO mice in LFB stained sections. Sections labeled with MBP-IHC are in line with LFB staining. G: Representative immunoblots for myelin-associated glycoprotein (MAG) expression in the dissected CC of cuprizone-exposed and untreated mice. Dividing lines above the numbered immunoblotlanes depict the control and cuprizone-treated samples from TRPA1 WT and KO groups. Even protein loadings were confirmed by anti-HSP90 antibody immunoblotting. H: shows semi-quantitative evaluation of myelination by LFB in the CC. Scale bars 200 µm (A–C) and 100 µm (D–F). WT CPZ versus KO CPZ ***P < 0.001 (H).

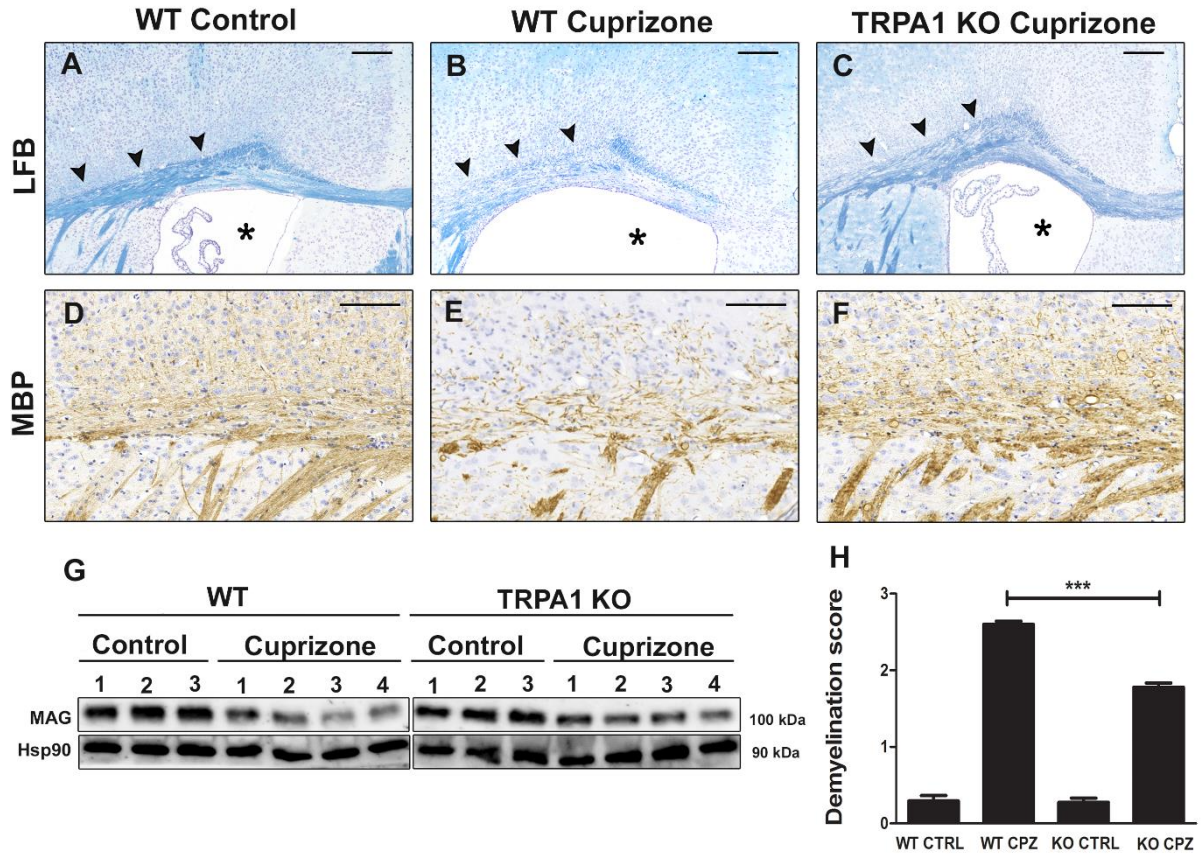

3.1.4 Mature OL loss is reduced in cuprizone-treated TRPA1 KO mice

Cuprizone treatment profoundly reduced the number of mature OLs in the CC of WT mice compared to untreated mice (***P<0.001) (Fig.6G,H and J). The mature OL count was also significantly reduced in cuprizone-treated KO mice compared to their controls but the extent of mature OL loss was significantly less pronounced than in cuprizone-treated WT mice (***P<0.001) (Fig.6H,I and J).

3.1.5 Cuprizone-induced gliosis and macrophage reaction is reduced in TRPA1 deficient Mice

Astrocyte and microglia/macrophage activation are closely correlated with demyelination in the cuprizone model (Gudi et al., 2014). Along with demyelination, cuprizone exposure induced a robust activation of microglia/macrophages and astrocytes in wild-type mice as indicated by Iba-1 and GFAP IHC (Fig.6B and E). Microglia and astrocytic reactions were less prominent in cuprizone-treated TRPA1 deficient mice (Fig.6C and F). No astrocyte activation or increased numbers of microglial cells were found in untreated TRPA1 deficient mice.

Fig.6: Effect of 6 weeks of cuprizone exposure on astrocyte, microglia/macrophage activation and OL loss in the CC of WT and TRPA1 KO mice. (A–F) Representative histopathological images of astrocytes and microglia/macrophage activation visualized by anti-GFAP and anti-Iba-1 IHC, respectively. Note that 6 weeks of cuprizone treatment induced a less pronounced activation of both astrocytes and microglia/macrophages in the CC of KO mice compared to WT mice. (G–I) Representative immunofluorescent images and (J) quantitative analysis of mature APC-positive OLs in the CC. Images were taken from the midline (G–I) and lateral part (A–F) of the CC as demonstrated by the red rectangles in the schematic drawing of the mouse brain (lower right panel). Scale bars 100 µm (A–C), 100 µm (D–F), and 100 µm (G–I). WT CTRL versus WT CPZ ***P < 0.001, WT CPZ versus KO CPZ ***P < 0.001 (J).

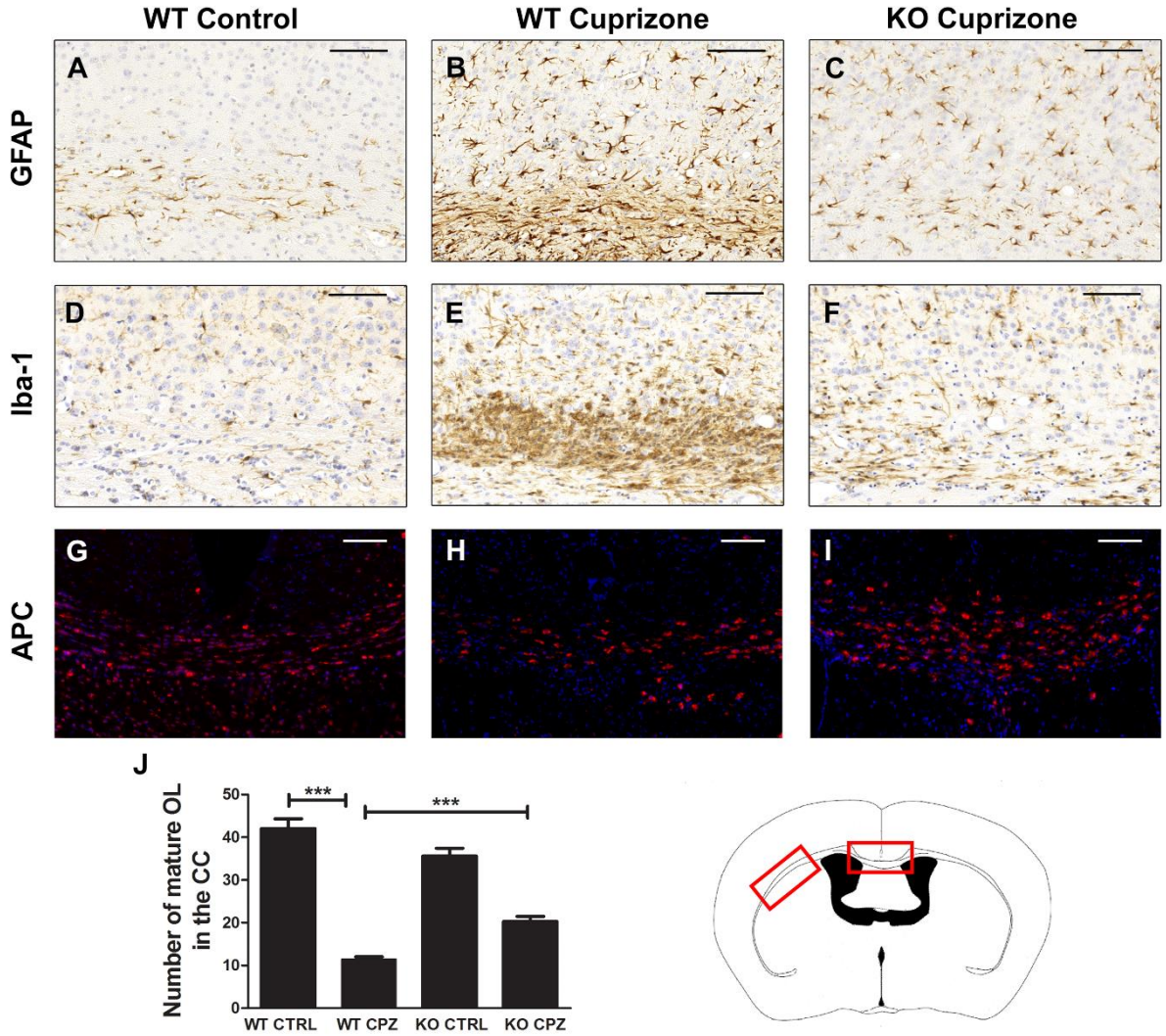

3.1.6 Number of premature oligodendrocytes is increased in cuprizone-treated WT mice

Immunofluorescent double-label experiments revealed that 6 weeks of cuprizone treatment decreased the number of Olig2/APC double positive cells (mature OLs) in the CC of WT mice compared to KO mice (data not shown). The number of cells immunoreactive for Olig2 only (considered as early OPC) (Islam et al., 2009) was also increased in cuprizone treated WT mice compared to KO mice. However, no significant difference was found in Olig2 immunoreactivity between the untreated WT and KO mice. Moreover, gene expression analysis revealed that 4 weeks of cuprizone exposure induced a significant *NG2* mRNA elevation in WT mice, but this treatment did not affect *NG2* mRNA level in TRPA1 KO mice (Fig.7A).

3.1.7 Expression of *Bak, IGF-1, FGF-2,* and *PDGFRα* mRNA in the CC

To determine the mechanism of cuprizone-induced oligodendrocyte loss in the CC, we performed *Bak, IGF-1, FGF-2,* and *PDGFRα* -specific qPCR analyses. *IGF-1* mRNA analysis revealed a remarkable, fourfold mRNA upregulation in cuprizone-treated WT animals. Cuprizone diet caused only twofold elevation of *IGF-1* between the untreated and cuprizone-fed TRPA1 KO groups (Fig.7B). We found that *PDGFRα* mRNA expression was not affected by cuprizone treatment in either WT or TRPA1 KO animals (Fig.7C). Although there was increased *FGF-2* mRNA expression in both naive and cuprizone-treated TRPA1 KO animals, a statistically significant upregulation was only observed in WT cuprizone-fed animals (threefold elevation, Fig.7D). Similarly to *NG2*, we detected approximately threefold upregulation of *Bak* mRNA in treated WT mice, but there was no significant difference between TRPA1 KO CTRL and CPZ groups (Fig.7E). No significant difference was detected in *TRPA1* expression between control and cuprizone-treated WT mice (data not shown).

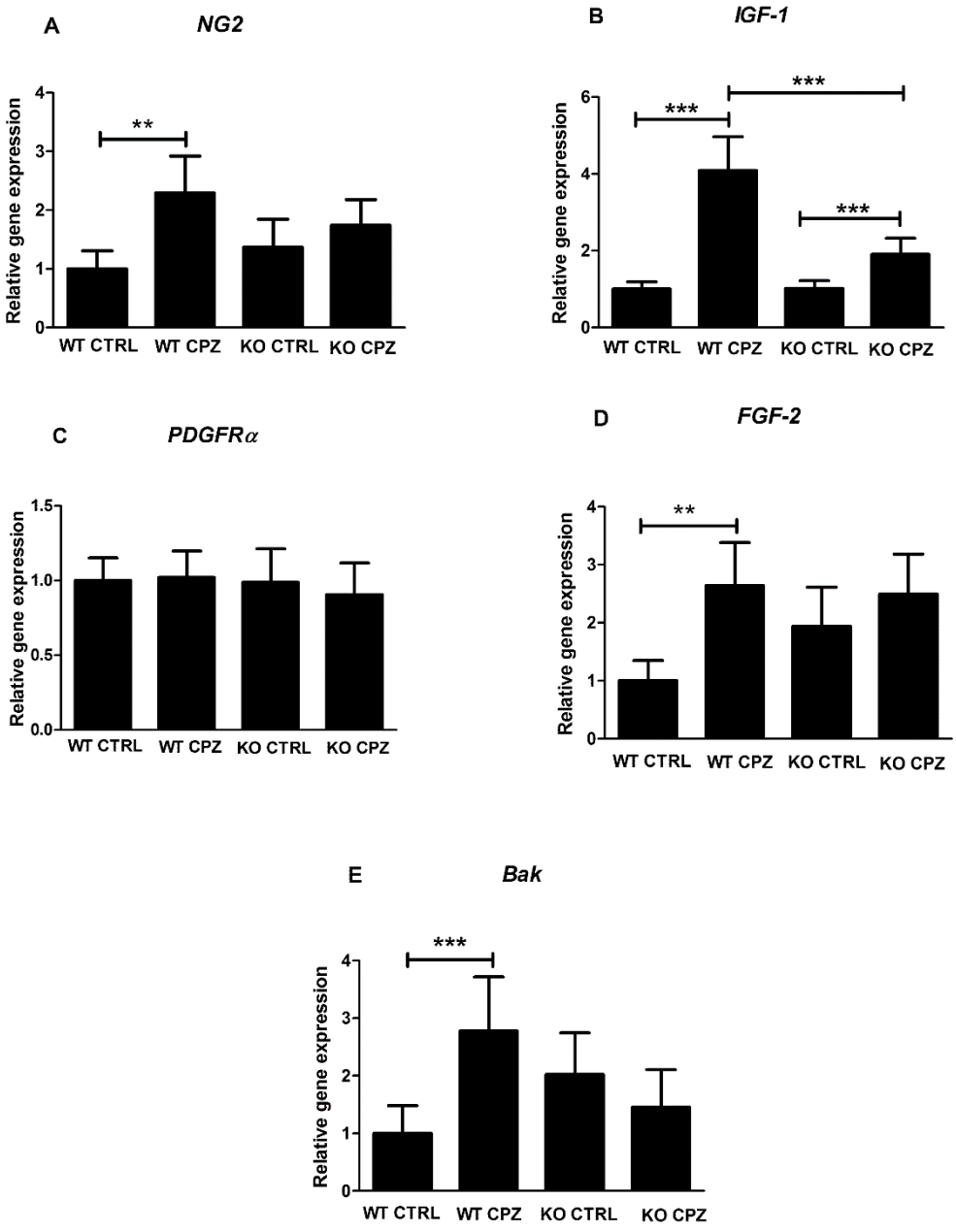

Fig.7: Gene expression analyses of NG2, IGF-1, FGF-2, PDGFRα, and Bak in the CC. Relative gene expression ratios of (A) chondroitin sulfate proteoglycan 4 (Cspg4) (NG2), (B) insulin-like growth factor 1 (IGF-1), (C) platelet-derived growth factor receptor alpha (PDGFRα), (D) fibroblast growth factor 2 (FGF-2) and (E) BCL2-Antagonist/Killer 1 (Bak1) in the dissected CC of cuprizone-treated and control mice. Columns represent the respective mRNA levels (mean±SEM) normalized to GAPDH as a housekeeping gene. Tissue samples were collected from two separate experiments. Each gene expression analysis was repeated three times and intergroup differences were tested by one-way ANOVA followed by Bonferroni's multiple comparison post hoc test: (A) WT CTRL versus WT CPZ **P < 0.01, (B) WT CTRL versus

WT CPZ ***P < 0.001, KO CTRL versus KO CPZ ***P < 0.001, WT CPZ versus KO CPZ ***P < 0.001, (D) WT CTRL versus WT CPZ **P < 0.01, and (E) WT CTRL versus WT CPZ ***P < 0.001.

3.1.8 TRPA1 activation modulates mitogen-activated protein kinase pathways in the cuprizone Model

Six weeks of cuprizone feeding significantly induced activation of the mitogen-activated protein kinases (MAPKs) JNK, ERK1/2 (**P<0.01 and *P<0.05), and c-Jun (*P<0.05) shown by immunoblotting using phosphorylation-dependent primary antibodies (Fig.8A,B and D). A tendency was seen for p38, although the difference measured by densitometry did not reach statistical significance (Fig.8C). The absence of TRPA1 enhanced the cuprizone-induced phosphorylation of p38-MAPK and ERK1/2, but again this was not statistically significant. In addition, TRPA1 deletion decreased p38, c-Jun phosphorylation (*P<0.05 and *P<0.05) and increased ERK1/2 phosphorylation (**P<0.01) in cuprizone naive knockout mice (Fig.8A,C and D). Basic level of phosphorylated JNK was increased in untreated TRPA1 knockout mice (**P<0.01), and cuprizone treatment did not influence its expression in this group (Fig.8B). In addition to the effect on MAPKs, densitometric analysis showed that cuprizone treatment did not affect the phosphorylation of MAPK downstream target c-Jun in the KO group (Fig.8D). The results are summarized in Fig.8.

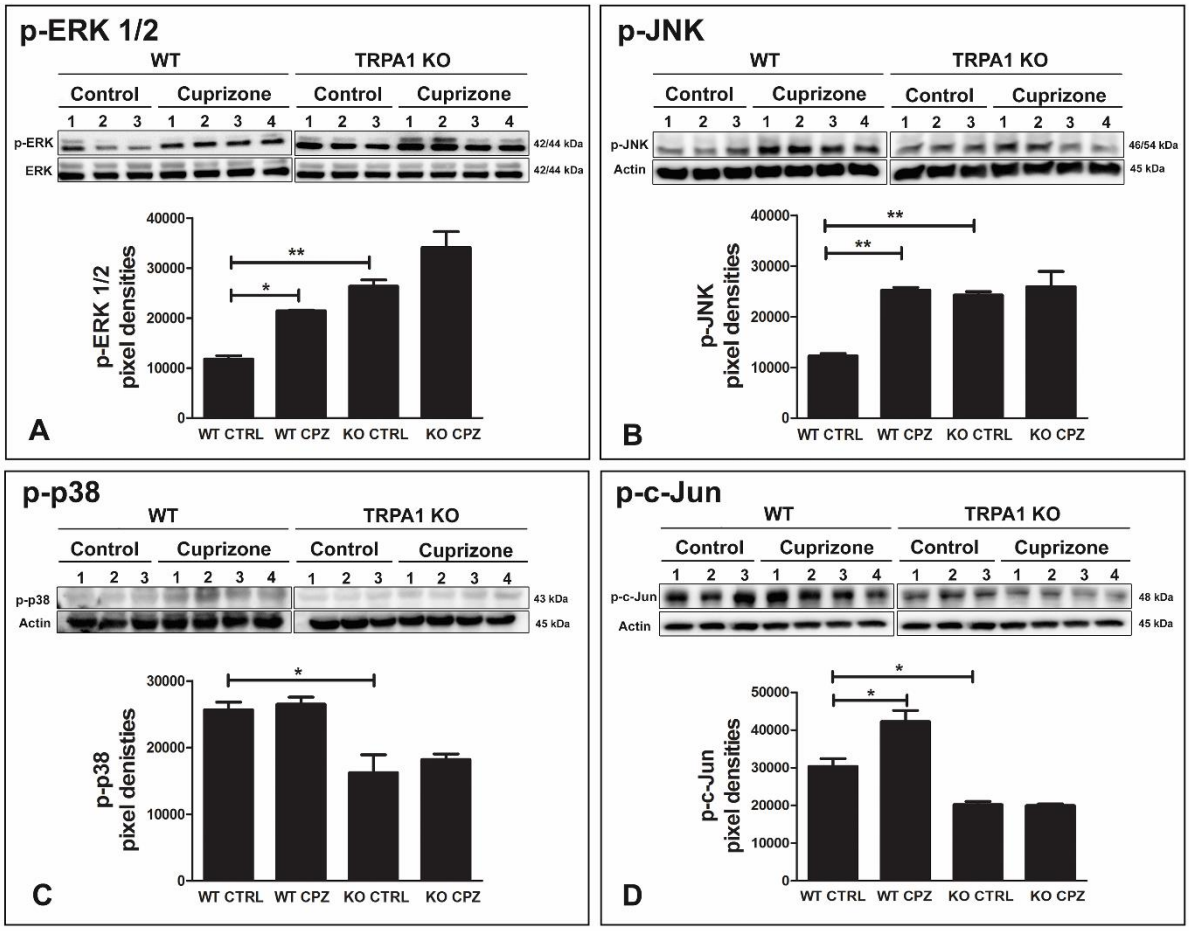

Fig.8: The effect of cuprizone treatment on the phosphorylation state of mitogen activated kinases (MAPK) and c-Jun in the CC of TRPA1 KO and WT mice. MAPK and c-Jun protein phosphorylation in the dissected CC of cuprizone-treated and untreated mice was detected by immunoblots utilizing phosphorylation-dependent antibodies (upper panels). Each panel shows representative immunoblots for (A) phospho-p44/42 MAPK (Thr202/Tyr204) (p-ERK1/2), (B) phospho-SAPK/JNK (Thr183/Tyr185) (p-JNK), (C) phospho-p38 (pThr180/pTyr182) (p-p38), (D) phospho-c-Jun (Ser73) (p-c-Jun) and their densitometric evaluation (lower panels). Even protein loadings were confirmed by an anti-b actin antibody and anti-nonphosphorylated ERK 1/2 antibody immunoblotting. Dividing lines above the numbered immunoblot lanes depict the control and cuprizone-treated samples from WT and TRPA1 KO groups. Tissue samples were collected from two separate experiments. Representative immunoblots are obtained from the same experiment and were processed parallel under same conditions. Each immunoblot analysis was repeated three times and intergroup differences were tested by one-way ANOVA followed by Bonferroni's multiple comparison post hoc test. Results on the diagrams are expressed as mean pixel densities±SD; (A) WT CTRL versus WT CPZ *P < 0.05, WT CTRL versus KO CTRL **P< 0.01, (B) WT CTRL versus WT CPZ **P < 0.01, WT CTRL versus

KO CTRL **P< 0.01, (C) WT CTRL versus KO CTRL *P< 0.05, (D) WT CTRL versus WT CPZ *P < 0.05 and WT CTRL versus KO CTRL *P < 0.05.

3.2 Quantitative comparison of primary cilia marker expression and length in the mouse brain

3.2.1 Characterization of AC3, Sstr3, and Arl13b expressing primary cilia of CNS cell types

To assess the distribution of ciliary markers in the mouse brain, we first analysed the localization of AC3, Sstr3, and Arl13b positive primary cilia of different CNS cell types. Brain sections were co-immunolabelled with antibodies to the three ciliary markers and with NeuN for neurons, GFAP for astrocytes, APC for mature oligodendrocytes or Iba-1 for microglia/macrophages. In line with previous reports (Bishop et al., 2007; Händel et al., 1999), the majority of AC3 positive and all Sstr3-positive primary cilia were detected on the surface of NeuN-labelled neurons (Fig.9A-B). While Sstr3-positive cilia were not found on the other investigated cell types, co-labelling also revealed the rare presence of AC3-positive cilia on GFAP-stained astrocytes (Bishop et al., 2007; Kasahara et al., 2014). Occurrence of Arl13b immunopositive cilia was strongly associated with GFAP positive astrocytes (Fig.9C). Although we also observed Arl13b positive primary cilia on neurons (Kasahara et al., 2014), the signal intensity of these cilia were faint and less apparent compared to the other two markers. Neither AC3 nor Arl13b immunoreactive cilia were observed on Iba-1-labelled microglia/macrophages or APC positive mature oligodendrocytes.

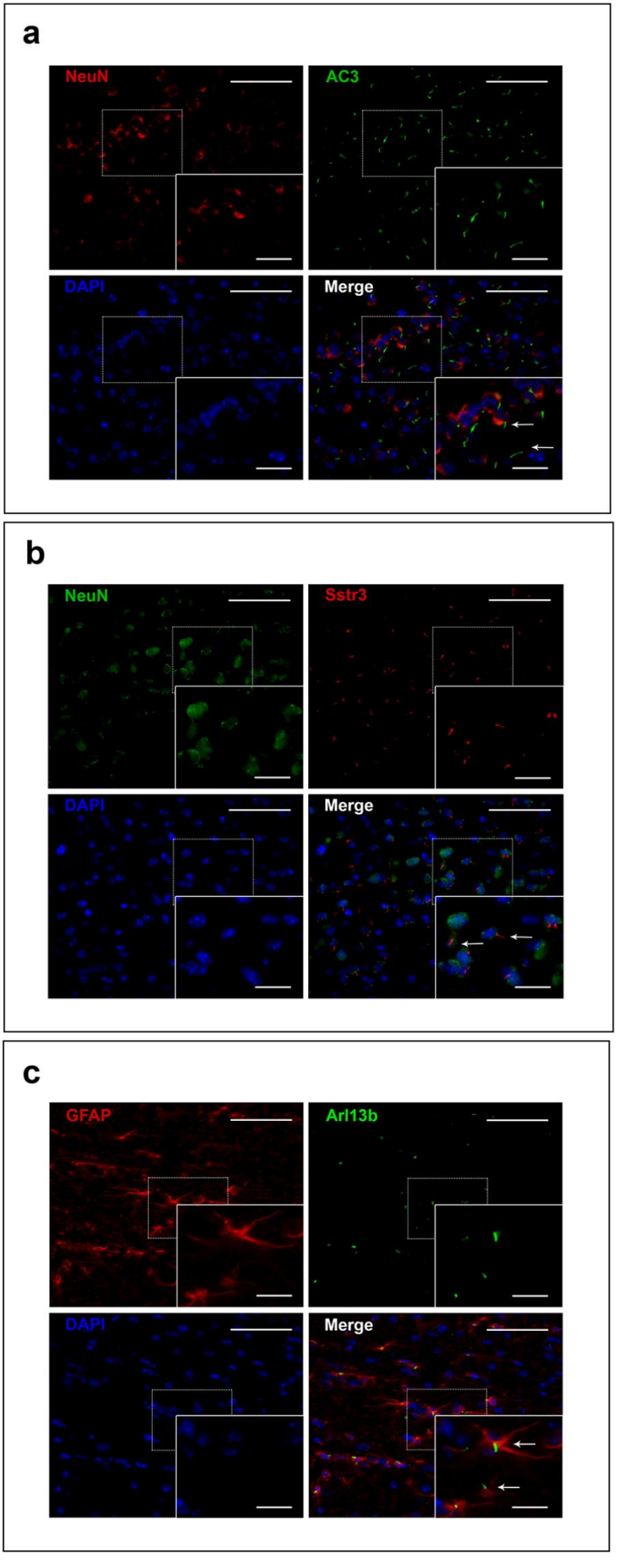

Fig.9: Expression of primary cilia markers in the 8-week-old WT mouse brain. a, b, c Representative double fluorescent images of neurons and astrocytes co-labelled for AC3, Sstr3, and Arl13b. a, b Primary cilia labelled with AC3 (green) and Sstr3 (red) localize to NeuN positive neurons (a—red and b—green). c Arl13b (green)-expressing primary cilia are associated with GFAP-positive astrocytes (red) as shown in corresponding overlays (scale bar 50 μm). Nuclei are visualized by DAPI (blue). The inserts in a, b, c panels indicate expression of the markers at higher magnification (scale bar 20 μm), and arrows show double labelled cells.

3.2.2 Comparative distribution of neuronal and astrocytic primary cilia in the mouse brain

It has been previously reported that expression of certain ciliary markers are restricted to different regions of the brain (Bishop et al., 2007; Händel et al., 1999). To investigate whether there is a regional preference of primary cilia marker expression, we counted and compared the number of $AC3^+/NeuN^+$ and $Sstr3^+/NeuN^+$ neuronal primary cilia ($AC3^+$NPC and $Sstr3^+$NPC) as well as the $Arl13b^+/GFAP^+$ positive astrocytic primary cilia ($Arl13b^+$AsPC) of distinct areas of the brain. Our results were generally consistent with the earlier described data by others and were summarized in Table 4. We found that AC3, Sstr3, and Arl13b positive primary cilia were evenly distributed in the cingular, sensory, motor, and piriform cortices omitting the most superficial layer (Fig.10A,B,C). Among these regions both AC3 and Sstr3 showed the highest density in the piriform cortex where 53.73 % and 29.68% of the cells had AC3- and Sstr3-positive cilia, respectively. The number of $Arl13b^+$AsPC was significantly less in all cortical regions (11.56–16.59%). High number and a higher density of $AC3^+$NPC were found in the olfactory tubercule (91.8%), accumbens nucleus (85.36%), and caudo/putamen (81.3%), whereas a low number of $Arl13b^+$AsPC (8.2–18.69%) and no Sstr3 immunoreactive neuronal cilia were detected in these regions. In contrast, $Sstr3^+$NPC were observed in the claustrum and endopiriform nucleus (21.51% and 29.21%); however, their number was significantly lower compared to $AC3^+$NPC (61.49 and 63.66%).

In the hippocampus, both $AC3^+$NPC and $Sstr3^+$NPC were detected in all subregions of the stratum pyramidale. The number and density of Sstr3 followed a decreasing tendency, namely CA3 > CA2 > CA1, respectively. Notably, we observed a CA2 intersecting area where Sstr3 immunoreactivity only appeared in a punctate form surrounding the cell nuclei. The overall expression pattern of Sstr3 was found to be inversely proportionate to the number of $AC3^+$NPC. This trend was also observed in the dentate gyrus. In contrast to the neuronal ciliary markers, $Arl13b^+$AsPC showed an even distribution in the stratum oriens and radiatum bordering the pyramidal layer. Importantly, the density of $Arl13b^+$AsPC was the highest in the stratum lacunosum-moleculare and polymorph layer in the hippocampal formation. We also found all three ciliary markers expressed in subnuclei of amygdala (Fig.10G,H and I). Although both $AC3^+$NPC and $Sstr3^+$NPC showed a higher density compared to $Arl13b^+$AsPC, the number of $AC3^+$NPC was significantly higher (61.67%) in contrast to $Sstr3^+$NPC (19.2%) or $Arl13b^+$AsPC (19.13%). In addition to the amygdala, the distribution and pattern of primary cilia also varied in the hypothalamic nuclei. Both $AC3^+$NPC and $Arl13b^+$AsPC were detected in all major subnuclei including the paraventricular (PVN), dorsomedial (DM), ventromedial

(VM), arcuate (ARC), and suprachiasmatic (SCN) nucleus (Fig.10D,E and F). The density and number of $AC3^{+}$NPC and $Arl13b^{+}$AsPC was the highest in the SCN (85.08%) and PVN (30.93%) regions, respectively. In contrast, ciliary expression of Sstr3 was limited to the VM in which 32.04% of the neurons had Sstr3-positive primary cilia. Although we did not find $Sstr3^{+}$NPC in the rest of the hypothalamic regions, we also observed a punctate Sstr3 immunoreactivity around cell nuclei similar to the hippocampal CA1-CA2 intersecting pattern.

Table 4: Percentage of AC3, Sstr3 and Arl13b (+) primary cilia in regions of the brain			
	AC3^{+}NPC	**Sstr3^{+}NPC**	**Arl13b^{+}AsPC**
Cortex (Cx) & additional regions			
Cingular Cx	66,35%	21,77%	11,88%
Motor Cx	55,27%	31,24%	13,49%
Somatosensory Cx	65,9%	22,54%	11,56%
Piriform Cx	53,73%	29,68%	16,59%
Olfactory Tubercule	91,8%	-	8,2%
Accumbens Nucleus	85,36%	-	14,64%
Caudo/putamen	81,31%	-	18,69%
Clasutrum	61,49%	21,51%	17,0%
Endopriform Nucleus	63,66%	29,21%	7,13%
Hippocampus			
CA1	49,78%	25,73%	24,49%
CA2	56,57%	35,32%	8,11%
CA3	35,64%	41,77%	22,59%
Dentate Gyrus	69,75%	9,25%	21,0%
Amygdala	61,67%	19,2%	19,13%
Hypothalamus			
Paraventricular Nucleus	69,07%	-	30,93%
Suprachiasmatic Nucleus	85,08%	-	14,92%
Arcuate Nucleus	82,25%	-	17,75%
Dorsomedial Nucleus	69,9%	-	30,1%
Ventromedial Nucleus	52,48%	32,04%	15,48%

Table 4: Quantitative comparison of the number of neuronal and astrocytic primary cilia markers in regions of the brain. Rows represent the number of AC3 positive neuronal cilia (AC3^{+}NPC), Sstr3 positive neuronal cilia (Sstr3^{+}NPC) and Arl13b positive astrocytic cilia (Arl13b^{+}AsPC) in total number of cilia counted in each region. The regional differences were tested by fractional of total analysis and data are expressed in percentage (%) (GraphPad Prism software Version 6).

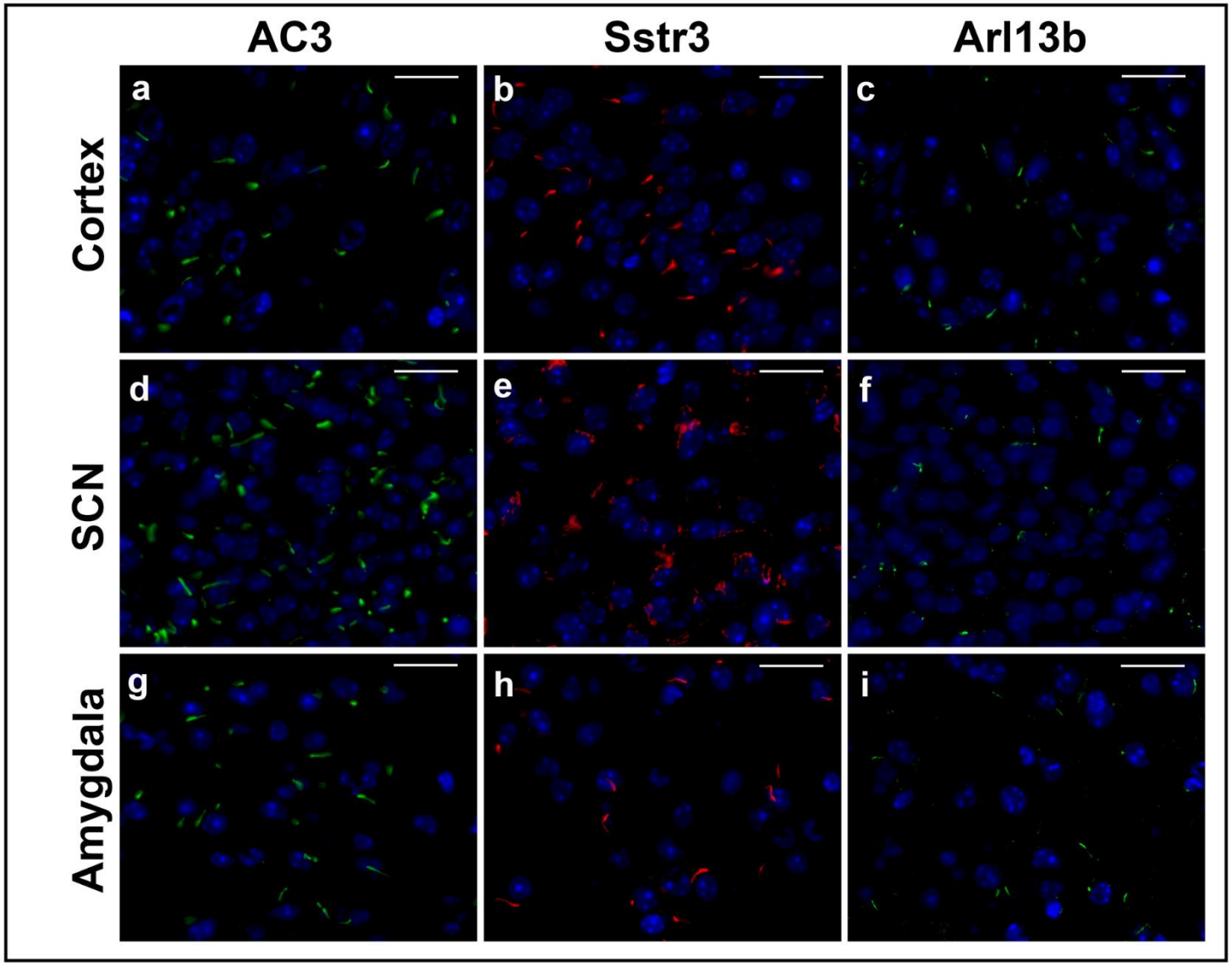

Fig.10: Expression pattern and distribution of primary cilia markers in the mouse brain. a–i Representative fluorescent images of multiple brain regions showing primary cilia labeled for AC3 (green), Sstr3 (red), and Arl13b (green). a–h The number and density of AC3- and Sstr3- expressing primary cilia are inversely proportionate as shown in the cortical region (a, b), suprachiasmatic (d, e), and amygdaloid nucleus (g, h). Note that Sstr3 localizes to primary cilia in the cortical area (b) and amygdala (h), while Sstr3 immunoreactivity can only be seen in the cytoplasm in the suprachiasmatic nucleus (SCN) (e). The number of Arl13b-expressing primary cilia is less compared to AC3 or Sstr3, and only a few Arl13b-expressing cilia shows strong signal intensity (c, f, and i). Nuclei are stained with DAPI (blue). Scale bar 20 μm.

3.2.3 Regional distribution of primary cilia is associated with alterations of their length

Recent studies have demonstrated that ciliary signalling proteins can modulate primary cilia functions by dynamically regulating their length (Miyoshi et al., 2014; Parker et al., 2016). Based on the observed distributional patterns, to examine possible regional functions of primary cilia in the CNS, we measured and compared the length of neuronal and astrocytic primary cilia in the mouse brain. We found that the average length of $AC3^+$NPC or $Sstr3^+$NPC was variable in the four investigated cortical regions within the range from 4.88 and 5.51 μm (cingular cortex) to 5.55 and 5.18 μm (piriform cortex), respectively.

Besides NPC, the average length of $Arl13b^+$AsPC varied between 2.95 and 3.33 μm. While $Arl13b^+$AsPC were significantly shorter compared to both types of NPC (***$P < 0.001$ and/or ****$P \leq 0.001$), comparison of AC3 and $Sstr3^+$NPC length did not reach a statistically significant value in either cortical region (Fig.11).

Among the investigated brain regions, the average length of $AC3^+$NPC were measured essentially longer in the areas of the olfactory tubercule (10.68 μm), accumbens nucleus (9.84 μm) and caudo/putamen (9.61 μm) compared to the length of $AC3^+$NPC measured in the cortices. Additionally, the average length of both AC3 and $Sstr3^+$NPC were similarly short in the claustrum (5.41 and 4.92 μm) and endopiriform nucleus (6.16 and 5.14 μm) as in the cortical areas. Notably, $AC3^+$NPC were significantly longer compared to $Sstr3^+$NPC in the endopiriform region (***$P < 0.001$). Moreover, the average length of $Arl13b^+$AsPC ranged between 3.37–4.2 μm and was also significantly shorter compared to $AC3^+$NPC and/or $Sstr3^+$NPC in these areas (Fig.11).

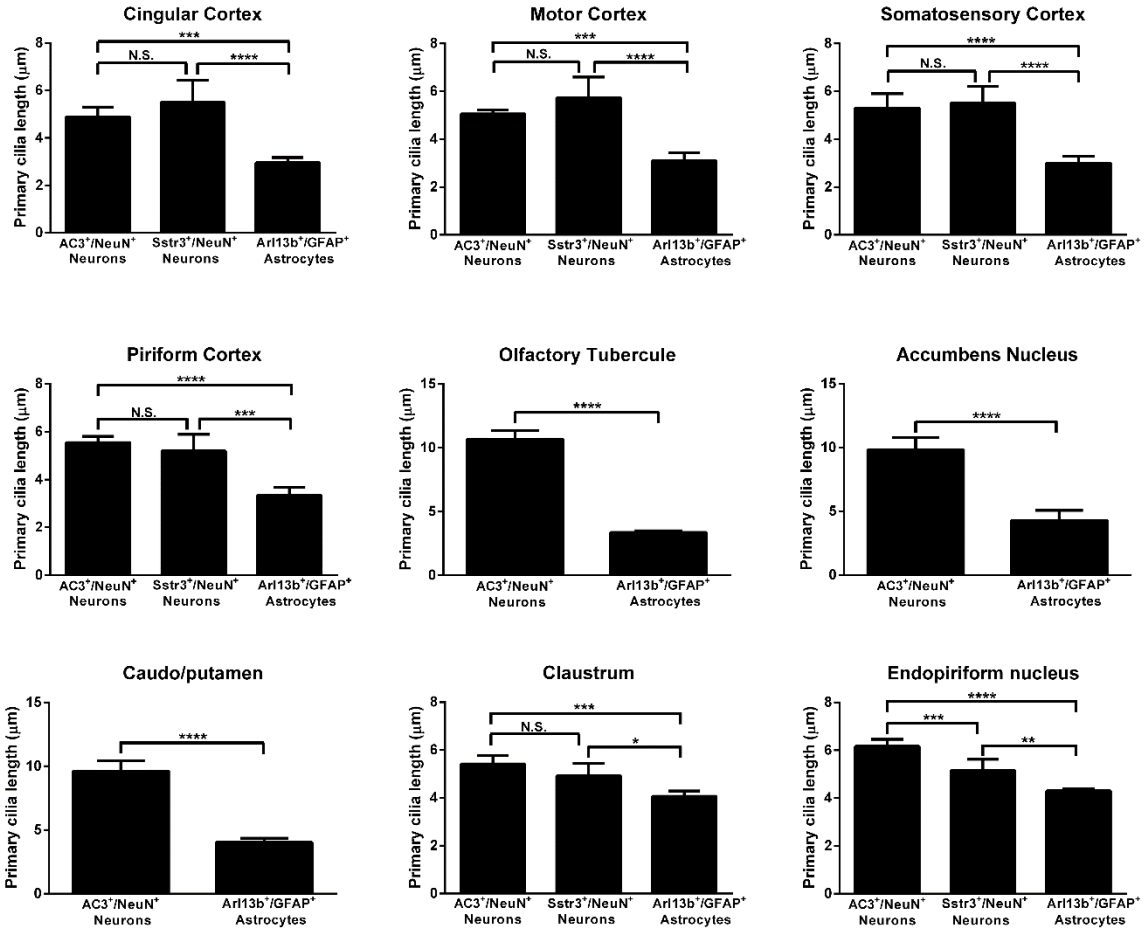

Fig.11: Comparison of primary cilia length in the cortices, olfactory tubercule, caudo/putamen, claustrum, endopriform, and accumbens nucleus. Histograms show the length of $AC3^+/NeuN^+$, $Sstr3^+/NeuN^+$, and $Arl13b^+/GFAP^+$ double positive primary cilia measured (n > 150) from 5 animals per region. Columns represent the average length (mean ± SEM) of each primary cilia marker per brain region. Measurements were repeated three times and statistical differences were tested by Student's t test or one-way ANOVA followed by Tukey's multiple comparison post hoc test (*P < 0.05, **P < 0.01, ***P < 0.001, ****P < 0.0001) (GraphPad Prism software Version 6).

In the hippocampal CA regions, the average lengths of AC3^{+}NPC (5.0–5.91 μm) and Sstr3^{+}NPC (3.79–5.46 μm) showed a similar tendency to the cortices (Fig.12 and 13). Importantly, AC3^{+}NPC (5.82 μm) were significantly longer compared to Sstr3^{+}NPC (3.79 μm) in the CA1 region (****P ≤ 0.001). In addition, no significant differences were found comparing the average length of the AC3 and Sstr3^{+}NPC in the dentate gyrus (3.2 and 2.78 μm) and subnuclei of the amygdala (6.73 and 6.48 μm). The average length of Arl13b^{+}AsPC in the amygdala and hippocampus were identical to the cortical values (2.8–3.2 μm) and were significantly shorter in all of these regions but the area of the dentate gyrus. We also found that AC3^{+}NPC were longer in the hypothalamus and its nuclei (Fig.12 and 13). Their average length varied between 8.0 μm (PVN) and 10.48 μm (VM). Sstr3- expressing NPC were also detected longer in the VM (8.18 μm); however, these primary cilia appeared to be significantly shorter compared to AC3^{+}NPC in this region (**P < 0.01). Repeatedly, Arl13b^{+}AsPC were found significantly shorter (3.6–4.09 μm) in all nuclei of the hypothalamus (****P ≤ 0.001).

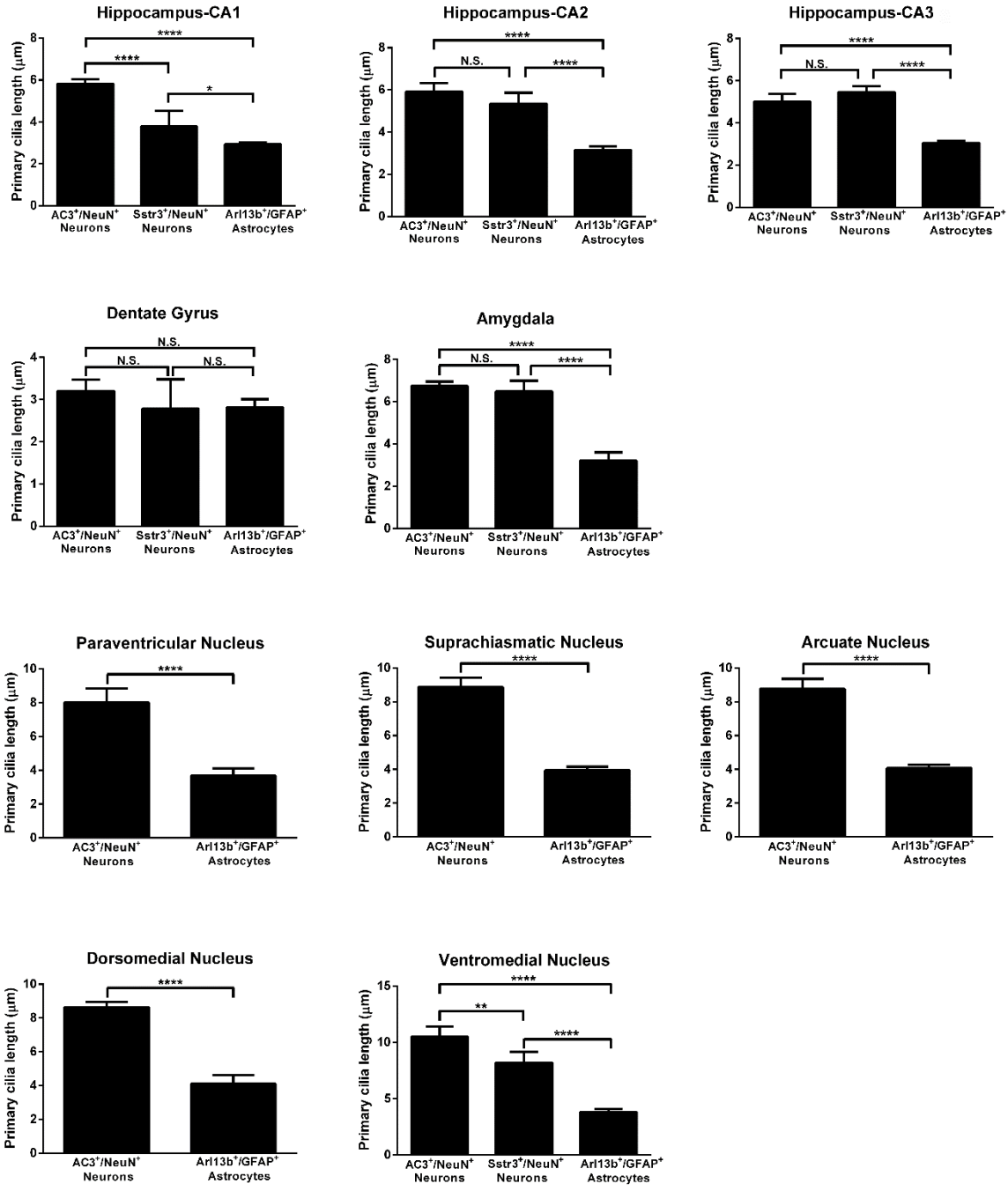

Fig.12: Comparison of primary cilia length in the hippocampal formation and hypothalamic nuclei. Histograms show the length of $AC3^+/NeuN^+$, $Sstr3^+/NeuN^+$, and $Arl13b^+/GFAP^+$ double positive primary cilia measured (n > 150) from 5 animals per region. Columns represent the average length (mean ± SEM) of each primary cilia marker per brain region. Measurements were repeated three times, and statistical differences were tested by Student's t test or one-way ANOVA followed by Tukey's multiple comparison post hoc test (*P < 0.05, **P < 0.01, ****P < 0.0001) (GraphPad Prism software Version 6).

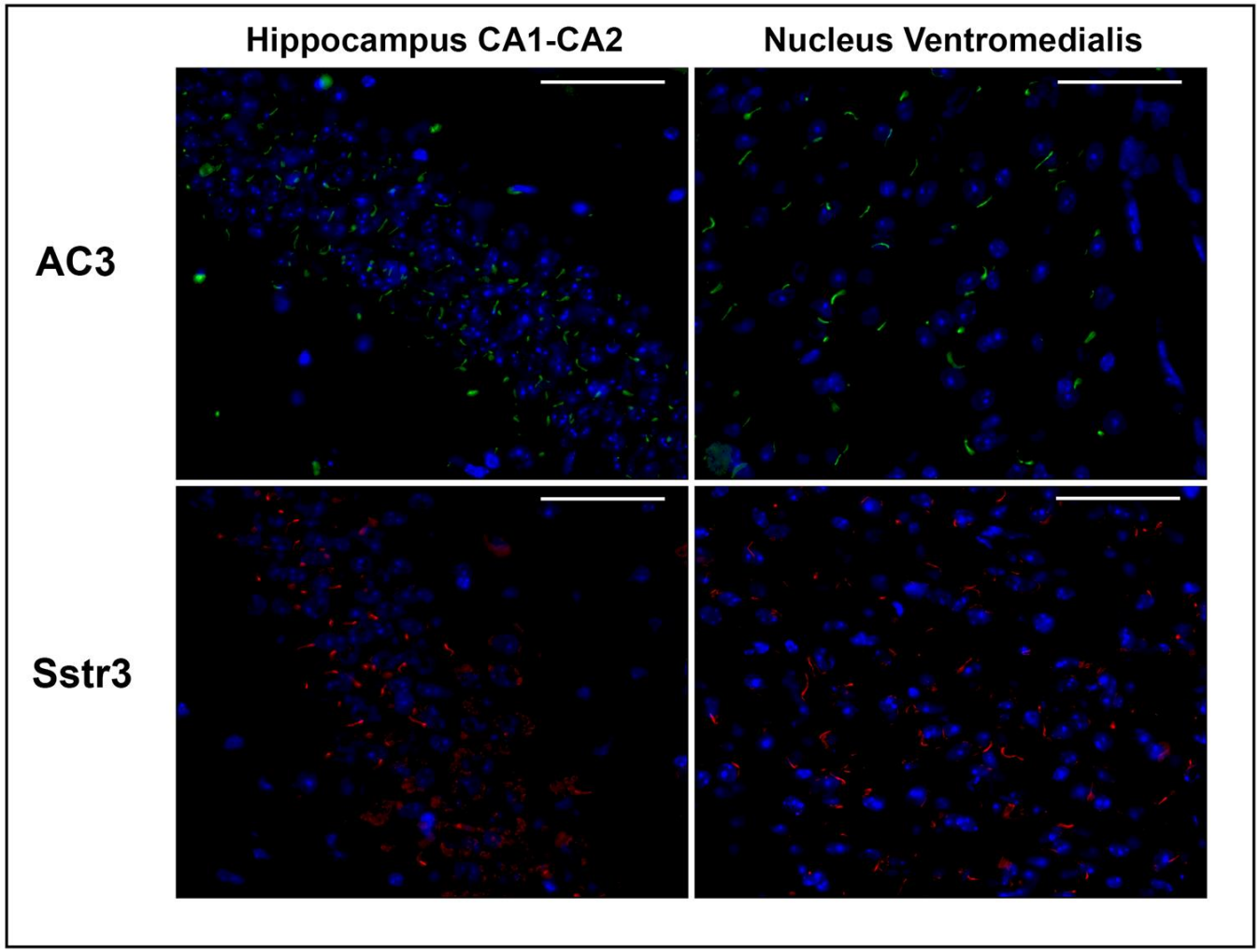

Fig.13: Representative fluorescent images of the expression pattern and length of primary cilia labelled for AC3 and Sstr3 in the mouse brain. Labelling for AC3 (green) and Sstr3 (red) reveals numerous short primary cilia the hippocampus CA regions; however, Sstr3 immunoreactivity can also be seen in the cytoplasm. Note that the length of AC3 (green)- and Sstr3 (red)-positive cilia are longer in the ventromedial nucleus. Nuclei are visualized by DAPI (blue). Scale bar 50 μm.

4. DISCUSSION

4.1 TRPA1 deficiency is protective in cuprizone-induced demyelination- A new target against oligodendrocyte apoptosis

In the present study, we investigated the distribution and possible regulatory role of TRPA1 receptors in the mouse CNS by utilizing the cuprizone-induced demyelination model. Our data indicate that TRPA1 deficiency attenuates the non-immune mediated, toxin-induced demyelination via a mechanism resulting the reduction of the apoptosis of mature OLs. Our findings also suggest that modulation of the function of TRPA1 may provide new therapeutic strategies for the treatment of patients with certain MS subtypes.

Our study commenced with a series of IHC experiments to assess the expression profile of TRPA1 within the CNS. We found that TRPA1 is expressed in several distinct regions of the mouse brain including the CC. Importantly, results of immunohistocehmical co-localization studies revealed that TRPA1 expression is restricted to astrocytes (Fig.4A-B). TRPA1 is generally known to be activated by a spectrum of noxious stimuli (such as different chemical compounds-induced inflammation, tissue damage as well as oxidative stress) (Bang et al., 2009; Bautista et al., 2013; Verkhratsky et al., 2014; Viana, 2016). Additionally, astrocytes play a pivotal role in influencing de- and remyelinating processes of the cuprizone-induced demyelination model (Skripuletz et al., 2013). Thus, it was intriguing to hypothesise that TRPA1 receptor might modulate this toxin-induced demyelination.

We show that demyelination occurred in both TRPA1 deficient and WT mice. However, the degree of demyelination was less severe in KO mice compared to WT mice (***$P<0.001$) (Fig.5C and H), suggesting a functional role of TRPA1 in the toxin-induced myelin damage. Primary OL death is one of the most prominent histopathological feature of the cuprizone model (Acs et al., 2009; Acs & Komoly, 2012; Praet et al., 2014). On a cellular level, TRPA1 deficiency significantly attenuated the loss of mature OLs (***$P<0.001$) (Fig.6G,H and J), suggesting a detrimental role of TRPA1 receptor activation in OL apoptosis. The complex course of toxic demyelination is also accompanied by a robust endogeneous form of reparatory process, in which mature OL loss and tissue damage can be partially or even fully restored by newly recruited and proliferating OPCs to achieve remyelination of lesions (Acs et al., 2009; Gudi et al., 2009; Mason, Jones, et al., 2000). These observations led us to hypothesise two possible scenarios: 1) either the higher number of mature OLs found in the CC of TRPA1 KO mice is due to a reduced vulnerability to cuprizone-induced apoptosis or 2) selective mature OL loss may be rapidly replaced by newly formed, proliferating OPCs facilitating an enhanced remyelination. We found that cuprizone administration did not increase the number of OPCs

(only Olig2 positive cells and NG2 expression) significantly in KO mice, supporting the notion that TRPA1 deficiency reduces apoptotic cell death, but it does not activate the proliferation and differentiation of OPCs. Besides the above described selective vulnerability of mature OLs, prominent astrocyte as well as microglia/macrophage activation are also well-known pathological hallmarks that accompany cuprizone-induced demyelination in a spatio-temporal manner (Gudi et al., 2014). Based on the differences observed in OL loss, we investigated whether the appearance and distribution of astrocyte and microglia/macrophage reactions also occur in a different pattern in cuprizone-treated TRPA1 KO mice (Fig.6). In line with previous reports (Acs et al., 2009) extensive astrocyte and microglia/macrophage reaction co-occurred with severe demyelination in the CC of WT mice, whereas a less prominent cellular response was observed in cuprizone exposed TRPA1 KO animals with a distribution pattern that coincides with surviving OLs. The notion of diminished glial reactions in KO mice imply a lower degree of tissue injury, which further reinforces the theory that TRPA1 deficiency could be beneficial. Since we found TRPA1 expression on astrocytes, these histopathological findings prompted us to presume that the absence and presence of the receptor might mediate opposing effects on cellular responses by predominantly affecting astrocytes. Therefore, we speculated a modulatory role in apoptosis- at least partially- by influencing interactions between OLs and astrocytes. It has been reported that TRPA1 activation can exert major changes on the physiological functions of astrocytes (Shigetomi et al., 2013; Shigetomi et al., 2011); and these cells can also directly alter the fate of OLs by releasing various biological molecules under different experimental conditions (Gudi et al., 2011; Kang et al., 2012; Linares et al., 2006; Zeger et al., 2007). However, it should be highlighted that a recent study reported TRPA1 receptor expression on OLs from rat and mouse cerebellum, *in vitro* (Hamilton et al., 2016). Although our results do not support that OLs express TRPA1 in mouse CNS, a possible direct mode of action of TRPA1 function on apoptotic cell death cannot be ruled out.

Growth factors (GFs) are tiny diffusible molecules that have a well- established role in the modulation of cellular processes. They are known to facilitate a multitude of different biological responses, however, their precise modulatory function is always organ and target cell specific (Cross et al., 1991; Shrivastava et al., 2016). In particular, GFs released by astrocytes have been demonstrated to influence the fate of cells participating in the myelination processes, such as regulating the proliferation and differentiation of OPCs as well as the survival of mature OLs (Acs et al., 2009). We observed that demyelination together with astrocyte and microglia/macrophage activation was attenuated in the absence of TRPA1 (Fig.5 and 6). Thus, we investigated whether genetic deficiency of TRPA1 might mitigate cuprizone-induced

mature OL death by altering the expression of GFs secreted by astrocytes. Within the CNS, platelet-derived growth factor receptor α (PDGFRα) and fibroblast growth factor 2 (FGF-2) are two major factors considered to promote proliferation and inhibit differentiation of premature OLs (Armstrong et al., 2002; McKinnon et al., 1990; Murtie et al., 2005; Woodruff et al., 2004). In line with previous observations (Acs et al., 2009), cuprizone treatment resulted in higher mRNA expression of *FGF-2* (**P < 0.01), but not *PDGFRα* in the CC of WT mice (Fig.7C,D). Importantly, mRNA levels of *PDGFRα* and *FGF-2* did not show a significant change in KO mice, further indicating that the preserved myelin status is not achieved by an enhanced proliferation and maturation of OPCs into myelin forming OLs. Chondroitin sulfate proteoglycan 4/neural/glial antigen 2 (NG2) is a marker of OPCs, which react to injury by proliferating around the lesion site and differentiating into OL (Hackett et al., 2016). Several studies have reported that $NG2^+$ OLs and PDGFRα are recruited to demyelinated lesions (Islam et al., 2009). Elevated *NG2* expression in cuprizone-treated WT mice might suggest a compensatory response to the extensive myelin damage (**P < 0.01) (Fig.7A). The unaltered *NG2* level in KO mice seems to be the result of less pronounced demyelination due to reduced OL apoptosis. Astrocytes are the main source of insulin-like growth factor I (IGF-1), which has been shown to be important in the recruitment, differentiation and maturation of OPCs and in protecting mature OLs under different toxic conditions (Komoly et al., 1992; Mason, Ye, et al., 2000; Zeger et al., 2007). Cuprizone treatment significantly induced *IGF-1* mRNA expression in WT mice (***P < 0.001) (Fig.7B), indicating that the recruitment of premature OLs is a result of robust astrogliosis and subsequent IGF-1 release. Although we observed higher *IGF-1* mRNA expression in KO mice treated with cuprizone (***P < 0.001), its level was significantly lower compared to WT mice (***P < 0.001). It could be the consequence of a less pronounced activation of astrocytes and diminished apoptotic cell death in the absence of enhanced recruitment of OPCs. Apoptosis of OLs is also connected to mitochondrial dysfunction during toxin-induced demyelination. It has been proposed that cuprizone toxicity results in impaired functioning of major cell stress and death related mitochondrial mechanisms and is also associated with a reduction of the mitochondrial transmembrane potential (Acs et al., 2013; Benardais et al., 2013; Praet et al., 2014). Among the different groups of mitochondria-linked molecules, members of the Bcl-2 family- involving both anti-apoptotic as well as pro-apoptotic (such as Bax, Bid and Bak) factors -have been reported to be major determinants of the fate of OLs (Itoh et al., 2003; Lindsten et al., 2000). In particular, Bak is well-known to be one crucial regulator of mitochondrial outer membrane permeabilization (MOMP), which subsequently allows the release of pro-apoptogenic proteins from the

mitochondria to the nucleus that commits the cell to undergo apoptosis (Cheng et al., 2001; Dewson et al., 2009; Wei et al., 2000; Wei et al., 2001). Notably, we found a significantly elevated level of *Bak* mRNA expression after cuprizone treatment in WT mice (***P < 0.001), but there were no significant changes in KO animals (Fig.7E). Thus, these results show strong consistency with our IHC findings suggesting that TRPA1 deficiency reduces the apoptosis of mature OLs during cuprizone diet. However, further studies are needed in the future to reveal the precise molecular mechanisms underlying TRPA1 activation and clarify its particular role in OL death.

As a next step in our study, we were intrigued to hypothesise that stimulation of TRPA1- being a non-selective cation channel involved in Ca^{2+} linked signal transmission (Hamilton et al., 2016; Raquibul Hasan et al., 2017; R. Hasan et al., 2018; Vangeel et al., 2019; Zygmunt et al., 2014)- might contribute to apoptotic cell death by allowing a higher intracellular Ca^{2+} concentration, which could lead to a facilitated activation of apoptotic signalling pathways in mature OLs during cuprizone challenge. According to current literature, TRPA1-coupled downstream signal transduction was connected to members of the mitogen- activated protein kinase (MAPK) cascades. For example, activation of extracellular regulated protein kinase (ERK1/2) and p38-mitogen-activated protein kinase (p38-MAPK) in DRG neurons occurs through TRPA1 in response to noxious gastric distension (Kondo et al., 2009; Kondo et al., 2010; Kondo et al., 2013). Members of the MAPK cascades (ERK1/2, c-Jun N-terminal kinase (JNK) and p38-MAPK) have a well-established role in the transduction of a broad spectrum of extracellular stimuli into diverse intracellular responses that determine fate of the cells towards survival or stress-induced apoptotic death (L. Chang et al., 2001; Widmann et al., 1999). It has been previously demonstrated that cuprizone-induced apoptosis is mediated via JNK and p38-MAPK pathways (Veto et al., 2010), thus we speculated that these pathways might be possible intersecting points of cuprizone toxicity and TRPA1 action. In line with literature data, we found increased level of JNK in the CC of cuprizone treated WT mice. In contrast, the level of JNK activation appeared to be consistently high in both naïve and cuprizone exposed TRPA1 KO mice (Fig.8B). Additionally, the basic level of p38 activation was significantly lower (*P< 0.05) and similar to JNK also remained unaffected after cuprizone challenge in KO compared to WT animals (Fig.8C), suggesting that the absence of TRPA1 might reduce the activation of p38-MAPK pathway and subsequently the death of OLs. Transcription factor c-Jun is a downstream target of JNK and p38-MAPK and its activation is considered to be an important trigger of apoptosis after various CNS insults (Crocker et al., 2001; Watson et al., 1998). Cuprizone exposure significantly increased c-Jun activation in WT mice (*P < 0.05), whereas

the basic level of c-Jun was significantly attenuated in naïve TRPA1 KO animals (*P < 0.05) and its level did not change following cuprizone treatment (Fig.8D). These findings further indicate the reduced apoptosis of OLs in cuprizone exposed TRPA1 deficient mice. Activation of ERK1/2-MAPK pathway has been demonstrated to play a pivotal role in promoting the survival of OLs under different experimental conditions (Domercq et al., 2011; J. Y. Lee et al., 2011; Xia et al., 1995). Cuprizone intoxication resulted in significant ERK1/2 activation (*P < 0.05) in WT group, which was further enhanced in the absence of TRPA1, indicating that a pronounced protective effect against cell death of mature OLs may be present in TRPA1 KO mice.

In summary, our findings strongly suggest that TRPA1 contributes to cuprizone-induced OL death by influencing the Ca^{2+} influx into the astrocytes and subsequently facilitating the activation of JNK and p38-MAPK pathways resulting in c-Jun activation in mature OLs. Although protective ERK1/2 pathway can be activated by cuprizone, this compensatory mechanism seems to be insufficient to prevent apoptotic cell death. However, TRPA1 deficiency attenuates the apoptosis in OLs by primarily suppressing the activation of p38-MAPK and c-Jun as well as by enhancing ERK1/2 pathways (Fig.14).

TRPA1 receptors can be activated by oxidative stress, endogenous electrophilic ligands released in inflammatory and degenerative processes in the CNS. We conclude that opening of these multisteric ion channels triggers the elevation of intracellular Ca^{2+} concentration. Activation of TRPA1 receptor- either indirectly by modulating astrocyte function and consequently astrocyte-OL crosstalk, or directly by acting on OLs—may contribute to OL death by supporting the pro-apoptotic p38-MAPK pathway resulting in c-Jun activation and consequent OL apoptosis. However, our data rather support the indirect effect of TRPA1 activation on OL death. TRPA1 receptor antagonists might successfully diminish the non-immune mediated degeneration in multiple sclerosis and could be promising drug candidates to limit CNS damage in demyelinating diseases.

Fig.14: Possible role of TRPA1 in cuprizone-induced oligodendrocyte loss. Schematic drawing summarizing the role of TRPA1 in cuprizone-induced phosphorylation of mitogen-activated protein kinase pathways (ERK1/2, JNK, and p38-MAPK) and transcription factor c-Jun in WT and TRPA1 KO mice. Left side panel: in WT mice cuprizone treatment induces the activation of proapoptotic JNK and p38-MAPK pathways leading to OL death. We hypothesize that TRPA1 on astrocytes contributes to OL loss by Ca^{2+} influx that allows the release of certain astrocyte factors enhancing the activation of JNK and p38-MAPK pathways as well as their nuclear downstream target c-Jun resulting apoptosis. Right side panel: In absence of TRPA1 receptor, the cuprizone-induced release of astrocyte factors is altered, which significantly increases ERK1/2 and reduces both p38-MAPK and c-Jun activation resulting less OL apoptosis. Red arrows indicate enhanced or decreased phosphorylation of proteins detected by immunoblot analysis (see Fig.8).

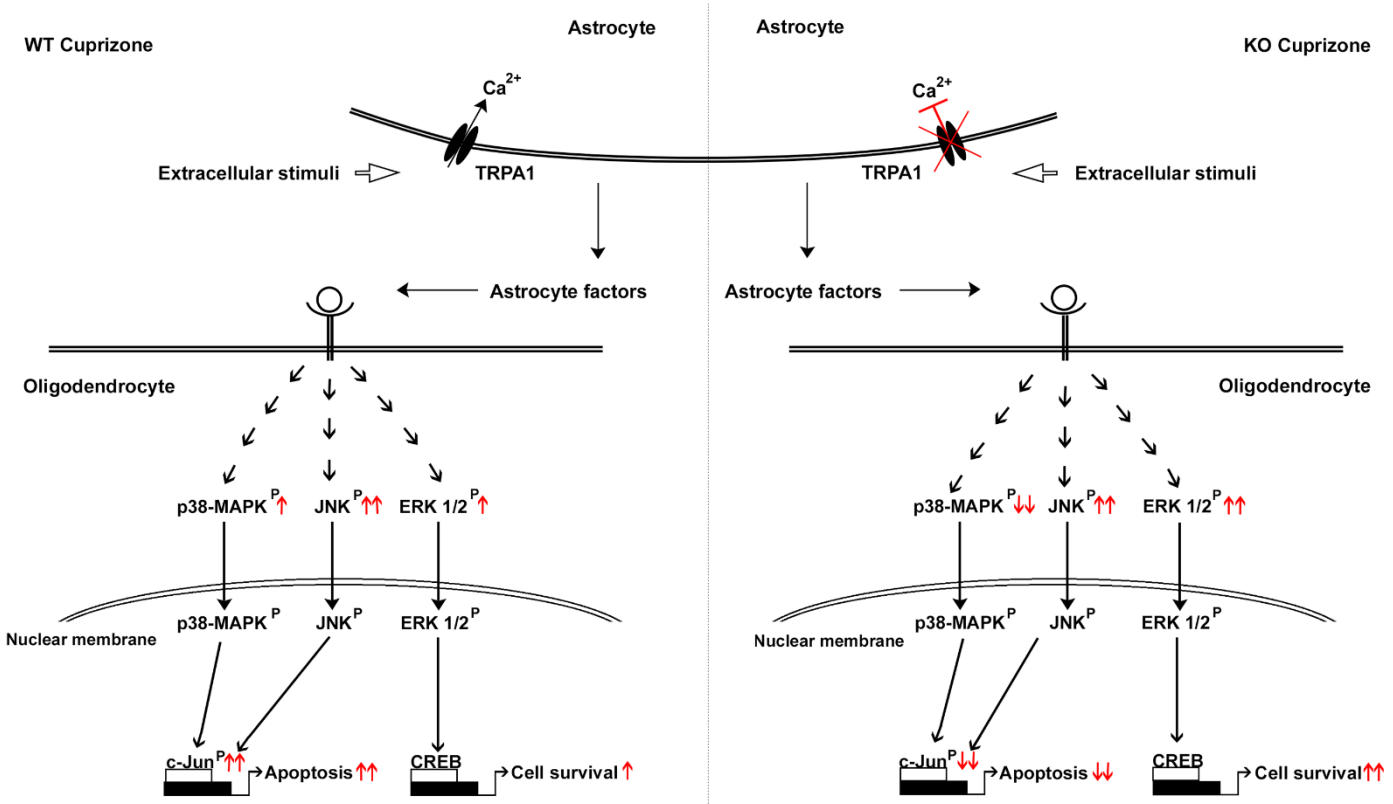

4.2 Quantitative comparison of primary cilia marker expression and length in the mouse brain

Several previous studies have shown that primary cilia play a critical role in the development and maintenance of neural homeostasis of the mammalian brain (Fry et al., 2014; J. H. Lee et al., 2010; Valente et al., 2014). Based on earlier observations (Bishop et al., 2007; Händel et al., 1999), possible functions of primary cilia can be specified by three major features: (1) the signalling molecules concentrated in the ciliary membrane, (2) the length of the structure, and (3) the cellular and regional localisation of the organelle within the CNS. Previous studies have elegantly mapped the distribution of AC3 and Sstr3-positive primary cilia in the brain (Bishop et al., 2007; Händel et al., 1999). In light of these fundamental reports, we intend to discuss our findings in connection with those and other studies underpinning a specific role of primary cilia in cell types and selected brain regions. Also, we intend to put emphasis on the regional traits and differences of ciliary marker expression that have not been described. One limitation of the present study is that accurate measurements of primary cilia length possess a technical challenge due to the 3D orientation and versatile expression of ciliary markers along the organelle's entire structural profile. However, currently, the main method of visualizing or quantifying primary cilia length on histological sections is still by immunofluorescence techniques utilizing cilia-specific antibodies. Therefore, we would like to highlight the possibility that our findings might only reflect the immunohistochemically measurable length of primary cilia, and novel methods need to be developed to capture the true length of these organelles.

In this study, first we aimed to characterise AC3, Sstr3 and Arl13b positive primary cilia expression on different CNS cell types. In accordance with earlier observations (Bishop et al., 2007; Händel et al., 1999) we found that both AC3 and Sstr3 markers are predominantly expressed on neuronal primary cilia (NPC) in the adult mouse brain. Notably, double immunolabelling also revealed faint Arl13b- positive primary cilia on neurons, however, clear and apparent Arl13b expression was strongly associated with primary cilia on astrocytes (astrocytic primary cilia/AsPC). Additionally, only a few AC3 immunoreactive cilia localized to astrocytes and neither of the markers were observed together with mature oligodendrocytes (OL) or microglia/macrophages. The expression and frequency of Sstr3 positive NPC has been reported to change in parallel with the embryonic and postnatal development of the CNS (Stanić et al., 2009). Moreover, it has been demonstrated that AC3 as well as Arl13b expression of NPC and AsPC appear in a reciprocal manner in young aged (P10) compared to adult mice (P56) (Kasahara et al., 2014). Thus, our findings further indicate developmentally specified functions

of primary cilia of CNS cell types, particularly on matured neurons and subpopulation of astrocytes.

To further elucidate the relationship between primary cilia and brain function, we conducted a series of comparative histopathological analysis targeting the 1) the expression pattern, 2) the length, 3) and the rate of occurrence of NPC and AsPC markers in regulatory centres of the brain. Based on currently available literature data linking primary cilia to brain function, traits of primary cilia were analysed in 19 dedicated region of the mouse brain (Fig.2). We confirmed that AC3 is the most abundant ciliary marker which can be detected throughout the brain. In contrast, the distribution of Sstr3 had a more restricted expression profile among the investigated areas. Importantly, the number and length of these NPC were variable and showed region-specific alternations. In particular, $AC3^+$ NPC were observed to be the densest and longest in the olfactory tubercule (fraction of total 91,8% and average length 10,68 μm), supporting previous studies that implicated their significant role in olfaction (Challis et al., 2015; Kaupp, 2010; Qiu et al., 2016; Wong et al., 2000). Additionally, the length of $AC3^+$ NPC was also measured longer in regions of the caudo/putamen (9,61 μm) and accumben nucleus (9,84 μm). Since the protein components of primary cilia are thought to reflect distinct functional traits and we found ciliary morphology alike the olfactory tubercule, it is possible that the proper functioning of these regions may also substantially depend on AC3-linked pathways similar to odorant signalling. However, further experiments are needed to address this possibility.

In addition to these findings, the expression pattern and length of $AC3^+$NPC were also comparable to $Sstr3^+$NPC within the rest of the investigated regions. It has been previously demonstrated that the presence of $Sstr3^+$NPC are scarce in areas where AC3 expressing cilia are prevalent (Bishop et al., 2007). Indeed, we show that the number of $Sstr3^+$NPC is inversely proportionate to $AC3^+$NPC counted in regions, particularly in the cortices and hippocampus. Consistent with previous data published (Berbari et al., 2007; Berbari, Lewis, et al., 2008; J. A. Green et al., 2016), our double immunolabelling experiments revealed two distinct expression profiles in the latter regions, indicating that only distinct population of neuron possess Sstr3-positive cilia. Noteworthy, in the hippocampus Sstr3 immunoreactivity only appeared in a punctate form surrounding the cell nuclei the intersecting area of the CA2 hippocampal pyramidal layer. Considering that Sstr3 is retained in the cellular compartment while AC3 localizes to the ciliary structure, it reinforces literature data about the localization of ciliary signalling proteins are under strict control and suggests that the precise functions of NPC may vary within neuronal subpopulations. It has been previously demonstrated that Sstr3-induced

signalling is interconnected with adenylyl cyclase in the hippocampus (Einstein et al., 2010), and genetic ablation of both AC3 and Sstr3 has a major impact on several region related functions such as forms of memory in mice (Xuanmao Chen et al., 2016; Einstein et al., 2010; Guadiana et al., 2013; Wang et al., 2011). Moreover, dynamic changes of ciliary protein expression and length have been also described in response to pharmacological or agonist treatment (J. A. Green et al., 2016; Parker et al., 2016). Therefore, it would be interesting to examine whether these specific neuronal primary cilia in the hippocampus may 1) transport receptors from the cells, 2) alter their morphology and length, 3) or modify neuronal function in the adult brain under different experimental conditions such as stress. Regarding the hippocampal formation, it should be also noted that the number and density of Sstr3+NPC detected in the dentate gyrus is in contrast with earlier published data (Stanić et al., 2009), in which the density of Sstr3 positive primary cilia was observed to increase in a gradual manner and sustained at higher levels in the adult rat brain. It has been described that differences within immunohistochemical procedures greatly define the sensitivity and specificity of ciliary protein and structure detection (Hua et al., 2017). Thus, one reason underlying this discrepancy may be due to our different immunolabelling technique applied (antibody and detecting method versus antisera) or our results may reflect age- and/or species-associated alternations between the brains of rodents.

Primary cilia have also been implicated in the hypothalamic control of appetite and feeding behaviour. Genetic modulation of ciliary expression can profoundly influence the regulation of food intake (Berbari et al., 2013; Davenport et al., 2007; Loktev et al., 2013; Mok et al., 2010; Mukhopadhyay et al., 2013; Qiu et al., 2016; Seo et al., 2009; Wang et al., 2009). In accordance with other data, we found numerous $AC3^{+}$ NPC in all hypothalamic subnuclei, indicating that AC3 positive cilia are probably involved in the central regulation of appetite. However, ciliary expression of Sstr3 was restricted to the ventromedial nucleus (VM). Interestingly, only punctate cellular Sstr3 immunoreactivity appeared in the rest of the hypothalamic nuclei, similarly to what we have seen in the hippocampus. This distinct expression pattern of Sstr3 indicates that certain hypothalamic neuronal cilia might have multiple functional properties beyond the regulation of homeostatic functions. In particular, neuronal primary cilia have been demonstrated to express both Sstr3 and kisspeptin receptor 1 (kiss1r) on different population of hypothalamic neurons that are well-known central effectors driving the neuroendocrine axis such as growth hormone (GH) and gonadotropin-releasing hormone (GnRH) secretion (Brazeau et al., 1973; Johansson et al., 1984; Koemeter-Cox et al., 2014; Patel, 1999; Yasuda et al., 1992). Additionally, Sstr3 expressing primary cilia on GH secreting cell have been

suggested to play an important role in sensing somatostatin ligands in the adenohypophysis of mice (Iwanaga et al., 2011). Based on our histological observations, our findings strongly support that $Sstr3^{+}$NPC might mediate the biological effect of somatostatin on neuroendocrine cells and also contribute to the complex regulation of local hypothalamic neural circuitry. Importantly, the measured length of both $AC3^{+}$- and $Sstr3^{+}$ NPC was generally longer (8,0-10,48μm) within the hypothalamic nuclei. Since the hypothalamus is known to harbour a sophisticated inner network, we speculate that enhanced ciliary length might be indispensable to sense multiple ligands and orchestrate a plethora of different signal transduction pathways that are required for region-specific functions. Indeed, it has been recently reported that cilia length on hypothalamic neurons are actively regulated according to different metabolic necessities and feeding state (Y. M. Han et al., 2014). Thus, it is intriguing to hypothesise that longer ciliary length may also correlate with the ability to alter ligand binding sites and amplify the efficacy of signal transduction by transporting receptors from the neuronal plasma membrane. Nonetheless, further studies are needed in the future to elucidate such possibilities. Although the presence of a single primary cilium on the surface of astrocytes have been long accepted and described (Berbari et al., 2007; Bishop et al., 2007; Danilov et al., 2009; Doetsch et al., 1999), less is known about their precise physiological functions on astrocytes. Consistent with previous work (Bishop et al., 2007; Kasahara et al., 2014), we confirmed that the majority of Arl13b- positive primary cilia localize to the surface of astrocytes (Arl13b- positive astrocytic primary cilia/Arl13b+AsPC), while AC3 immunoreactivity was scarce, only a few AC3 positive primary cilia were detected on these cell types. Astrocytes are known to fulfil a multitude of different functions in the CNS (Parpura et al., 2012; Verkhratsky et al., 2010). Considering their paramount importance in the homeostatic maintenance of the brain, this preferential expression profile suggest that there might be different populations of astrocytes and Arl13b-signalling may provide an additional mechanism in regulating their region dependent functions. One particular observation is that the number and density of $Arl13^{+}$AsPC was higher in layers surrounding the hippocampal stratum granulare, a region important in generating new neurons from adult stem/progenitor cells (Ming et al., 2011; Walton, 2012). Notably, primary cilia in the CNS are known to mediate signalling pathways- such as Shh- that are critical during organogenesis and essential to maintain the cellular homeostasis throughout adult life (Alvarez-Satta et al., 2019; Bangs et al., 2017; Park et al., 2019). Conditional deletion of Arl13b or other ciliary structural proteins disrupt cilium mediated Shh signalling (Caspary et al., 2007; Larkins et al., 2011) and hippocampal neurogenesis in the mouse brain (Breunig et al., 2008; Y.-G. Han et al., 2008). Thus, our results suggest that Arl13b signalling through the

non-germinal astrocytes may contribute to a permissive environment to maintain neurogenesis in the dentate gyrus during perinatal as well as postnatal life. It should be also highlighted that we found significantly shorter AsPC compared to NPC within all investigated brain regions (Fig. 11 and 12). Quantitative comparison of AsPC length revealed differences among CNS regions, however, in some of the areas—linked average lengths of ARl13b expressing cilia differ from those previously described (Kasahara et al., 2014). Based on our immunohistocehmical findings, we assumed the divergence arose from the experimental technique/protocol and antibody applied likewise the disparate expression pattern of $Sstr3^{+}$NPC observed in the hippocampal formation.

Arl13b belongs to the Ras GTPase superfamily and has well-established functions in diverse cellular processes. For example, primary cilia-mediated Arl13b signalling is required for ciliary microtubule organization, ciliary membrane trafficking pathways, neuronal migration and formation of polarized radial glial scaffold in the developing nervous system (Caspary et al., 2007; Cevik et al., 2010; Higginbotham et al., 2012; Higginbotham et al., 2013; Humbert et al., 2012; Li et al., 2010). Signalling through $AC3^{+}$AsPC have been suggested to provide and additional mechanism affecting synaptic transmission (Bishop et al., 2007). Therefore, it is intriguing to speculate a similar regulatory role influencing the biological functions of astrocytes. Nevertheless, the general presence and functional implications of Arl13b on astrocytic cilia is yet to be investigated in future experiments.

4.3 Summary of the thesis and future perspectives

4.3.1 TRPA1 deficiency is protective in cuprizone-induced demyelination—A new target against oligodendrocyte apoptosis

MS is a chronic, inflammatory, degenerative and progressive disease of the CNS. Currently used immunomodulatory therapies are only able to counteract the inflammatory nature of the disease and these drugs have little efficacy on long term progression of clinical disabilities. Thus, adequate management of MS therapy requires new pharmacological targets to inhibit demyelination or promote CNS repair. In the present study we investigated the expression and possible role of TRPA1 in the cuprizone-induced experimental demyelination model. We show that TRPA1 is expressed on astrocytes in the mouse CNS under physiological conditions. Moreover, we demonstrate that the genetic deficiency of TRPA1 significantly attenuates the demyelination in cuprizone exposed animals by reducing the apoptosis of mature OLs. Based on our data, we propose that TRPA1 activation regulates MAPK signalling pathways and their downstream effectors that ultimately enhances the apoptosis of mature OLs. Additionally, this mechanism is possibly mediated through an interplay between TRPA1 activation to modify astrocyte functions. We conclude that inhibition of TRPA1 receptors might diminish the degenerative pathology of MS and could be a promising therapeutic target in the future.

4.3.2 Quantitative comparison of primary cilia marker expression and length in the mouse brain

Primary cilia are tiny antenna-like cellular appendages that provide important sensory and signalling functions in the mammalian organ systems, particularly in the CNS. In recent years, the clinical and biological relevance of these organelles gained increasing attention, which uncovered that primary cilia dysfunction may be the underlying cause of numerous human diseases such as congenital ciliopathies, certain types of CNS tumors or other neurological disorders. Although primary cilia are found to be widely distributed in the brain, the precise role of these organelles are just beginning to be understood. Notably, studies of the last decade have highlighted that functions of neuronal cilia are reflected by the signalling molecules enriched in the ciliary membrane, their morphology, and localization in the CNS. In the present study, we conducted a comparative and quantitative histopathological analysis of the expression pattern, distribution and length of primary cilia expressing AC3, Sstr3 as well as Arl13b in the adult mouse brain. We show that primary cilia of neurons and astrocytes display a well-characterised ciliary marker expression profile throughout the investigated brain regions. Additionally, quantitative comparison of their length, density and occurrence rate revealed

apparent differences among regulatory centres of the CNS, further indicating possible, yet unknown roles of primary cilia in brain functions. Overall, our study provides a comprehensive overview of the cellular organization and morphological traits of primary cilia in regions of the physiological adult mouse brain, which serves an important tool in understanding the role of these organelles in future experiments. Additionally, considering the genetic aetiology of numerous human neurodegenerative diseases, the characterization of dysfunctional primary cilia on post- mortem human brain tissues might provide a different aspect of understanding disease pathogenesis and may open novel therapeutic avenues for clinical management of neurological disorders such as Parkinson’s disease or Multiple Sclerosis.

5. REFERENCES

Acs, P., & Kalman, B. (2012). Pathogenesis of multiple sclerosis: what can we learn from the cuprizone model. *Methods Mol Biol, 900*, 403-431. doi: 10.1007/978-1-60761-720-4_20

Acs, P., Kipp, M., Norkute, A., Johann, S., Clarner, T., Braun, A., . . . Beyer, C. (2009). 17beta-estradiol and progesterone prevent cuprizone provoked demyelination of corpus callosum in male mice. *Glia, 57*(8), 807-814. doi: 10.1002/glia.20806

Acs, P., & Komoly, S. (2012). Selective ultrastructural vulnerability in the cuprizone-induced experimental demyelination. *Ideggyogy Sz, 65*(7-8), 266-270.

Acs, P., Selak, M. A., Komoly, S., & Kalman, B. (2013). Distribution of oligodendrocyte loss and mitochondrial toxicity in the cuprizone-induced experimental demyelination model. *J Neuroimmunol, 262*(1-2), 128-131. doi: 10.1016/j.jneuroim.2013.06.012

Alvarez-Satta, M., Castro-Sanchez, S., & Valverde, D. (2015). Alstrom syndrome: current perspectives. *Appl Clin Genet, 8*, 171-179. doi: 10.2147/tacg.s56612

Alvarez-Satta, M., Moreno-Cugnon, L., & Matheu, A. (2019). Primary cilium and brain aging: role in neural stem cells, neurodegenerative diseases and glioblastoma. *Ageing Res Rev, 52*, 53-63. doi: 10.1016/j.arr.2019.04.004

Amador-Arjona, A., Elliott, J., Miller, A., Ginbey, A., Pazour, G. J., Enikolopov, G., . . . Terskikh, A. V. (2011). Primary cilia regulate proliferation of amplifying progenitors in adult hippocampus: implications for learning and memory. *J Neurosci, 31*(27), 9933-9944. doi: 10.1523/jneurosci.1062-11.2011

Amor, S., O'Neill, J. K., Morris, M. M., Smith, R. M., Wraith, D. C., Groome, N., . . . Baker, D. (1996). Encephalitogenic epitopes of myelin basic protein, proteolipid protein, myelin oligodendrocyte glycoprotein for experimental allergic encephalomyelitis induction in Biozzi ABH (H-2Ag7) mice share an amino acid motif. *J Immunol, 156*(8), 3000-3008.

Andersson, D. A., Gentry, C., Moss, S., & Bevan, S. (2008). Transient receptor potential A1 is a sensory receptor for multiple products of oxidative stress. *J Neurosci, 28*(10), 2485-2494. doi: 10.1523/jneurosci.5369-07.2008

Armato, U., Chakravarthy, B., Pacchiana, R., & Whitfield, J. F. (2013). Alzheimer's disease: an update of the roles of receptors, astrocytes and primary cilia (review). *Int J Mol Med, 31*(1), 3-10. doi: 10.3892/ijmm.2012.1162

Armstrong, R. C., Le, T. Q., Frost, E. E., Borke, R. C., & Vana, A. C. (2002). Absence of fibroblast growth factor 2 promotes oligodendroglial repopulation of demyelinated white matter. *J Neurosci, 22*(19), 8574-8585.

Ascherio, A., & Munger, K. L. (2010). Epstein-barr virus infection and multiple sclerosis: a review. *J Neuroimmune Pharmacol, 5*(3), 271-277. doi: 10.1007/s11481-010-9201-3

Ascherio, A., & Munger, K. L. (2016). Epidemiology of Multiple Sclerosis: From Risk Factors to Prevention-An Update. *Semin Neurol, 36*(2), 103-114. doi: 10.1055/s-0036-1579693

Avidor-Reiss, T., & Leroux, M. R. (2015). Shared and Distinct Mechanisms of Compartmentalized and Cytosolic Ciliogenesis. *Curr Biol, 25*(23), R1143-1150. doi: 10.1016/j.cub.2015.11.001

Ayuso, T., Aznar, P., Soriano, L., Olaskoaga, A., Roldan, M., Otano, M., . . . Mendioroz, M. (2017). Vitamin D receptor gene is epigenetically altered and transcriptionally up-regulated in multiple sclerosis. *PLoS One, 12*(3), e0174726. doi: 10.1371/journal.pone.0174726

Badano, J. L., Mitsuma, N., Beales, P. L., & Katsanis, N. (2006). The Ciliopathies: An Emerging Class of Human Genetic Disorders. *Annual Review of Genomics and Human Genetics, 7*(1), 125-148. doi: 10.1146/annurev.genom.7.080505.115610

Bae, J. E., Kang, G. M., Min, S. H., Jo, D. S., Jung, Y. K., Kim, K., & Kim, M. S. (2019). Primary cilia mediate mitochondrial stress responses to promote dopamine neuron survival in a Parkinson's disease model. *10*(12), 952. doi: 10.1038/s41419-019-2184-y

Bandell, M., Story, G. M., Hwang, S. W., Viswanath, V., Eid, S. R., Petrus, M. J., . . . Patapoutian, A. (2004). Noxious cold ion channel TRPA1 is activated by pungent compounds and bradykinin. *Neuron, 41*(6), 849-857.

Bang, S., & Hwang, S. W. (2009). Polymodal ligand sensitivity of TRPA1 and its modes of interactions. *J Gen Physiol, 133*(3), 257-262. doi: 10.1085/jgp.200810138

Bangs, F., & Anderson, K. V. (2017). Primary Cilia and Mammalian Hedgehog Signaling. *Cold Spring Harb Perspect Biol, 9*(5). doi: 10.1101/cshperspect.a028175

Barker, A. R., Thomas, R., & Dawe, H. R. (2014). Meckel-Gruber syndrome and the role of primary cilia in kidney, skeleton, and central nervous system development. *Organogenesis, 10*(1), 96-107. doi: 10.4161/org.27375

Barnett, M. H., & Prineas, J. W. (2004). Relapsing and remitting multiple sclerosis: pathology of the newly forming lesion. *Ann Neurol, 55*(4), 458-468. doi: 10.1002/ana.20016

Barnett, M. H., & Sutton, I. (2006). The pathology of multiple sclerosis: a paradigm shift. *Curr Opin Neurol, 19*(3), 242-247. doi: 10.1097/01.wco.0000227032.47458.cb

Bartholomaus, I., Kawakami, N., Odoardi, F., Schlager, C., Miljkovic, D., Ellwart, J. W., . . . Flugel, A. (2009). Effector T cell interactions with meningeal vascular structures in nascent autoimmune CNS lesions. *Nature, 462*(7269), 94-98. doi: 10.1038/nature08478

Basso, A. S., Frenkel, D., Quintana, F. J., Costa-Pinto, F. A., Petrovic-Stojkovic, S., Puckett, L., . . . Weiner, H. L. (2008). Reversal of axonal loss and disability in a mouse model of progressive multiple sclerosis. *J Clin Invest, 118*(4), 1532-1543. doi: 10.1172/jci33464

Basten, S. G., & Giles, R. H. (2013). Functional aspects of primary cilia in signaling, cell cycle and tumorigenesis. *Cilia, 2*(1), 6. doi: 10.1186/2046-2530-2-6

Bautista, D. M., Jordt, S. E., Nikai, T., Tsuruda, P. R., Read, A. J., Poblete, J., . . . Julius, D. (2006). TRPA1 mediates the inflammatory actions of environmental irritants and proalgesic agents. *Cell, 124*(6), 1269-1282. doi: 10.1016/j.cell.2006.02.023

Bautista, D. M., Movahed, P., Hinman, A., Axelsson, H. E., Sterner, O., Hogestatt, E. D., . . . Zygmunt, P. M. (2005). Pungent products from garlic activate the sensory ion channel TRPA1. *Proc Natl Acad Sci U S A, 102*(34), 12248-12252. doi: 10.1073/pnas.0505356102

Bautista, D. M., Pellegrino, M., & Tsunozaki, M. (2013). TRPA1: A gatekeeper for inflammation. *Annu Rev Physiol, 75*, 181-200. doi: 10.1146/annurev-physiol-030212-183811

Benardais, K., Kotsiari, A., Skuljec, J., Koutsoudaki, P. N., Gudi, V., Singh, V., . . . Stangel, M. (2013). Cuprizone [bis(cyclohexylidenehydrazide)] is selectively toxic for mature oligodendrocytes. *Neurotox Res, 24*(2), 244-250. doi: 10.1007/s12640-013-9380-9

Bender, S. J., & Weiss, S. R. (2010). Pathogenesis of murine coronavirus in the central nervous system. *J Neuroimmune Pharmacol, 5*(3), 336-354. doi: 10.1007/s11481-010-9202-2

Berard, J. L., Wolak, K., Fournier, S., & David, S. (2010). Characterization of relapsing-remitting and chronic forms of experimental autoimmune encephalomyelitis in C57BL/6 mice. *Glia, 58*(4), 434-445. doi: 10.1002/glia.20935

Berbari, N. F., Bishop, G. A., Askwith, C. C., Lewis, J. S., & Mykytyn, K. (2007). Hippocampal neurons possess primary cilia in culture. *J Neurosci Res, 85*(5), 1095-1100. doi: 10.1002/jnr.21209

Berbari, N. F., Johnson, A. D., Lewis, J. S., Askwith, C. C., & Mykytyn, K. (2008). Identification of ciliary localization sequences within the third intracellular loop of G protein-coupled receptors. *Mol Biol Cell, 19*(4), 1540-1547. doi: 10.1091/mbc.E07-09-0942

Berbari, N. F., Lewis, J. S., Bishop, G. A., Askwith, C. C., & Mykytyn, K. (2008). Bardet-Biedl syndrome proteins are required for the localization of G protein-coupled receptors to primary cilia. *Proc Natl Acad Sci U S A, 105*(11), 4242-4246. doi: 10.1073/pnas.0711027105

Berbari, N. F., Pasek, R. C., Malarkey, E. B., Yazdi, S. M., McNair, A. D., Lewis, W. R., . . . Yoder, B. K. (2013). Leptin resistance is a secondary consequence of the obesity in ciliopathy mutant mice. *Proc Natl Acad Sci U S A, 110*(19), 7796-7801. doi: 10.1073/pnas.1210192110

Berghoff, S. A., Gerndt, N., Winchenbach, J., Stumpf, S. K., Hosang, L., Odoardi, F., . . . Saher, G. (2017). Dietary cholesterol promotes repair of demyelinated lesions in the adult brain. *Nat Commun, 8*, 14241. doi: 10.1038/ncomms14241

Bettelli, E., Baeten, D., Jager, A., Sobel, R. A., & Kuchroo, V. K. (2006). Myelin oligodendrocyte glycoprotein-specific T and B cells cooperate to induce a Devic-like disease in mice. *J Clin Invest, 116*(9), 2393-2402. doi: 10.1172/jci28334

Bettelli, E., Pagany, M., Weiner, H. L., Linington, C., Sobel, R. A., & Kuchroo, V. K. (2003). Myelin oligodendrocyte glycoprotein-specific T cell receptor transgenic mice develop spontaneous autoimmune optic neuritis. *J Exp Med, 197*(9), 1073-1081. doi: 10.1084/jem.20021603

Bieber, A. J., Ure, D. R., & Rodriguez, M. (2005). Genetically dominant spinal cord repair in a murine model of chronic progressive multiple sclerosis. *J Neuropathol Exp Neurol, 64*(1), 46-57.

Billiau, A., & Matthys, P. (2001). Modes of action of Freund's adjuvants in experimental models of autoimmune diseases. *J Leukoc Biol, 70*(6), 849-860.

Bishop, G. A., Berbari, N. F., Lewis, J., & Mykytyn, K. (2007). Type III adenylyl cyclase localizes to primary cilia throughout the adult mouse brain. *J Comp Neurol, 505*(5), 562-571. doi: 10.1002/cne.21510

Bitsch, A., Schuchardt, J., Bunkowski, S., Kuhlmann, T., & Bruck, W. (2000). Acute axonal injury in multiple sclerosis. Correlation with demyelination and inflammation. *Brain, 123 (Pt 6)*, 1174-1183.

Bittner, S., Afzali, A. M., Wiendl, H., & Meuth, S. G. (2014). Myelin oligodendrocyte glycoprotein (MOG35-55) induced experimental autoimmune encephalomyelitis (EAE) in C57BL/6 mice. *J Vis Exp*(86). doi: 10.3791/51275

Blakemore, W. F. (1972). Observations on oligodendrocyte degeneration, the resolution of status spongiosus and remyelination in cuprizone intoxication in mice. *J Neurocytol, 1*(4), 413-426.

Blakemore, W. F. (1982). Ethidium bromide induced demyelination in the spinal cord of the cat. *Neuropathol Appl Neurobiol, 8*(5), 365-375.

Bleau, C., Filliol, A., Samson, M., & Lamontagne, L. (2015). Brain Invasion by Mouse Hepatitis Virus Depends on Impairment of Tight Junctions and Beta Interferon Production in Brain Microvascular Endothelial Cells. *J Virol, 89*(19), 9896-9908. doi: 10.1128/jvi.01501-15

Bo, L., Vedeler, C. A., Nyland, H. I., Trapp, B. D., & Mork, S. J. (2003). Subpial demyelination in the cerebral cortex of multiple sclerosis patients. *J Neuropathol Exp Neurol, 62*(7), 723-732. doi: 10.1093/jnen/62.7.723

Brailov, I., Bancila, M., Brisorgueil, M. J., Miquel, M. C., Hamon, M., & Verge, D. (2000). Localization of 5-HT(6) receptors at the plasma membrane of neuronal cilia in the rat brain. *Brain Res, 872*(1-2), 271-275. doi: 10.1016/s0006-8993(00)02519-1

Bramow, S., Frischer, J. M., Lassmann, H., Koch-Henriksen, N., Lucchinetti, C. F., Sørensen, P. S., & Laursen, H. (2010). Demyelination versus remyelination in progressive multiple sclerosis. *Brain, 133*(10), 2983-2998. doi: 10.1093/brain/awq250

Brazeau, P., Vale, W., Burgus, R., Ling, N., Butcher, M., Rivier, J., & Guillemin, R. (1973). Hypothalamic Polypeptide That Inhibits the Secretion of Immunoreactive Pituitary Growth Hormone. *Science, 179*(4068), 77-79. doi: 10.1126/science.179.4068.77

Breunig, J. J., Sarkisian, M. R., Arellano, J. I., Morozov, Y. M., Ayoub, A. E., Sojitra, S., . . . Town, T. (2008). Primary cilia regulate hippocampal neurogenesis by mediating sonic hedgehog signaling. *Proc Natl Acad Sci U S A, 105*(35), 13127-13132. doi: 10.1073/pnas.0804558105

Brombin, C., & Di Serio, C. (2016). Evaluating treatment effect within a multivariate stochastic ordering framework: Nonparametric combination methodology applied to a study on multiple sclerosis. *Stat Methods Med Res, 25*(1), 366-384. doi: 10.1177/0962280212454203

Brownell, B., & Hughes, J. T. (1962). The distribution of plaques in the cerebrum in multiple sclerosis. *J Neurol Neurosurg Psychiatry, 25*, 315-320. doi: 10.1136/jnnp.25.4.315

Burton, J. M., O'Connor, P. W., Hohol, M., & Beyene, J. (2009). Oral versus intravenous steroids for treatment of relapses in multiple sclerosis. *Cochrane Database Syst Rev*(3), Cd006921. doi: 10.1002/14651858.CD006921.pub2

Campbell, G. R., Ziabreva, I., Reeve, A. K., Krishnan, K. J., Reynolds, R., Howell, O., . . . Mahad, D. J. (2011). Mitochondrial DNA deletions and neurodegeneration in multiple sclerosis. *Ann Neurol, 69*(3), 481-492. doi: 10.1002/ana.22109

Canterini, S., Dragotto, J., Dardis, A., Zampieri, S., De Stefano, M. E., Mangia, F., . . . Fiorenza, M. T. (2017). Shortened primary cilium length and dysregulated Sonic hedgehog signaling in Niemann-Pick C1 disease. *Hum Mol Genet, 26*(12), 2277-2289. doi: 10.1093/hmg/ddx118

Canto, E., & Oksenberg, J. R. (2018). Multiple sclerosis genetics. *Multiple Sclerosis Journal, 24*(1), 75-79. doi: 10.1177/1352458517737371

Capone, F., Capone, G., Motolese, F., Voci, A., Caminiti, M. L., Musumeci, G., & Di Lazzaro, V. (2019). Spinal cord dysfunction contributes to balance impairment in multiple sclerosis patients. *Clin Neurol Neurosurg, 184*, 105451. doi: 10.1016/j.clineuro.2019.105451

Carrieri, P. B., Provitera, V., De Rosa, T., Tartaglia, G., Gorga, F., & Perrella, O. (1998). Profile of cerebrospinal fluid and serum cytokines in patients with relapsing-remitting multiple sclerosis: a correlation with clinical activity. *Immunopharmacol Immunotoxicol, 20*(3), 373-382. doi: 10.3109/08923979809034820

Caspary, T., Larkins, C. E., & Anderson, K. V. (2007). The graded response to Sonic Hedgehog depends on cilia architecture. *Dev Cell, 12*(5), 767-778. doi: 10.1016/j.devcel.2007.03.004

Cevik, S., Hori, Y., Kaplan, O. I., Kida, K., Toivenon, T., Foley-Fisher, C., . . . Blacque, O. E. (2010). Joubert syndrome Arl13b functions at ciliary membranes and stabilizes protein transport in Caenorhabditis elegans. *Journal of Cell Biology, 188*(6), 953-969. doi: 10.1083/jcb.200908133

Chakravarthy, B., Gaudet, C., Menard, M., Atkinson, T., Chiarini, A., Dal Pra, I., & Whitfield, J. (2010). The p75 neurotrophin receptor is localized to primary cilia in adult murine hippocampal dentate gyrus granule cells. *Biochem Biophys Res Commun, 401*(3), 458-462. doi: 10.1016/j.bbrc.2010.09.081

Chakravarthy, B., Gaudet, C., Menard, M., Brown, L., Atkinson, T., Laferla, F. M., . . . Whitfield, J. (2012). Reduction of the immunostainable length of the hippocampal dentate granule cells' primary cilia in 3xAD-transgenic mice producing human Abeta(1-42) and tau. *Biochem Biophys Res Commun, 427*(1), 218-222. doi: 10.1016/j.bbrc.2012.09.056

Challis, Rosemary C., Tian, H., Wang, J., He, J., Jiang, J., Chen, X., . . . Ma, M. (2015). An Olfactory Cilia Pattern in the Mammalian Nose Ensures High Sensitivity to Odors. *Current Biology, 25*(19), 2503-2512. doi: 10.1016/j.cub.2015.07.065

Chang, A., Tourtellotte, W. W., Rudick, R., & Trapp, B. D. (2002). Premyelinating oligodendrocytes in chronic lesions of multiple sclerosis. *N Engl J Med, 346*(3), 165-173. doi: 10.1056/NEJMoa010994

Chang, L., & Karin, M. (2001). Mammalian MAP kinase signalling cascades. *Nature, 410*(6824), 37-40. doi: 10.1038/35065000

Chen, X., Luo, J., Leng, Y., Yang, Y., Zweifel, L. S., Palmiter, R. D., & Storm, D. R. (2016). Ablation of Type III Adenylyl Cyclase in Mice Causes Reduced Neuronal Activity, Altered Sleep Pattern, and Depression-like Phenotypes. *Biological Psychiatry, 80*(11), 836-848. doi: 10.1016/j.biopsych.2015.12.012

Chen, X., Winkler-Pickett, R. T., Carbonetti, N. H., Ortaldo, J. R., Oppenheim, J. J., & Howard, O. M. (2006). Pertussis toxin as an adjuvant suppresses the number and function of CD4+CD25+ T regulatory cells. *Eur J Immunol, 36*(3), 671-680. doi: 10.1002/eji.200535353

Cheng, E. H., Wei, M. C., Weiler, S., Flavell, R. A., Mak, T. W., Lindsten, T., & Korsmeyer, S. J. (2001). BCL-2, BCL-X(L) sequester BH3 domain-only molecules preventing BAX- and BAK-mediated mitochondrial apoptosis. *Mol Cell, 8*(3), 705-711.

Citterio, A., La Mantia, L., Ciucci, G., Candelise, L., Brusaferri, F., Midgard, R., & Filippini, G. (2000). Corticosteroids or ACTH for acute exacerbations in multiple sclerosis. *Cochrane Database of Systematic Reviews*(4). doi: 10.1002/14651858.CD001331

Clapham, D. E., Runnels, L. W., & Strubing, C. (2001). The TRP ion channel family. *Nat Rev Neurosci, 2*(6), 387-396. doi: 10.1038/35077544

Coghe, G., & Corona, F. (2019). Is There Any Relationship between Upper and Lower Limb Impairments in People with Multiple Sclerosis? A Kinematic Quantitative Analysis. *2019*, 9149201. doi: 10.1155/2019/9149201

Compston, D. A., Batchelor, J. R., & McDonald, W. I. (1976). B-lymphocyte alloantigens associated with multiple sclerosis. *Lancet, 2*(7998), 1261-1265.

Cowley, T. J., & Weiss, S. R. (2010). Murine coronavirus neuropathogenesis: determinants of virulence. *J Neurovirol, 16*(6), 427-434. doi: 10.3109/13550284.2010.529238

Crocker, S. J., Lamba, W. R., Smith, P. D., Callaghan, S. M., Slack, R. S., Anisman, H., & Park, D. S. (2001). c-Jun mediates axotomy-induced dopamine neuron death in vivo. *Proc Natl Acad Sci U S A, 98*(23), 13385-13390. doi: 10.1073/pnas.231177098

Cross, M., & Dexter, T. M. (1991). Growth factors in development, transformation, and tumorigenesis. *Cell, 64*(2), 271-280. doi: 10.1016/0092-8674(91)90638-f

Cruz-Orengo, L., Dhaka, A., Heuermann, R. J., Young, T. J., Montana, M. C., Cavanaugh, E. J., . . . Story, G. M. (2008). Cutaneous nociception evoked by 15-delta PGJ2 via activation of ion channel TRPA1. *Mol Pain, 4*, 30. doi: 10.1186/1744-8069-4-30

D'Souza-Schorey, C., & Chavrier, P. (2006). ARF proteins: roles in membrane traffic and beyond. *Nature Reviews Molecular Cell Biology, 7*(5), 347-358. doi: 10.1038/nrm1910

Dandekar, A. A., Anghelina, D., & Perlman, S. (2004). Bystander CD8 T-cell-mediated demyelination is interferon-gamma-dependent in a coronavirus model of multiple sclerosis. *Am J Pathol, 164*(2), 363-369.

Dandekar, A. A., Wu, G. F., Pewe, L., & Perlman, S. (2001). Axonal damage is T cell mediated and occurs concomitantly with demyelination in mice infected with a neurotropic coronavirus. *J Virol, 75*(13), 6115-6120. doi: 10.1128/jvi.75.13.6115-6120.2001

Danilov, A. I., Gomes-Leal, W., Ahlenius, H., Kokaia, Z., Carlemalm, E., & Lindvall, O. (2009). Ultrastructural and antigenic properties of neural stem cells and their progeny in adult rat subventricular zone. *Glia, 57*(2), 136-152. doi: 10.1002/glia.20741

Das Sarma, J., Kenyon, L. C., Hingley, S. T., & Shindler, K. S. (2009). Mechanisms of primary axonal damage in a viral model of multiple sclerosis. *J Neurosci, 29*(33), 10272-10280. doi: 10.1523/jneurosci.1975-09.2009

Davenport, J. R., Watts, A. J., Roper, V. C., Croyle, M. J., van Groen, T., Wyss, J. M., . . . Yoder, B. K. (2007). Disruption of Intraflagellar Transport in Adult Mice Leads to Obesity and Slow-Onset Cystic Kidney Disease. *Current Biology, 17*(18), 1586-1594. doi: 10.1016/j.cub.2007.08.034

De Angelis, F., John, N. A., & Brownlee, W. J. (2018). Disease-modifying therapies for multiple sclerosis. *Bmj, 363*, k4674. doi: 10.1136/bmj.k4674

DeBerry, J. J., Schwartz, E. S., & Davis, B. M. (2014). TRPA1 mediates bladder hyperalgesia in a mouse model of cystitis. *Pain, 155*(7), 1280-1287. doi: 10.1016/j.pain.2014.03.023

Degelman, M. L., & Herman, K. M. (2017). Smoking and multiple sclerosis: A systematic review and meta-analysis using the Bradford Hill criteria for causation. *Mult Scler Relat Disord, 17*, 207-216. doi: 10.1016/j.msard.2017.07.020

Delgado, O., Batten, K. G., Richardson, J. A., Xie, X. J., Gazdar, A. F., Kaisani, A. A., . . . Shay, J. W. (2014). Radiation-enhanced lung cancer progression in a transgenic mouse model of lung cancer is predictive of outcomes in human lung and breast cancer. *Clin Cancer Res, 20*(6), 1610-1622. doi: 10.1158/1078-0432.CCR-13-2589

Dendrou, C. A., Fugger, L., & Friese, M. A. (2015). Immunopathology of multiple sclerosis. *Nat Rev Immunol, 15*(9), 545-558. doi: 10.1038/nri3871

Denic, A., Johnson, A. J., Bieber, A. J., Warrington, A. E., Rodriguez, M., & Pirko, I. (2011). The relevance of animal models in multiple sclerosis research. *Pathophysiology, 18*(1), 21-29. doi: 10.1016/j.pathophys.2010.04.004

Desjardins, P., Frost, E., & Morais, R. (1985). Ethidium bromide-induced loss of mitochondrial DNA from primary chicken embryo fibroblasts. *Mol Cell Biol, 5*(5), 1163-1169.

Dewson, G., Kratina, T., Czabotar, P., Day, C. L., Adams, J. M., & Kluck, R. M. (2009). Bak activation for apoptosis involves oligomerization of dimers via their alpha6 helices. *Mol Cell, 36*(4), 696-703. doi: 10.1016/j.molcel.2009.11.008

Dhekne, H. S., & Yanatori, I. (2018). A pathway for Parkinson's Disease LRRK2 kinase to block primary cilia and Sonic hedgehog signaling in the brain. *7*. doi: 10.7554/eLife.40202

Di Pietro, C., Marazziti, D., La Sala, G., Abbaszadeh, Z., Golini, E., Matteoni, R., & Tocchini-Valentini, G. P. (2017). Primary Cilia in the Murine Cerebellum and in Mutant Models of Medulloblastoma. *Cell Mol Neurobiol, 37*(1), 145-154. doi: 10.1007/s10571-016-0354-3

Doetsch, F., García-Verdugo, J. M., & Alvarez-Buylla, A. (1999). Regeneration of a germinal layer in the adult mammalian brain. *Proceedings of the National Academy of Sciences, 96*(20), 11619-11624. doi: 10.1073/pnas.96.20.11619

Domercq, M., Alberdi, E., Sanchez-Gomez, M. V., Ariz, U., Perez-Samartin, A., & Matute, C. (2011). Dual-specific phosphatase-6 (Dusp6) and ERK mediate AMPA receptor-induced oligodendrocyte death. *J Biol Chem, 286*(13), 11825-11836. doi: 10.1074/jbc.M110.153049

Domire, J. S., Green, J. A., Lee, K. G., Johnson, A. D., Askwith, C. C., & Mykytyn, K. (2011). Dopamine receptor 1 localizes to neuronal cilia in a dynamic process that requires the Bardet-Biedl syndrome proteins. *Cellular and Molecular Life Sciences, 68*(17), 2951-2960. doi: 10.1007/s00018-010-0603-4

Dumas, A., Amiable, N., de Rivero Vaccari, J. P., Chae, J. J., Keane, R. W., Lacroix, S., & Vallieres, L. (2014). The inflammasome pyrin contributes to pertussis toxin-induced IL-1beta synthesis, neutrophil intravascular crawling and autoimmune encephalomyelitis. *PLoS Pathog, 10*(5), e1004150. doi: 10.1371/journal.ppat.1004150

Dummer, A., Poelma, C., DeRuiter, M. C., Goumans, M.-J. T. H., & Hierck, B. P. (2016). Measuring the primary cilium length: improved method for unbiased high-throughput analysis. *Cilia, 5*(1), 7. doi: 10.1186/s13630-016-0028-2

Einstein, E. B., Patterson, C. A., Hon, B. J., Regan, K. A., Reddi, J., Melnikoff, D. E., . . . Tallent, M. K. (2010). Somatostatin Signaling in Neuronal Cilia Is Criticalfor Object Recognition Memory. *The Journal of Neuroscience, 30*(12), 4306-4314. doi: 10.1523/jneurosci.5295-09.2010

Ellmerich, S., Takacs, K., Mycko, M., Waldner, H., Wahid, F., Boyton, R. J., . . . Altmann, D. M. (2004). Disease-related epitope spread in a humanized T cell receptor transgenic model of multiple sclerosis. *Eur J Immunol, 34*(7), 1839-1848. doi: 10.1002/eji.200324044

Engel, M. A., Leffler, A., Niedermirtl, F., Babes, A., Zimmermann, K., Filipovic, M. R., . . . Reeh, P. W. (2011). TRPA1 and substance P mediate colitis in mice. *Gastroenterology, 141*(4), 1346-1358. doi: 10.1053/j.gastro.2011.07.002

Evangelou, N., Konz, D., Esiri, M. M., Smith, S., Palace, J., & Matthews, P. M. (2000). Regional axonal loss in the corpus callosum correlates with cerebral white matter lesion volume and distribution in multiple sclerosis. *Brain, 123 (Pt 9)*, 1845-1849. doi: 10.1093/brain/123.9.1845

Fabbri, L., Bost, F., & Mazure, N. M. (2019). Primary Cilium in Cancer Hallmarks. *Int J Mol Sci, 20*(6), 1336. doi: 10.3390/ijms20061336

Faissner, S., & Gold, R. (2018). Efficacy and Safety of the Newer Multiple Sclerosis Drugs Approved Since 2010. *CNS Drugs, 32*(3), 269-287. doi: 10.1007/s40263-018-0488-6

Faissner, S., & Gold, R. (2019). Progressive multiple sclerosis: latest therapeutic developments and future directions. *Ther Adv Neurol Disord, 12*, 1756286419878323. doi: 10.1177/1756286419878323

Fischer, M. T., Sharma, R., Lim, J. L., Haider, L., Frischer, J. M., Drexhage, J., . . . Lassmann, H. (2012). NADPH oxidase expression in active multiple sclerosis lesions in relation to oxidative tissue damage and mitochondrial injury. *Brain, 135*(Pt 3), 886-899. doi: 10.1093/brain/aws012

Fischer, M. T., Wimmer, I., Hoftberger, R., Gerlach, S., Haider, L., Zrzavy, T., . . . Lassmann, H. (2013). Disease-specific molecular events in cortical multiple sclerosis lesions. *Brain, 136*(Pt 6), 1799-1815. doi: 10.1093/brain/awt110

Fletcher, J. M., Lalor, S. J., Sweeney, C. M., Tubridy, N., & Mills, K. H. (2010). T cells in multiple sclerosis and experimental autoimmune encephalomyelitis. *Clin Exp Immunol, 162*(1), 1-11. doi: 10.1111/j.1365-2249.2010.04143.x

Flugel, A., Berkowicz, T., Ritter, T., Labeur, M., Jenne, D. E., Li, Z., . . . Wekerle, H. (2001). Migratory activity and functional changes of green fluorescent effector cells before and during experimental autoimmune encephalomyelitis. *Immunity, 14*(5), 547-560.

FOG, T. (1950). TOPOGRAPHIC DISTRIBUTION OF PLAQUES IN THE SPINAL CORD IN MULTIPLE SCLEROSIS. *Archives of Neurology & Psychiatry, 63*(3), 382-414. doi: 10.1001/archneurpsyc.1950.02310210028003

Forsythe, E., & Beales, P. L. (2013). Bardet–Biedl syndrome. *European Journal of Human Genetics, 21*(1), 8-13. doi: 10.1038/ejhg.2012.115

Forsythe, E., Kenny, J., Bacchelli, C., & Beales, P. L. (2018). Managing Bardet–Biedl Syndrome—Now and in the Future. *Frontiers in Pediatrics, 6*(23). doi: 10.3389/fped.2018.00023

Franklin, K. B. J., & Paxinos, G. (2008). *The mouse brain : in stereotaxic coordinates. Compact third edition*. New York [etc.]: Academic Press.

Frischer, J. M., Bramow, S., Dal-Bianco, A., Lucchinetti, C. F., Rauschka, H., Schmidbauer, M., . . . Lassmann, H. (2009). The relation between inflammation and neurodegeneration in multiple sclerosis brains. *Brain, 132*(Pt 5), 1175-1189. doi: 10.1093/brain/awp070

Fry, A. M., Leaper, M. J., & Bayliss, R. (2014). The primary cilium. *Organogenesis, 10*(1), 62-68. doi: 10.4161/org.28910

Garcia, G., 3rd, Raleigh, D. R., & Reiter, J. F. (2018). How the Ciliary Membrane Is Organized Inside-Out to Communicate Outside-In. *Curr Biol, 28*(8), R421-r434. doi: 10.1016/j.cub.2018.03.010

Garg, N., & Smith, T. W. (2015). An update on immunopathogenesis, diagnosis, and treatment of multiple sclerosis. *Brain Behav, 5*(9), e00362. doi: 10.1002/brb3.362

Gerdes, J. M., Davis, E. E., & Katsanis, N. (2009). The Vertebrate Primary Cilium in Development, Homeostasis, and Disease. *Cell, 137*(1), 32-45. doi: 10.1016/j.cell.2009.03.023

Ghezzi, A. (2018). European and American Guidelines for Multiple Sclerosis Treatment. *Neurol Ther, 7*(2), 189-194. doi: 10.1007/s40120-018-0112-1

Gillingham, A. K., & Munro, S. (2007). The small G proteins of the Arf family and their regulators. *Annu Rev Cell Dev Biol, 23*, 579-611. doi: 10.1146/annurev.cellbio.23.090506.123209

Gold, R., Buttgereit, F., & Toyka, K. V. (2001). Mechanism of action of glucocorticosteroid hormones: possible implications for therapy of neuroimmunological disorders. *J Neuroimmunol, 117*(1-2), 1-8. doi: 10.1016/s0165-5728(01)00330-7

Goldenberg, M. M. (2012). Multiple sclerosis review. *P t, 37*(3), 175-184.

Gomez, O., Sanchez-Rodriguez, A., Le, M., Sanchez-Caro, C., Molina-Holgado, F., & Molina-Holgado, E. (2011). Cannabinoid receptor agonists modulate oligodendrocyte differentiation by activating PI3K/Akt and the mammalian target of rapamycin (mTOR) pathways. *Br J Pharmacol, 163*(7), 1520-1532. doi: 10.1111/j.1476-5381.2011.01414.x

Goncalves, J., & Pelletier, L. (2017). The Ciliary Transition Zone: Finding the Pieces and Assembling the Gate. *Mol Cells, 40*(4), 243-253. doi: 10.14348/molcells.2017.0054

Göbel, K., Ruck, T., & Meuth, S. G. (2018). Cytokine signaling in multiple sclerosis: Lost in translation. *Multiple Sclerosis Journal, 24*(4), 432-439. doi: 10.1177/1352458518763094

Grace, M. S., Baxter, M., Dubuis, E., Birrell, M. A., & Belvisi, M. G. (2014). Transient receptor potential (TRP) channels in the airway: role in airway disease. *Br J Pharmacol, 171*(10), 2593-2607. doi: 10.1111/bph.12538

Green, A. J., McQuaid, S., Hauser, S. L., Allen, I. V., & Lyness, R. (2010). Ocular pathology in multiple sclerosis: retinal atrophy and inflammation irrespective of disease duration. *Brain, 133*(6), 1591-1601. doi: 10.1093/brain/awq080

Green, J. A., Schmid, C. L., Bley, E., Monsma, P. C., Brown, A., Bohn, L. M., & Mykytyn, K. (2016). Recruitment of β-Arrestin into Neuronal Cilia Modulates Somatostatin Receptor Subtype 3 Ciliary Localization. *Mol Cell Biol, 36*(1), 223-235. doi: 10.1128/mcb.00765-15

Gregory, S. G., Schmidt, S., Seth, P., Oksenberg, J. R., Hart, J., Prokop, A., . . . Multiple Sclerosis Genetics, G. (2007). Interleukin 7 receptor alpha chain (IL7R) shows allelic and functional association with multiple sclerosis. *Nat Genet, 39*(9), 1083-1091. doi: 10.1038/ng2103

Grigoriadis, N., & van Pesch, V. (2015). A basic overview of multiple sclerosis immunopathology. *Eur J Neurol, 22 Suppl 2*, 3-13. doi: 10.1111/ene.12798

Grochowsky, A., & Gunay-Aygun, M. (2019). Clinical characteristics of individual organ system disease in non-motile ciliopathies. *Transl Sci Rare Dis, 4*(1-2), 1-23. doi: 10.3233/trd-190033

Guadiana, S. M., Semple-Rowland, S., Daroszewski, D., Madorsky, I., Breunig, J. J., Mykytyn, K., & Sarkisian, M. R. (2013). Arborization of Dendrites by Developing Neocortical Neurons Is Dependent on Primary

Cilia and Type 3 Adenylyl Cyclase. *The Journal of Neuroscience, 33*(6), 2626-2638. doi: 10.1523/jneurosci.2906-12.2013

Gudi, V., Gingele, S., Skripuletz, T., & Stangel, M. (2014). Glial response during cuprizone-induced de- and remyelination in the CNS: lessons learned. *Front Cell Neurosci, 8*, 73. doi: 10.3389/fncel.2014.00073

Gudi, V., Moharregh-Khiabani, D., Skripuletz, T., Koutsoudaki, P. N., Kotsiari, A., Skuljec, J., . . . Stangel, M. (2009). Regional differences between grey and white matter in cuprizone induced demyelination. *Brain Res, 1283*, 127-138. doi: 10.1016/j.brainres.2009.06.005

Gudi, V., Skuljec, J., Yildiz, O., Frichert, K., Skripuletz, T., Moharregh-Khiabani, D., . . . Stangel, M. (2011). Spatial and temporal profiles of growth factor expression during CNS demyelination reveal the dynamics of repair priming. *PLoS One, 6*(7), e22623. doi: 10.1371/journal.pone.0022623

Hackett, A. R., Lee, D. H., Dawood, A., Rodriguez, M., Funk, L., Tsoulfas, P., & Lee, J. K. (2016). STAT3 and SOCS3 regulate NG2 cell proliferation and differentiation after contusive spinal cord injury. *Neurobiol Dis, 89*, 10-22. doi: 10.1016/j.nbd.2016.01.017

Haider, L., Simeonidou, C., Steinberger, G., Hametner, S., Grigoriadis, N., Deretzi, G., . . . Frischer, J. M. (2014). Multiple sclerosis deep grey matter: the relation between demyelination, neurodegeneration, inflammation and iron. *J Neurol Neurosurg Psychiatry, 85*(12), 1386-1395. doi: 10.1136/jnnp-2014-307712

Haider, L., Zrzavy, T., Hametner, S., Hoftberger, R., Bagnato, F., Grabner, G., . . . Lassmann, H. (2016). The topograpy of demyelination and neurodegeneration in the multiple sclerosis brain. *Brain, 139*(Pt 3), 807-815. doi: 10.1093/brain/awv398

Hall, S. M. (1972). The effect of injections of lysophosphatidyl choline into white matter of the adult mouse spinal cord. *J Cell Sci, 10*(2), 535-546.

Hamilton, N. B., Kolodziejczyk, K., Kougioumtzidou, E., & Attwell, D. (2016). Proton-gated Ca(2+)-permeable TRP channels damage myelin in conditions mimicking ischaemia. *Nature, 529*(7587), 523-527. doi: 10.1038/nature16519

Hamon, M., Doucet, E., Lefèvre, K., Miquel, M.-C., Lanfumey, L., Insausti, R., . . . Vergé, D. (1999). Antibodies and Antisense Oligonucleotide for Probing the Distribution and Putative Functions of Central 5-HT6Receptors. *Neuropsychopharmacology, 21*(1), 68-76. doi: 10.1016/S0893-133X(99)00044-5

Han, Y.-G., Kim, H. J., Dlugosz, A. A., Ellison, D. W., Gilbertson, R. J., & Alvarez-Buylla, A. (2009). Dual and opposing roles of primary cilia in medulloblastoma development. *Nat Med, 15*(9), 1062-1065. doi: 10.1038/nm.2020

Han, Y.-G., Spassky, N., Romaguera-Ros, M., Garcia-Verdugo, J.-M., Aguilar, A., Schneider-Maunoury, S., & Alvarez-Buylla, A. (2008). Hedgehog signaling and primary cilia are required for the formation of adult neural stem cells. *Nat Neurosci, 11*(3), 277-284. doi: 10.1038/nn2059

Han, Y. G., & Alvarez-Buylla, A. (2010). Role of primary cilia in brain development and cancer. *Curr Opin Neurobiol, 20*(1), 58-67. doi: 10.1016/j.conb.2009.12.002

Han, Y. G., Spassky, N., Romaguera-Ros, M., Garcia-Verdugo, J. M., Aguilar, A., Schneider-Maunoury, S., & Alvarez-Buylla, A. (2008). Hedgehog signaling and primary cilia are required for the formation of adult neural stem cells. *Nat Neurosci, 11*(3), 277-284. doi: 10.1038/nn2059

Han, Y. M., Kang, G. M., Byun, K., Ko, H. W., Kim, J., Shin, M.-S., . . . Kim, M.-S. (2014). Leptin-promoted cilia assembly is critical for normal energy balance. *J Clin Invest, 124*(5), 2193-2197. doi: 10.1172/JCI69395

Handel, A. E., Williamson, A. J., Disanto, G., Dobson, R., Giovannoni, G., & Ramagopalan, S. V. (2011). Smoking and multiple sclerosis: an updated meta-analysis. *PLoS One, 6*(1), e16149. doi: 10.1371/journal.pone.0016149

Händel, M., Schulz, S., Stanarius, A., Schreff, M., Erdtmann-Vourliotis, M., Schmidt, H., . . . Höllt, V. (1999). Selective targeting of somatostatin receptor 3 to neuronal cilia. *Neuroscience, 89*(3), 909-926. doi: https://doi.org/10.1016/S0306-4522(98)00354-6

Hao, L., & ElShamy, W. M. (2007). BRCA1-IRIS activates cyclin D1 expression in breast cancer cells by downregulating the JNK phosphatase DUSP3/VHR. *Int J Cancer, 121*(1), 39-46. doi: 10.1002/ijc.22597

Harbo, H. F., Gold, R., & Tintore, M. (2013). Sex and gender issues in multiple sclerosis. *Ther Adv Neurol Disord, 6*(4), 237-248. doi: 10.1177/1756285613488434

Hartill, V., Szymanska, K., Sharif, S. M., Wheway, G., & Johnson, C. A. (2017). Meckel–Gruber Syndrome: An Update on Diagnosis, Clinical Management, and Research Advances. *Frontiers in Pediatrics, 5*(244). doi: 10.3389/fped.2017.00244

Hasan, R., Leeson-Payne, A. T. S., Jaggar, J. H., & Zhang, X. (2017). Calmodulin is responsible for Ca2+-dependent regulation of TRPA1 Channels. *Sci Rep, 7*(1), 45098. doi: 10.1038/srep45098

Hasan, R., & Zhang, X. (2018). Ca(2+) Regulation of TRP Ion Channels. *Int J Mol Sci, 19*(4). doi: 10.3390/ijms19041256

Häusser-Kinzel, S., & Weber, M. S. (2019). The Role of B Cells and Antibodies in Multiple Sclerosis, Neuromyelitis Optica, and Related Disorders. *Frontiers in Immunology, 10*(201). doi: 10.3389/fimmu.2019.00201

Hayashi, J., Tanaka, M., Sato, W., Ozawa, T., Yonekawa, H., Kagawa, Y., & Ohta, S. (1990). Effects of ethidium bromide treatment of mouse cells on expression and assembly of nuclear-coded subunits of complexes involved in the oxidative phosphorylation. *Biochem Biophys Res Commun, 167*(1), 216-221.

Hearn, T. (2019). ALMS1 and Alstrom syndrome: a recessive form of metabolic, neurosensory and cardiac deficits. *J Mol Med (Berl), 97*(1), 1-17. doi: 10.1007/s00109-018-1714-x

Hedström, A. K., Katsoulis, M., Hössjer, O., Bomfim, I. L., Oturai, A., Sondergaard, H. B., . . . Alfredsson, L. (2017). The interaction between smoking and HLA genes in multiple sclerosis: replication and refinement. *Eur J Epidemiol, 32*(10), 909-919. doi: 10.1007/s10654-017-0250-2

Henderson, A. P., Barnett, M. H., Parratt, J. D., & Prineas, J. W. (2009). Multiple sclerosis: distribution of inflammatory cells in newly forming lesions. *Ann Neurol, 66*(6), 739-753. doi: 10.1002/ana.21800

Henze, T., Rieckmann, P., & Toyka, K. V. (2006). Symptomatic treatment of multiple sclerosis. Multiple Sclerosis Therapy Consensus Group (MSTCG) of the German Multiple Sclerosis Society. *Eur Neurol, 56*(2), 78-105. doi: 10.1159/000095699

Higginbotham, H., Eom, T.-Y., Mariani, Laura E., Bachleda, A., Hirt, J., Gukassyan, V., . . . Anton, E. S. (2012). Arl13b in Primary Cilia Regulates the Migration and Placement of Interneurons in the Developing Cerebral Cortex. *Dev Cell, 23*(5), 925-938. doi: 10.1016/j.devcel.2012.09.019

Higginbotham, H., Guo, J., Yokota, Y., Umberger, N. L., Su, C.-Y., Li, J., . . . Anton, E. S. (2013). Arl13b-regulated cilia activities are essential for polarized radial glial scaffold formation. *Nat Neurosci, 16*(8), 1000-1007. doi: 10.1038/nn.3451

Hilgendorf, K. I., Johnson, C. T., & Jackson, P. K. (2016). The primary cilium as a cellular receiver: organizing ciliary GPCR signaling. *Current Opinion in Cell Biology, 39*, 84-92. doi: https://doi.org/10.1016/j.ceb.2016.02.008

Hiremath, M. M., Chen, V. S., Suzuki, K., Ting, J. P., & Matsushima, G. K. (2008). MHC class II exacerbates demyelination in vivo independently of T cells. *J Neuroimmunol, 203*(1), 23-32. doi: 10.1016/j.jneuroim.2008.06.034

Hiremath, M. M., Saito, Y., Knapp, G. W., Ting, J. P., Suzuki, K., & Matsushima, G. K. (1998). Microglial/macrophage accumulation during cuprizone-induced demyelination in C57BL/6 mice. *J Neuroimmunol, 92*(1-2), 38-49.

Hjelmstrom, P., Juedes, A. E., Fjell, J., & Ruddle, N. H. (1998). B-cell-deficient mice develop experimental allergic encephalomyelitis with demyelination after myelin oligodendrocyte glycoprotein sensitization. *J Immunol, 161*(9), 4480-4483.

Hoff, J. M., Dhayalan, M., Midelfart, A., Tharaldsen, A. R., & Bo, L. (2019). Visual dysfunction in multiple sclerosis. *Tidsskr Nor Laegeforen, 139*(11). doi: 10.4045/tidsskr.18.0786

Hollenbach, J. A., & Oksenberg, J. R. (2015). The immunogenetics of multiple sclerosis: A comprehensive review. *J Autoimmun, 64*, 13-25. doi: 10.1016/j.jaut.2015.06.010

Holley, J. E., Gveric, D., Newcombe, J., Cuzner, M. L., & Gutowski, N. J. (2003). Astrocyte characterization in the multiple sclerosis glial scar. *Neuropathol Appl Neurobiol, 29*(5), 434-444. doi: 10.1046/j.1365-2990.2003.00491.x

Hu, L., Wang, B., & Zhang, Y. (2017). Serotonin 5-HT6 receptors affect cognition in a mouse model of Alzheimer's disease by regulating cilia function. *Alzheimers Res Ther, 9*(1), 76. doi: 10.1186/s13195-017-0304-4

Hua, K., & Ferland, R. J. (2017). Fixation methods can differentially affect ciliary protein immunolabeling. *Cilia, 6*(1), 5. doi: 10.1186/s13630-017-0045-9

Humbert, M. C., Weihbrecht, K., Searby, C. C., Li, Y., Pope, R. M., Sheffield, V. C., & Seo, S. (2012). ARL13B, PDE6D, and CEP164 form a functional network for INPP5E ciliary targeting. *Proceedings of the National Academy of Sciences, 109*(48), 19691-19696. doi: 10.1073/pnas.1210916109

International Multiple Sclerosis Genetics, C., Beecham, A. H., Patsopoulos, N. A., Xifara, D. K., Davis, M. F., Kemppinen, A., . . . McCauley, J. L. (2013). Analysis of immune-related loci identifies 48 new susceptibility variants for multiple sclerosis. *Nat Genet, 45*(11), 1353-1360. doi: 10.1038/ng.2770

International Multiple Sclerosis Genetics, C., Wellcome Trust Case Control, C., Sawcer, S., Hellenthal, G., Pirinen, M., Spencer, C. C., . . . Compston, A. (2011). Genetic risk and a primary role for cell-mediated immune mechanisms in multiple sclerosis. *Nature, 476*(7359), 214-219. doi: 10.1038/nature10251

Islam, M. S., Tatsumi, K., Okuda, H., Shiosaka, S., & Wanaka, A. (2009). Olig2-expressing progenitor cells preferentially differentiate into oligodendrocytes in cuprizone-induced demyelinated lesions. *Neurochem Int, 54*(3-4), 192-198. doi: 10.1016/j.neuint.2008.10.011

Itoh, T., Itoh, A., & Pleasure, D. (2003). Bcl-2-related protein family gene expression during oligodendroglial differentiation. *J Neurochem, 85*(6), 1500-1512. doi: 10.1046/j.1471-4159.2003.01795.x

Iwanaga, T., Miki, T., & Takahashi-Iwanaga, H. (2011). Restricted expression of somatostatin receptor 3 to primary cilia in the pancreatic islets and adenohypophysis of mice. *Biomedical Research, 32*(1), 73-81. doi: 10.2220/biomedres.32.73

Izawa, I., Goto, H., Kasahara, K., & Inagaki, M. (2015). Current topics of functional links between primary cilia and cell cycle. *Cilia, 4*(1), 12. doi: 10.1186/s13630-015-0021-1

Jan, D. M., Pietro, M., Gayle, B. C., & Jurgen, K. N. (2011). Alstrom Syndrome: Genetics and Clinical Overview. *Current Genomics, 12*(3), 225-235. doi: http://dx.doi.org/10.2174/138920211795677912

Jean, I., Allamargot, C., Barthelaix-Pouplard, A., & Fressinaud, C. (2002). Axonal lesions and PDGF-enhanced remyelination in the rat corpus callosum after lysolecithin demyelination. *Neuroreport, 13*(5), 627-631.

Jeffery, N. D., & Blakemore, W. F. (1995). Remyelination of mouse spinal cord axons demyelinated by local injection of lysolecithin. *J Neurocytol, 24*(10), 775-781. doi: 10.1007/bf01191213

Jersild, C., Fog, T., Hansen, G. S., Thomsen, M., Svejgaard, A., & Dupont, B. (1973). Histocompatibility determinants in multiple sclerosis, with special reference to clinical course. *Lancet, 2*(7840), 1221-1225.

Ji, Q., Castelli, L., & Goverman, J. M. (2013). MHC class I-restricted myelin epitopes are cross-presented by Tip-DCs that promote determinant spreading to CD8(+) T cells. *Nat Immunol, 14*(3), 254-261. doi: 10.1038/ni.2513

Johansson, O., Hökfelt, T., & Elde, R. P. (1984). Immunohistochemical distribution of somatostatin-like immunoreactivity in the central nervous system of the adult rat. *Neuroscience, 13*(2), 265-IN262. doi: https://doi.org/10.1016/0306-4522(84)90233-1

Kaliszewski, M., Knott, A. B., & Bossy-Wetzel, E. (2015). Primary cilia and autophagic dysfunction in Huntington's disease. *Cell Death Differ, 22*(9), 1413-1424. doi: 10.1038/cdd.2015.80

Kamradt, T., Soloway, P. D., Perkins, D. L., & Gefter, M. L. (1991). Pertussis toxin prevents the induction of peripheral T cell anergy and enhances the T cell response to an encephalitogenic peptide of myelin basic protein. *J Immunol, 147*(10), 3296-3302.

Kang, Z., Liu, L., Spangler, R., Spear, C., Wang, C., Gulen, M. F., . . . Li, X. (2012). IL-17-induced Act1-mediated signaling is critical for cuprizone-induced demyelination. *J Neurosci, 32*(24), 8284-8292. doi: 10.1523/jneurosci.0841-12.2012

Kasahara, K., Miyoshi, K., Murakami, S., Miyazaki, I., & Asanuma, M. (2014). Visualization of astrocytic primary cilia in the mouse brain by immunofluorescent analysis using the cilia marker Arl13b. *Acta Med Okayama, 68*(6), 317-322. doi: 10.18926/amo/53020

Kaupp, U. B. (2010). Olfactory signalling in vertebrates and insects: differences and commonalities. *Nature Reviews Neuroscience, 11*(3), 188-200. doi: 10.1038/nrn2789

Kebir, H., Ifergan, I., Alvarez, J. I., Bernard, M., Poirier, J., Arbour, N., . . . Prat, A. (2009). Preferential recruitment of interferon-gamma-expressing TH17 cells in multiple sclerosis. *Ann Neurol, 66*(3), 390-402. doi: 10.1002/ana.21748

Kenny, J., Forsythe, E., Beales, P., & Bacchelli, C. (2017). Toward personalized medicine in Bardet-Biedl syndrome. *Per Med, 14*(5), 447-456. doi: 10.2217/pme-2017-0019

Kerschensteiner, M., Gallmeier, E., Behrens, L., Leal, V. V., Misgeld, T., Klinkert, W. E., . . . Hohlfeld, R. (1999). Activated human T cells, B cells, and monocytes produce brain-derived neurotrophic factor in vitro and in inflammatory brain lesions: a neuroprotective role of inflammation? *J Exp Med, 189*(5), 865-870. doi: 10.1084/jem.189.5.865

Keryer, G., Pineda, J. R., Liot, G., Kim, J., Dietrich, P., Benstaali, C., . . . Saudou, F. (2011). Ciliogenesis is regulated by a huntingtin-HAP1-PCM1 pathway and is altered in Huntington disease. *J Clin Invest, 121*(11), 4372-4382. doi: 10.1172/jci57552

Khatri, P., Obernier, K., Simeonova, I. K., Hellwig, A., Hölzl-Wenig, G., Mandl, C., . . . Ciccolini, F. (2014). Proliferation and cilia dynamics in neural stem cells prospectively isolated from the SEZ. *Sci Rep, 4*(1), 3803. doi: 10.1038/srep03803

Kim, J. Y., Lee, Y. W., Kim, J. H., Lee, W. T., Park, K. A., & Lee, J. E. (2015). Agmatine Attenuates Brain Edema and Apoptotic Cell Death after Traumatic Brain Injury. *J Korean Med Sci, 30*(7), 943-952. doi: 10.3346/jkms.2015.30.7.943

Kim, T. S., & Perlman, S. (2005). Virus-specific antibody, in the absence of T cells, mediates demyelination in mice infected with a neurotropic coronavirus. *Am J Pathol, 166*(3), 801-809. doi: 10.1016/s0002-9440(10)62301-2

Kim, Y. J., & Kim, J. (2019). Therapeutic perspectives for structural and functional abnormalities of cilia. *Cell Mol Life Sci, 76*(19), 3695-3709. doi: 10.1007/s00018-019-03158-6

Kipp, M., Clarner, T., Dang, J., Copray, S., & Beyer, C. (2009). The cuprizone animal model: new insights into an old story. *Acta Neuropathol, 118*(6), 723-736. doi: 10.1007/s00401-009-0591-3

Kirschen, G. W., Liu, H., Lang, T., Liang, X., Ge, S., & Xiong, Q. (2017). The radial organization of neuronal primary cilia is acutely disrupted by seizure and ischemic brain injury. *Front Biol (Beijing), 12*(2), 124-138. doi: 10.1007/s11515-017-1447-1

Koch, M. W., Metz, L. M., & Kovalchuk, O. (2013). Epigenetic changes in patients with multiple sclerosis. *Nat Rev Neurol, 9*(1), 35-43. doi: 10.1038/nrneurol.2012.226

Koemeter-Cox, A. I., Sherwood, T. W., Green, J. A., Steiner, R. A., Berbari, N. F., Yoder, B. K., . . . Mykytyn, K. (2014). Primary cilia enhance kisspeptin receptor signaling on gonadotropin-releasing hormone neurons. *Proceedings of the National Academy of Sciences, 111*(28), 10335-10340. doi: 10.1073/pnas.1403286111

Komoly, S., Hudson, L. D., Webster, H. D., & Bondy, C. A. (1992). Insulin-like growth factor I gene expression is induced in astrocytes during experimental demyelination. *Proc Natl Acad Sci U S A, 89*(5), 1894-1898.

Komoly, S., Jeyasingham, M. D., Pratt, O. E., & Lantos, P. L. (1987). Decrease in oligodendrocyte carbonic anhydrase activity preceding myelin degeneration in cuprizone induced demyelination. *J Neurol Sci, 79*(1-2), 141-148.

Kondo, T., Obata, K., Miyoshi, K., Sakurai, J., Tanaka, J., Miwa, H., & Noguchi, K. (2009). Transient receptor potential A1 mediates gastric distention-induced visceral pain in rats. *Gut, 58*(10), 1342-1352. doi: 10.1136/gut.2008.175901

Kondo, T., Oshima, T., Obata, K., Sakurai, J., Knowles, C. H., Matsumoto, T., . . . Miwa, H. (2010). Role of transient receptor potential A1 in gastric nociception. *Digestion, 82*(3), 150-155. doi: 10.1159/000310836

Kondo, T., Sakurai, J., Miwa, H., & Noguchi, K. (2013). Activation of p38 MAPK through transient receptor potential A1 in a rat model of gastric distension-induced visceral pain. *Neuroreport, 24*(2), 68-72. doi: 10.1097/WNR.0b013e32835c7df2

Kotter, M. R., Setzu, A., Sim, F. J., Van Rooijen, N., & Franklin, R. J. (2001). Macrophage depletion impairs oligodendrocyte remyelination following lysolecithin-induced demyelination. *Glia, 35*(3), 204-212.

Koutsoudaki, P. N., Skripuletz, T., Gudi, V., Moharregh-Khiabani, D., Hildebrandt, H., Trebst, C., & Stangel, M. (2009). Demyelination of the hippocampus is prominent in the cuprizone model. *Neurosci Lett, 451*(1), 83-88. doi: 10.1016/j.neulet.2008.11.058

Krishnamoorthy, G., Lassmann, H., Wekerle, H., & Holz, A. (2006). Spontaneous opticospinal encephalomyelitis in a double-transgenic mouse model of autoimmune T cell/B cell cooperation. *J Clin Invest, 116*(9), 2385-2392. doi: 10.1172/jci28330

Kuhlmann, T., Miron, V., Cui, Q., Wegner, C., Antel, J., & Bruck, W. (2008). Differentiation block of oligodendroglial progenitor cells as a cause for remyelination failure in chronic multiple sclerosis. *Brain, 131*(Pt 7), 1749-1758. doi: 10.1093/brain/awn096

Kutzelnigg, A., Faber-Rod, J. C., Bauer, J., Lucchinetti, C. F., Sorensen, P. S., Laursen, H., . . . Lassmann, H. (2007). Widespread demyelination in the cerebellar cortex in multiple sclerosis. *Brain Pathol, 17*(1), 38-44. doi: 10.1111/j.1750-3639.2006.00041.x

Kutzelnigg, A., & Lassmann, H. (2014). Pathology of multiple sclerosis and related inflammatory demyelinating diseases. *Handb Clin Neurol, 122*, 15-58. doi: 10.1016/B978-0-444-52001-2.00002-9

Kutzelnigg, A., Lucchinetti, C. F., Stadelmann, C., Bruck, W., Rauschka, H., Bergmann, M., . . . Lassmann, H. (2005). Cortical demyelination and diffuse white matter injury in multiple sclerosis. *Brain, 128*(Pt 11), 2705-2712. doi: 10.1093/brain/awh641

Kuypers, N. J., James, K. T., Enzmann, G. U., Magnuson, D. S., & Whittemore, S. R. (2013). Functional consequences of ethidium bromide demyelination of the mouse ventral spinal cord. *Exp Neurol, 247*, 615-622. doi: 10.1016/j.expneurol.2013.02.014

Larkins, C. E., Aviles, G. D. G., East, M. P., Kahn, R. A., & Caspary, T. (2011). Arl13b regulates ciliogenesis and the dynamic localization of Shh signaling proteins. *Mol Biol Cell, 22*(23), 4694-4703. doi: 10.1091/mbc.e10-12-0994

Lassmann, H. (2018). Multiple Sclerosis Pathology. *Cold Spring Harb Perspect Med, 8*(3). doi: 10.1101/cshperspect.a028936

Lassmann, H., & Bradl, M. (2017). Multiple sclerosis: experimental models and reality. *Acta Neuropathol, 133*(2), 223-244. doi: 10.1007/s00401-016-1631-4

Lassmann, H., Bruck, W., & Lucchinetti, C. F. (2007). The immunopathology of multiple sclerosis: an overview. *Brain Pathol, 17*(2), 210-218. doi: 10.1111/j.1750-3639.2007.00064.x

Lau, L. W., Keough, M. B., Haylock-Jacobs, S., Cua, R., Doring, A., Sloka, S., . . . Yong, V. W. (2012). Chondroitin sulfate proteoglycans in demyelinated lesions impair remyelination. *Ann Neurol, 72*(3), 419-432. doi: 10.1002/ana.23599

Lee, J., & Chung, Y. D. (2015). Ciliary subcompartments: how are they established and what are their functions? *BMB Rep, 48*(7), 380-387. doi: 10.5483/bmbrep.2015.48.7.084

Lee, J. H., & Gleeson, J. G. (2010). The role of primary cilia in neuronal function. *Neurobiol Dis, 38*(2), 167-172. doi: https://doi.org/10.1016/j.nbd.2009.12.022

Lee, J. Y., Oh, T. H., & Yune, T. Y. (2011). Ghrelin inhibits hydrogen peroxide-induced apoptotic cell death of oligodendrocytes via ERK and p38MAPK signaling. *Endocrinology, 152*(6), 2377-2386. doi: 10.1210/en.2011-0090

Lee, S. M., Cho, Y. S., Kim, T. H., Jin, M. U., Ahn, D. K., Noguchi, K., & Bae, Y. C. (2012). An ultrastructural evidence for the expression of transient receptor potential ankyrin 1 (TRPA1) in astrocytes in the rat trigeminal caudal nucleus. *J Chem Neuroanat, 45*(1-2), 45-49. doi: 10.1016/j.jchemneu.2012.07.003

Legroux, L., & Arbour, N. (2015). Multiple Sclerosis and T Lymphocytes: An Entangled Story. *J Neuroimmune Pharmacol, 10*(4), 528-546. doi: 10.1007/s11481-015-9614-0

Leray, E., Moreau, T., Fromont, A., & Edan, G. (2016). Epidemiology of multiple sclerosis. *Rev Neurol (Paris), 172*(1), 3-13. doi: 10.1016/j.neurol.2015.10.006

Levin, L. I., Munger, K. L., O'Reilly, E. J., Falk, K. I., & Ascherio, A. (2010). Primary infection with the Epstein-Barr virus and risk of multiple sclerosis. *Ann Neurol, 67*(6), 824-830. doi: 10.1002/ana.21978

Li, Y., Wei, Q., Zhang, Y., Ling, K., & Hu, J. (2010). The small GTPases ARL-13 and ARL-3 coordinate intraflagellar transport and ciliogenesis. *Journal of Cell Biology, 189*(6), 1039-1051. doi: 10.1083/jcb.200912001

Lill, C. M., Schjeide, B. M., Graetz, C., Liu, T., Damotte, V., Akkad, D. A., . . . Bertram, L. (2013). Genome-wide significant association of ANKRD55 rs6859219 and multiple sclerosis risk. *J Med Genet, 50*(3), 140-143. doi: 10.1136/jmedgenet-2012-101411

Linares, D., Taconis, M., Mana, P., Correcha, M., Fordham, S., Staykova, M., & Willenborg, D. O. (2006). Neuronal nitric oxide synthase plays a key role in CNS demyelination. *J Neurosci, 26*(49), 12672-12681. doi: 10.1523/jneurosci.0294-06.2006

Lindsten, T., Ross, A. J., King, A., Zong, W. X., Rathmell, J. C., Shiels, H. A., . . . Thompson, C. B. (2000). The combined functions of proapoptotic Bcl-2 family members bak and bax are essential for normal development of multiple tissues. *Mol Cell, 6*(6), 1389-1399.

Linington, C., Bradl, M., Lassmann, H., Brunner, C., & Vass, K. (1988). Augmentation of demyelination in rat acute allergic encephalomyelitis by circulating mouse monoclonal antibodies directed against a myelin/oligodendrocyte glycoprotein. *Am J Pathol, 130*(3), 443-454.

Lipphardt, M., Muhlhausen, J., Kitze, B., Heigl, F., Mauch, E., Helms, H. J., . . . Koziolek, M. J. (2019). Immunoadsorption or plasma exchange in steroid-refractory multiple sclerosis and neuromyelitis optica. *J Clin Apher, 34*(4), 381-391. doi: 10.1002/jca.21686

Lipton, H. L., Twaddle, G., & Jelachich, M. L. (1995). The predominant virus antigen burden is present in macrophages in Theiler's murine encephalomyelitis virus-induced demyelinating disease. *J Virol, 69*(4), 2525-2533.

Liu, H., Kiseleva, A. A., & Golemis, E. A. (2018). Ciliary signalling in cancer. *Nat Rev Cancer, 18*(8), 511-524. doi: 10.1038/s41568-018-0023-6

Liu, Y. P., Tsai, I. C., Morleo, M., Oh, E. C., Leitch, C. C., Massa, F., . . . Katsanis, N. (2014). Ciliopathy proteins regulate paracrine signaling by modulating proteasomal degradation of mediators. *J Clin Invest, 124*(5), 2059-2070. doi: 10.1172/JCI71898

Loktev, Alexander V., & Jackson, Peter K. (2013). Neuropeptide Y Family Receptors Traffic via the Bardet-Biedl Syndrome Pathway to Signal in Neuronal Primary Cilia. *Cell Reports, 5*(5), 1316-1329. doi: 10.1016/j.celrep.2013.11.011

Lu, C., Pelech, S., Zhang, H., Bond, J., Spach, K., Noubade, R., . . . Teuscher, C. (2008). Pertussis toxin induces angiogenesis in brain microvascular endothelial cells. *J Neurosci Res, 86*(12), 2624-2640. doi: 10.1002/jnr.21716

Lu, H., Toh, M. T., Narasimhan, V., Thamilselvam, S. K., Choksi, S. P., & Roy, S. (2015). A function for the Joubert syndrome protein Arl13b in ciliary membrane extension and ciliary length regulation. *Developmental Biology, 397*(2), 225-236. doi: https://doi.org/10.1016/j.ydbio.2014.11.009

Lublin, F. D., Reingold, S. C., Cohen, J. A., Cutter, G. R., Sorensen, P. S., Thompson, A. J., . . . Polman, C. H. (2014). Defining the clinical course of multiple sclerosis: the 2013 revisions. *Neurology, 83*(3), 278-286. doi: 10.1212/WNL.0000000000000560

Lucarelli, M., Di Pietro, C., La Sala, G., Fiorenza, M. T., Marazziti, D., & Canterini, S. (2019). Anomalies in Dopamine Transporter Expression and Primary Cilium Distribution in the Dorsal Striatum of a Mouse Model of Niemann-Pick C1 Disease. *Front Cell Neurosci, 13*, 226. doi: 10.3389/fncel.2019.00226

Lucchinetti, C., Bruck, W., Parisi, J., Scheithauer, B., Rodriguez, M., & Lassmann, H. (2000). Heterogeneity of multiple sclerosis lesions: implications for the pathogenesis of demyelination. *Ann Neurol, 47*(6), 707-717.

Lucchinetti, C. F., Bruck, W., Rodriguez, M., & Lassmann, H. (1996). Distinct patterns of multiple sclerosis pathology indicates heterogeneity on pathogenesis. *Brain Pathol, 6*(3), 259-274.

Ma, X., Peterson, R., & Turnbull, J. (2011). Adenylyl cyclase type 3, a marker of primary cilia, is reduced in primary cell culture and in lumbar spinal cord in situ in G93A SOD1 mice. *BMC Neurosci, 12*, 71. doi: 10.1186/1471-2202-12-71

Magliozzi, R., Howell, O., Vora, A., Serafini, B., Nicholas, R., Puopolo, M., . . . Aloisi, F. (2007). Meningeal B-cell follicles in secondary progressive multiple sclerosis associate with early onset of disease and severe cortical pathology. *Brain, 130*(Pt 4), 1089-1104. doi: 10.1093/brain/awm038

Mahad, D. H., Trapp, B. D., & Lassmann, H. (2015). Pathological mechanisms in progressive multiple sclerosis. *Lancet Neurol, 14*(2), 183-193. doi: 10.1016/S1474-4422(14)70256-X

Marabita, F., Almgren, M., Sjoholm, L. K., Kular, L., Liu, Y., James, T., . . . Jagodic, M. (2017). Smoking induces DNA methylation changes in Multiple Sclerosis patients with exposure-response relationship. *Sci Rep, 7*(1), 14589. doi: 10.1038/s41598-017-14788-w

Marik, C., Felts, P. A., Bauer, J., Lassmann, H., & Smith, K. J. (2007). Lesion genesis in a subset of patients with multiple sclerosis: a role for innate immunity? *Brain, 130*(Pt 11), 2800-2815. doi: 10.1093/brain/awm236

Marshall, W. F., & Nonaka, S. (2006). Cilia: Tuning in to the Cell's Antenna. *Current Biology, 16*(15), R604-R614. doi: 10.1016/j.cub.2006.07.012

Mason, J. L., Jones, J. J., Taniike, M., Morell, P., Suzuki, K., & Matsushima, G. K. (2000). Mature oligodendrocyte apoptosis precedes IGF-1 production and oligodendrocyte progenitor accumulation and differentiation during demyelination/remyelination. *J Neurosci Res, 61*(3), 251-262. doi: 10.1002/1097-4547(20000801)61:3<251::aid-jnr3>3.0.co;2-w

Mason, J. L., Langaman, C., Morell, P., Suzuki, K., & Matsushima, G. K. (2001). Episodic demyelination and subsequent remyelination within the murine central nervous system: changes in axonal calibre. *Neuropathol Appl Neurobiol, 27*(1), 50-58.

Mason, J. L., Ye, P., Suzuki, K., D'Ercole, A. J., & Matsushima, G. K. (2000). Insulin-like growth factor-1 inhibits mature oligodendrocyte apoptosis during primary demyelination. *J Neurosci, 20*(15), 5703-5708.

Matsushima, G. K., & Morell, P. (2001). The neurotoxicant, cuprizone, as a model to study demyelination and remyelination in the central nervous system. *Brain Pathol, 11*(1), 107-116.

McDonald, I., & Compston, A. (2005). The symptoms and signs of multiple sclerosis *McAlpine's Multiple Sclerosis* (pp. 287-346).

McKay, K. A., Kwan, V., Duggan, T., & Tremlett, H. (2015). Risk factors associated with the onset of relapsing-remitting and primary progressive multiple sclerosis: a systematic review. *Biomed Res Int, 2015*, 817238. doi: 10.1155/2015/817238

McKinnon, R. D., Matsui, T., Dubois-Dalcq, M., & Aaronson, S. A. (1990). FGF modulates the PDGF-driven pathway of oligodendrocyte development. *Neuron, 5*(5), 603-614.

McMahon, E. J., Bailey, S. L., Castenada, C. V., Waldner, H., & Miller, S. D. (2005). Epitope spreading initiates in the CNS in two mouse models of multiple sclerosis. *Nat Med, 11*(3), 335-339. doi: 10.1038/nm1202

McRae, B. L., Vanderlugt, C. L., Dal Canto, M. C., & Miller, S. D. (1995). Functional evidence for epitope spreading in the relapsing pathology of experimental autoimmune encephalomyelitis. *J Exp Med, 182*(1), 75-85.

Mendel, I., Kerlero de Rosbo, N., & Ben-Nun, A. (1995). A myelin oligodendrocyte glycoprotein peptide induces typical chronic experimental autoimmune encephalomyelitis in H-2b mice: fine specificity and T cell receptor V beta expression of encephalitogenic T cells. *Eur J Immunol, 25*(7), 1951-1959. doi: 10.1002/eji.1830250723

Miller, S. D., Vanderlugt, C. L., Begolka, W. S., Pao, W., Yauch, R. L., Neville, K. L., . . . Kim, B. S. (1997). Persistent infection with Theiler's virus leads to CNS autoimmunity via epitope spreading. *Nat Med, 3*(10), 1133-1136. doi: 10.1038/nm1097-1133

Ming, G. L., & Song, H. (2011). Adult neurogenesis in the mammalian brain: significant answers and significant questions. *Neuron, 70*(4), 687-702. doi: 10.1016/j.neuron.2011.05.001

Miron, V. E., Boyd, A., Zhao, J. W., Yuen, T. J., Ruckh, J. M., Shadrach, J. L., . . . Ffrench-Constant, C. (2013). M2 microglia and macrophages drive oligodendrocyte differentiation during CNS remyelination. *Nat Neurosci, 16*(9), 1211-1218. doi: 10.1038/nn.3469

Miyazaki, Y., Li, R., Rezk, A., Misirliyan, H., Moore, C., Farooqi, N., . . . Bar-Or, A. (2014). A novel microRNA-132-sirtuin-1 axis underlies aberrant B-cell cytokine regulation in patients with relapsing-remitting multiple sclerosis [corrected]. *PLoS One, 9*(8), e105421. doi: 10.1371/journal.pone.0105421

Miyoshi, K., Kasahara, K., Miyazaki, I., & Asanuma, M. (2009). Lithium treatment elongates primary cilia in the mouse brain and in cultured cells. *Biochem Biophys Res Commun, 388*(4), 757-762. doi: https://doi.org/10.1016/j.bbrc.2009.08.099

Miyoshi, K., Kasahara, K., Murakami, S., Takeshima, M., Kumamoto, N., Sato, A., . . . Asanuma, M. (2014). Lack of Dopaminergic Inputs Elongates the Primary Cilia of Striatal Neurons. *PLoS One, 9*(5), e97918. doi: 10.1371/journal.pone.0097918

Mok, C., Héon, E., & Zhen, M. (2010). Ciliary dysfunction and obesity. *Clinical Genetics, 77*(1), 18-27. doi: 10.1111/j.1399-0004.2009.01305.x

Montalban, X., Gold, R., Thompson, A. J., Otero-Romero, S., Amato, M. P., Chandraratna, D., . . . Zipp, F. (2018). ECTRIMS/EAN Guideline on the pharmacological treatment of people with multiple sclerosis. *Multiple Sclerosis Journal, 24*(2), 96-120. doi: 10.1177/1352458517751049

Morell, P., Barrett, C. V., Mason, J. L., Toews, A. D., Hostettler, J. D., Knapp, G. W., & Matsushima, G. K. (1998). Gene expression in brain during cuprizone-induced demyelination and remyelination. *Mol Cell Neurosci, 12*(4-5), 220-227. doi: 10.1006/mcne.1998.0715

Motl, R. W., Snook, E. M., & Schapiro, R. T. (2008). Symptoms and physical activity behavior in individuals with multiple sclerosis. *Res Nurs Health, 31*(5), 466-475. doi: 10.1002/nur.20274

Motter, A. L., & Ahern, G. P. (2012). TRPA1 is a polyunsaturated fatty acid sensor in mammals. *PLoS One, 7*(6), e38439. doi: 10.1371/journal.pone.0038439

Mukhopadhyay, S., & Jackson, P. K. (2013). Cilia, tubby mice, and obesity. *Cilia, 2*, 1. doi: 10.1186/2046-2530-2-1

Munger, K. L., Levin, L. I., Hollis, B. W., Howard, N. S., & Ascherio, A. (2006). Serum 25-hydroxyvitamin D levels and risk of multiple sclerosis. *JAMA, 296*(23), 2832-2838. doi: 10.1001/jama.296.23.2832

Murtie, J. C., Zhou, Y. X., Le, T. Q., Vana, A. C., & Armstrong, R. C. (2005). PDGF and FGF2 pathways regulate distinct oligodendrocyte lineage responses in experimental demyelination with spontaneous remyelination. *Neurobiol Dis, 19*(1-2), 171-182. doi: 10.1016/j.nbd.2004.12.006

Mustafa, R., Kreiner, G., Kaminska, K., Wood, A. J., Kirsch, J., Tucker, K. L., & Parlato, R. (2019). Targeted Depletion of Primary Cilia in Dopaminoceptive Neurons in a Preclinical Mouse Model of Huntington's Disease. *Front Cell Neurosci, 13*, 565. doi: 10.3389/fncel.2019.00565

Nachury, M. V. (2018). The molecular machines that traffic signaling receptors into and out of cilia. *Curr Opin Cell Biol, 51*, 124-131. doi: 10.1016/j.ceb.2018.03.004

Nagata, K., Duggan, A., Kumar, G., & Garcia-Anoveros, J. (2005). Nociceptor and hair cell transducer properties of TRPA1, a channel for pain and hearing. *J Neurosci, 25*(16), 4052-4061. doi: 10.1523/jneurosci.0013-05.2005

Naito, S., Namerow, N., Mickey, M. R., & Terasaki, P. I. (1972). Multiple sclerosis: association with HL-A3. *Tissue Antigens, 2*(1), 1-4.

Nakayama, K., & Katoh, Y. (2017). Ciliary protein trafficking mediated by IFT and BBSome complexes with the aid of kinesin-2 and dynein-2 motors. *The Journal of Biochemistry, 163*(3), 155-164. doi: 10.1093/jb/mvx087

Nielsen, T. R., Rostgaard, K., Nielsen, N. M., Koch-Henriksen, N., Haahr, S., Sorensen, P. S., & Hjalgrim, H. (2007). Multiple sclerosis after infectious mononucleosis. *Arch Neurol, 64*(1), 72-75. doi: 10.1001/archneur.64.1.72

Nikic, I., Merkler, D., Sorbara, C., Brinkoetter, M., Kreutzfeldt, M., Bareyre, F. M., . . . Kerschensteiner, M. (2011). A reversible form of axon damage in experimental autoimmune encephalomyelitis and multiple sclerosis. *Nat Med, 17*(4), 495-499. doi: 10.1038/nm.2324

Nilius, B., Appendino, G., & Owsianik, G. (2012). The transient receptor potential channel TRPA1: from gene to pathophysiology. *Pflugers Arch, 464*(5), 425-458. doi: 10.1007/s00424-012-1158-z

Norkute, A., Hieble, A., Braun, A., Johann, S., Clarner, T., Baumgartner, W., . . . Kipp, M. (2009). Cuprizone treatment induces demyelination and astrocytosis in the mouse hippocampus. *J Neurosci Res, 87*(6), 1343-1355. doi: 10.1002/jnr.21946

Noseworthy, J. H., Lucchinetti, C., Rodriguez, M., & Weinshenker, B. G. (2000). Multiple sclerosis. *N Engl J Med, 343*(13), 938-952. doi: 10.1056/NEJM200009283431307

O'Gorman, C., Lin, R., Stankovich, J., & Broadley, S. A. (2013). Modelling genetic susceptibility to multiple sclerosis with family data. *Neuroepidemiology, 40*(1), 1-12. doi: 10.1159/000341902

Ou, Y., Ruan, Y., Cheng, M., Moser, J. J., Rattner, J. B., & van der Hoorn, F. A. (2009). Adenylate cyclase regulates elongation of mammalian primary cilia. *Experimental Cell Research, 315*(16), 2802-2817. doi: https://doi.org/10.1016/j.yexcr.2009.06.028

Oxford, G. S., & Hurley, J. (2013). The role of TRP channels in migraine. *Open Pain J*(6), 37-49.

Pachner, A. R., Li, L., & Lagunoff, D. (2011). Plasma cells in the central nervous system in the Theiler's virus model of multiple sclerosis. *J Neuroimmunol, 232*(1-2), 35-40. doi: 10.1016/j.jneuroim.2010.09.026

Parisi, M. A. (2009). Clinical and molecular features of Joubert syndrome and related disorders. *American Journal of Medical Genetics Part C: Seminars in Medical Genetics, 151C*(4), 326-340. doi: 10.1002/ajmg.c.30229

Parisi, M. A. (2019). The molecular genetics of Joubert syndrome and related ciliopathies: The challenges of genetic and phenotypic heterogeneity. *Transl Sci Rare Dis, 4*(1-2), 25-49. doi: 10.3233/trd-190041

Park, S. M., Jang, H. J., & Lee, J. H. (2019). Roles of Primary Cilia in the Developing Brain. *Front Cell Neurosci, 13*(218). doi: 10.3389/fncel.2019.00218

Parker, A. K., Le, M. M., Smith, T. S., Hoang-Minh, L. B., Atkinson, E. W., Ugartemendia, G., . . . Sarkisian, M. R. (2016). Neonatal seizures induced by pentylenetetrazol or kainic acid disrupt primary cilia growth on developing mouse cortical neurons. *Exp Neurol, 282*, 119-127. doi: https://doi.org/10.1016/j.expneurol.2016.05.015

Parpura, V., Heneka, M. T., Montana, V., Oliet, S. H., Schousboe, A., Haydon, P. G., . . . Verkhratsky, A. (2012). Glial cells in (patho)physiology. *J Neurochem, 121*(1), 4-27. doi: 10.1111/j.1471-4159.2012.07664.x

Pasquini, L. A., Calatayud, C. A., Bertone Una, A. L., Millet, V., Pasquini, J. M., & Soto, E. F. (2007). The neurotoxic effect of cuprizone on oligodendrocytes depends on the presence of pro-inflammatory cytokines secreted by microglia. *Neurochem Res, 32*(2), 279-292. doi: 10.1007/s11064-006-9165-0

Patel, Y. C. (1999). Somatostatin and Its Receptor Family. *Frontiers in Neuroendocrinology, 20*(3), 157-198. doi: https://doi.org/10.1006/frne.1999.0183

Patrikios, P., Stadelmann, C., Kutzelnigg, A., Rauschka, H., Schmidbauer, M., Laursen, H., . . . Lassmann, H. (2006). Remyelination is extensive in a subset of multiple sclerosis patients. *Brain, 129*(Pt 12), 3165-3172. doi: 10.1093/brain/awl217

Paxinos, G., & Franklin, K. B. J. (2001). *The Mouse Brain in Stereotaxic Coordinates*. San Diego: Academic Press.

Perrin Ross, A., Ben-Zacharia, A., Harris, C., & Smrtka, J. (2013). Multiple Sclerosis, Relapses, and the Mechanism of Action of Adrenocorticotropic Hormone. *Frontiers in Neurology, 4*(21). doi: 10.3389/fneur.2013.00021

Petrov, D., Pedros, I., Artiach, G., Sureda, F. X., Barroso, E., Pallas, M., . . . Camins, A. (2015). High-fat diet-induced deregulation of hippocampal insulin signaling and mitochondrial homeostasis deficiences contribute to Alzheimer disease pathology in rodents. *Biochim Biophys Acta, 1852*(9), 1687-1699. doi: 10.1016/j.bbadis.2015.05.004

Pierrot-Deseilligny, C., & Souberbielle, J. C. (2017). Vitamin D and multiple sclerosis: An update. *Mult Scler Relat Disord, 14*, 35-45. doi: 10.1016/j.msard.2017.03.014

Pierson, E., Simmons, S. B., Castelli, L., & Goverman, J. M. (2012). Mechanisms regulating regional localization of inflammation during CNS autoimmunity. *Immunol Rev, 248*(1), 205-215. doi: 10.1111/j.1600-065X.2012.01126.x

Pissios, P., Bradley, R. L., & Maratos-Flier, E. (2006). Expanding the Scales: The Multiple Roles of MCH in Regulating Energy Balance and Other Biological Functions. *Endocrine Reviews, 27*(6), 606-620. doi: 10.1210/er.2006-0021

Plemel, J. R., Michaels, N. J., Weishaupt, N., Caprariello, A. V., Keough, M. B., Rogers, J. A., . . . Yong, V. W. (2018). Mechanisms of lysophosphatidylcholine-induced demyelination: A primary lipid disrupting myelinopathy. *66*(2), 327-347. doi: 10.1002/glia.23245

Popescu, B. F. G., & Lucchinetti, C. F. (2016). Chapter 9 - Neuropathology of Multiple Sclerosis. In A. Minagar (Ed.), *Mult Scler* (pp. 181-200). San Diego: Academic Press.

Pott, F., Gingele, S., Clarner, T., Dang, J., Baumgartner, W., Beyer, C., & Kipp, M. (2009). Cuprizone effect on myelination, astrogliosis and microglia attraction in the mouse basal ganglia. *Brain Res, 1305*, 137-149. doi: 10.1016/j.brainres.2009.09.084

Praet, J., Guglielmetti, C., Berneman, Z., Van der Linden, A., & Ponsaerts, P. (2014). Cellular and molecular neuropathology of the cuprizone mouse model: clinical relevance for multiple sclerosis. *Neurosci Biobehav Rev, 47*, 485-505. doi: 10.1016/j.neubiorev.2014.10.004

Prineas, J. W., Barnard, R. O., Kwon, E. E., Sharer, L. R., & Cho, E. S. (1993). Multiple sclerosis: remyelination of nascent lesions. *Ann Neurol, 33*(2), 137-151. doi: 10.1002/ana.410330203

Procaccini, C., De Rosa, V., Pucino, V., Formisano, L., & Matarese, G. (2015). Animal models of Multiple Sclerosis. *Eur J Pharmacol, 759*, 182-191. doi: 10.1016/j.ejphar.2015.03.042

Qiu, L., LeBel, R. P., Storm, D. R., & Chen, X. (2016). Type 3 adenylyl cyclase: a key enzyme mediating the cAMP signaling in neuronal cilia. *Int J Physiol Pathophysiol Pharmacol, 8*(3), 95-108.

Rae-Grant, A., Day, G. S., Marrie, R. A., Rabinstein, A., Cree, B. A. C., Gronseth, G. S., . . . Pringsheim, T. (2018). Comprehensive systematic review summary: Disease-modifying therapies for adults with multiple sclerosis: Report of the Guideline Development, Dissemination, and Implementation Subcommittee of the American Academy of Neurology. *Neurology, 90*(17), 789-800. doi: 10.1212/wnl.0000000000005345

Reiter, J. F., & Leroux, M. R. (2017). Genes and molecular pathways underpinning ciliopathies. *Nat Rev Mol Cell Biol, 18*(9), 533-547. doi: 10.1038/nrm.2017.60

Robertson, N. P., Fraser, M., Deans, J., Clayton, D., Walker, N., & Compston, D. A. (1996). Age-adjusted recurrence risks for relatives of patients with multiple sclerosis. *Brain, 119 (Pt 2)*, 449-455.

Rodriguez, E. G., Wegner, C., Kreutzfeldt, M., Neid, K., Thal, D. R., Jürgens, T., . . . Merkler, D. (2014). Oligodendroglia in cortical multiple sclerosis lesions decrease with disease progression, but regenerate after repeated experimental demyelination. *Acta Neuropathol, 128*(2), 231-246. doi: 10.1007/s00401-014-1260-8

Rodriguez, M., & David, C. S. (1985). Demyelination induced by Theiler's virus: influence of the H-2 haplotype. *J Immunol, 135*(3), 2145-2148.

Rodriguez, M., Leibowitz, J. L., & Lampert, P. W. (1983). Persistent infection of oligodendrocytes in Theiler's virus-induced encephalomyelitis. *Ann Neurol, 13*(4), 426-433. doi: 10.1002/ana.410130409

Rommer, P. S., Eichstadt, K., Ellenberger, D., Flachenecker, P., & Friede, T. (2019). Symptomatology and symptomatic treatment in multiple sclerosis: Results from a nationwide MS registry. *25*(12), 1641-1652. doi: 10.1177/1352458518799580

Rommer, P. S., Milo, R., Han, M. H., Satyanarayan, S., Sellner, J., Hauer, L., . . . Stuve, O. (2019). Immunological Aspects of Approved MS Therapeutics. *Front Immunol, 10*, 1564. doi: 10.3389/fimmu.2019.01564

Ruiz, F., Vigne, S., & Pot, C. (2019). Resolution of inflammation during multiple sclerosis. *41*(6), 711-726. doi: 10.1007/s00281-019-00765-0

Ruther, B. J., Scheld, M., Dreymueller, D., Clarner, T., Kress, E., & Brandenburg, L. O. (2017). Combination of cuprizone and experimental autoimmune encephalomyelitis to study inflammatory brain lesion formation and progression. *65*(12), 1900-1913. doi: 10.1002/glia.23202

Sarkisian, M. R., & Semple-Rowland, S. L. (2019). Emerging Roles of Primary Cilia in Glioma. *Front Cell Neurosci, 13*, 55. doi: 10.3389/fncel.2019.00055

Sattar, S., & Gleeson, J. G. (2011). The ciliopathies in neuronal development: a clinical approach to investigation of Joubert syndrome and Joubert syndrome-related disorders. *Dev Med Child Neurol, 53*(9), 793-798. doi: 10.1111/j.1469-8749.2011.04021.x

Scheld, M., Ruther, B. J., Grosse-Veldmann, R., Ohl, K., Tenbrock, K., Dreymuller, D., . . . Kipp, M. (2016). Neurodegeneration Triggers Peripheral Immune Cell Recruitment into the Forebrain. *J Neurosci, 36*(4), 1410-1415. doi: 10.1523/jneurosci.2456-15.2016

Schetters, S. T. T., Gomez-Nicola, D., Garcia-Vallejo, J. J., & Van Kooyk, Y. (2017). Neuroinflammation: Microglia and T Cells Get Ready to Tango. *Front Immunol, 8*, 1905. doi: 10.3389/fimmu.2017.01905

Schou, K. B., Pedersen, L. B., & Christensen, S. T. (2015). Ins and outs of GPCR signaling in primary cilia. *EMBO reports, 16*(9), 1099-1113. doi: 10.15252/embr.201540530

Schulz, K., Kroner, A., & David, S. (2012). Iron efflux from astrocytes plays a role in remyelination. *J Neurosci, 32*(14), 4841-4847. doi: 10.1523/jneurosci.5328-11.2012

Seo, S., Guo, D.-F., Bugge, K., Morgan, D. A., Rahmouni, K., & Sheffield, V. C. (2009). Requirement of Bardet-Biedl syndrome proteins for leptin receptor signaling. *Human Molecular Genetics, 18*(7), 1323-1331. doi: 10.1093/hmg/ddp031

Serafini, B., Rosicarelli, B., Magliozzi, R., Stigliano, E., & Aloisi, F. (2004). Detection of ectopic B-cell follicles with germinal centers in the meninges of patients with secondary progressive multiple sclerosis. *Brain Pathol, 14*(2), 164-174.

Shigetomi, E., Jackson-Weaver, O., Huckstepp, R. T., O'Dell, T. J., & Khakh, B. S. (2013). TRPA1 channels are regulators of astrocyte basal calcium levels and long-term potentiation via constitutive D-serine release. *J Neurosci, 33*(24), 10143-10153. doi: 10.1523/jneurosci.5779-12.2013

Shigetomi, E., Tong, X., Kwan, K. Y., Corey, D. P., & Khakh, B. S. (2011). TRPA1 channels regulate astrocyte resting calcium and inhibitory synapse efficacy through GAT-3. *Nat Neurosci, 15*(1), 70-80. doi: 10.1038/nn.3000

Shin, J. S., Kwon, Y. N., Choi, Y., Lee, J. Y., Lee, Y. I., Hwang, J. H., . . . Kim, S. M. (2019). Comparison of psychiatric disturbances in patients with multiple sclerosis and neuromyelitis optica. *Medicine (Baltimore), 98*(38), e17184. doi: 10.1097/md.0000000000017184

Shindler, K. S., Kenyon, L. C., Dutt, M., Hingley, S. T., & Das Sarma, J. (2008). Experimental optic neuritis induced by a demyelinating strain of mouse hepatitis virus. *J Virol, 82*(17), 8882-8886. doi: 10.1128/jvi.00920-08

Shrivastava, R., & Bhadauria, S. (2016). Role of Growth Factor Signaling in Cancer *Defence Life Science Journal, 1*(1), 37-47. doi: https://doi.org/10.14429/dlsj.1.10059

Silveira, C., Guedes, R., Maia, D., Curral, R., & Coelho, R. (2019). Neuropsychiatric Symptoms of Multiple Sclerosis: State of the Art. *Psychiatry Investig*. doi: 10.30773/pi.2019.0106

Singla, V., & Reiter, J. F. (2006). The Primary Cilium as the Cell's Antenna: Signaling at a Sensory Organelle. *Science, 313*(5787), 629-633. doi: 10.1126/science.1124534

Sisignano, M., Park, C. K., Angioni, C., Zhang, D. D., von Hehn, C., Cobos, E. J., . . . Brenneis, C. (2012). 5,6-EET is released upon neuronal activity and induces mechanical pain hypersensitivity via TRPA1 on central afferent terminals. *J Neurosci, 32*(18), 6364-6372. doi: 10.1523/jneurosci.5793-11.2012

Skripuletz, T., Bussmann, J. H., Gudi, V., Koutsoudaki, P. N., Pul, R., Moharregh-Khiabani, D., . . . Stangel, M. (2010). Cerebellar cortical demyelination in the murine cuprizone model. *Brain Pathol, 20*(2), 301-312. doi: 10.1111/j.1750-3639.2009.00271.x

Skripuletz, T., Hackstette, D., Bauer, K., Gudi, V., Pul, R., Voss, E., . . . Stangel, M. (2013). Astrocytes regulate myelin clearance through recruitment of microglia during cuprizone-induced demyelination. *Brain, 136*(Pt 1), 147-167. doi: 10.1093/brain/aws262

Skripuletz, T., Lindner, M., Kotsiari, A., Garde, N., Fokuhl, J., Linsmeier, F., . . . Stangel, M. (2008). Cortical demyelination is prominent in the murine cuprizone model and is strain-dependent. *Am J Pathol, 172*(4), 1053-1061. doi: 10.2353/ajpath.2008.070850

Smith, P. A., Heijmans, N., Ouwerling, B., Breij, E. C., Evans, N., van Noort, J. M., . . . Amor, S. (2005). Native myelin oligodendrocyte glycoprotein promotes severe chronic neurological disease and demyelination in Biozzi ABH mice. *Eur J Immunol, 35*(4), 1311-1319. doi: 10.1002/eji.200425842

Sofologi, M., Koutsouraki, E., Tsolaki, M., Tsolaki, A., Koukoulidis, T., Theofilidis, A., . . . Moraitou, D. (2019). Analyzing social cognition and understanding of social inferences in patients with multiple sclerosis. A comparative study. *Hell J Nucl Med, 22 Suppl 2*, 15-26.

Soulika, A. M., Lee, E., McCauley, E., Miers, L., Bannerman, P., & Pleasure, D. (2009). Initiation and progression of axonopathy in experimental autoimmune encephalomyelitis. *J Neurosci, 29*(47), 14965-14979. doi: 10.1523/jneurosci.3794-09.2009

Stadelmann, C., Kerschensteiner, M., Misgeld, T., Bruck, W., Hohlfeld, R., & Lassmann, H. (2002). BDNF and gp145trkB in multiple sclerosis brain lesions: neuroprotective interactions between immune and neuronal cells? *Brain, 125*(Pt 1), 75-85. doi: 10.1093/brain/awf015

Stanić, D., Malmgren, H., He, H., Scott, L., Aperia, A., & Hökfelt, T. (2009). Developmental changes in frequency of the ciliary somatostatin receptor 3 protein. *Brain Res, 1249*, 101-112. doi: https://doi.org/10.1016/j.brainres.2008.10.024

Storch, M. K., Bauer, J., Linington, C., Olsson, T., Weissert, R., & Lassmann, H. (2006). Cortical demyelination can be modeled in specific rat models of autoimmune encephalomyelitis and is major histocompatibility complex (MHC) haplotype-related. *J Neuropathol Exp Neurol, 65*(12), 1137-1142. doi: 10.1097/01.jnen.0000248547.13176.9d

Story, G. M., Peier, A. M., Reeve, A. J., Eid, S. R., Mosbacher, J., Hricik, T. R., . . . Patapoutian, A. (2003). ANKTM1, a TRP-like channel expressed in nociceptive neurons, is activated by cold temperatures. *Cell, 112*(6), 819-829.

Stys, P. K., Zamponi, G. W., van Minnen, J., & Geurts, J. J. (2012). Will the real multiple sclerosis please stand up? *Nat Rev Neurosci, 13*(7), 507-514. doi: 10.1038/nrn3275

Suzuki, K., & Kikkawa, Y. (1969). Status spongiosus of CNS and hepatic changes induced by cuprizone (biscyclohexanone oxalyldihydrazone). *Am J Pathol, 54*(2), 307-325.

Tanuma, N., Sakuma, H., Sasaki, A., & Matsumoto, Y. (2006). Chemokine expression by astrocytes plays a role in microglia/macrophage activation and subsequent neurodegeneration in secondary progressive multiple sclerosis. *Acta Neuropathol, 112*(2), 195-204. doi: 10.1007/s00401-006-0083-7

Taylor-Clark, T. E., McAlexander, M. A., Nassenstein, C., Sheardown, S. A., Wilson, S., Thornton, J., . . . Undem, B. J. (2008). Relative contributions of TRPA1 and TRPV1 channels in the activation of vagal bronchopulmonary C-fibres by the endogenous autacoid 4-oxononenal. *J Physiol, 586*(14), 3447-3459. doi: 10.1113/jphysiol.2008.153585

Taylor-Clark, T. E., Nassenstein, C., McAlexander, M. A., & Undem, B. J. (2009). TRPA1: a potential target for anti-tussive therapy. *Pulm Pharmacol Ther, 22*(2), 71-74. doi: 10.1016/j.pupt.2008.12.019

Taylor-Clark, T. E., Undem, B. J., Macglashan, D. W., Jr., Ghatta, S., Carr, M. J., & McAlexander, M. A. (2008). Prostaglandin-induced activation of nociceptive neurons via direct interaction with transient receptor potential A1 (TRPA1). *Mol Pharmacol, 73*(2), 274-281. doi: 10.1124/mol.107.040832

Thompson, A. J., Banwell, B. L., Barkhof, F., Carroll, W. M., Coetzee, T., Comi, G., . . . Cohen, J. A. (2018). Diagnosis of multiple sclerosis: 2017 revisions of the McDonald criteria. *Lancet Neurol, 17*(2), 162-173. doi: 10.1016/s1474-4422(17)30470-2

Thompson, A. J., Baranzini, S. E., Geurts, J., Hemmer, B., & Ciccarelli, O. (2018). Multiple sclerosis. *Lancet, 391*(10130), 1622-1636. doi: 10.1016/s0140-6736(18)30481-1

Tong, C. K., Han, Y. G., Shah, J. K., Obernier, K., Guinto, C. D., & Alvarez-Buylla, A. (2014). Primary cilia are required in a unique subpopulation of neural progenitors. *Proc Natl Acad Sci U S A, 111*(34), 12438-12443. doi: 10.1073/pnas.1321425111

Torkildsen, O., Brunborg, L. A., Myhr, K. M., & Bo, L. (2008). The cuprizone model for demyelination. *Acta Neurol Scand Suppl, 188*, 72-76. doi: 10.1111/j.1600-0404.2008.01036.x

Trapp, B. D., & Nave, K. A. (2008). Multiple sclerosis: an immune or neurodegenerative disorder? *Annu Rev Neurosci, 31*, 247-269. doi: 10.1146/annurev.neuro.30.051606.094313

Trapp, B. D., Peterson, J., Ransohoff, R. M., Rudick, R., Mork, S., & Bo, L. (1998). Axonal transection in the lesions of multiple sclerosis. *N Engl J Med, 338*(5), 278-285. doi: 10.1056/nejm199801293380502

Trapp, B. D., & Stys, P. K. (2009). Virtual hypoxia and chronic necrosis of demyelinated axons in multiple sclerosis. *Lancet Neurol, 8*(3), 280-291. doi: 10.1016/S1474-4422(09)70043-2

Trevisan, G., Hoffmeister, C., Rossato, M. F., Oliveira, S. M., Silva, M. A., Silva, C. R., . . . Ferreira, J. (2014). TRPA1 receptor stimulation by hydrogen peroxide is critical to trigger hyperalgesia and inflammation in a model of acute gout. *Free Radic Biol Med, 72*, 200-209. doi: 10.1016/j.freeradbiomed.2014.04.021

Tsunoda, I., & Fujinami, R. S. (2002). Inside-Out versus Outside-In models for virus induced demyelination: axonal damage triggering demyelination. *Springer Semin Immunopathol, 24*(2), 105-125. doi: 10.1007/s00281-002-0105-z

Tsunoda, I., & Fujinami, R. S. (2010). Neuropathogenesis of Theiler's murine encephalomyelitis virus infection, an animal model for multiple sclerosis. *J Neuroimmune Pharmacol, 5*(3), 355-369. doi: 10.1007/s11481-009-9179-x

Tsunoda, I., Kuang, L. Q., & Fujinami, R. S. (2002). Induction of autoreactive CD8+ cytotoxic T cells during Theiler's murine encephalomyelitis virus infection: implications for autoimmunity. *J Virol, 76*(24), 12834-12844.

Tullman, M. J., Oshinsky, R. J., Lublin, F. D., & Cutter, G. R. (2004). Clinical characteristics of progressive relapsing multiple sclerosis. *Mult Scler, 10*(4), 451-454. doi: 10.1191/1352458504ms1059oa

Tzartos, J. S., Craner, M. J., Friese, M. A., Jakobsen, K. B., Newcombe, J., Esiri, M. M., & Fugger, L. (2011). IL-21 and IL-21 receptor expression in lymphocytes and neurons in multiple sclerosis brain. *Am J Pathol, 178*(2), 794-802. doi: 10.1016/j.ajpath.2010.10.043

Tzartos, J. S., Friese, M. A., Craner, M. J., Palace, J., Newcombe, J., Esiri, M. M., & Fugger, L. (2008). Interleukin-17 production in central nervous system-infiltrating T cells and glial cells is associated with active disease in multiple sclerosis. *Am J Pathol, 172*(1), 146-155. doi: 10.2353/ajpath.2008.070690

Valente, E. M., Rosti, R. O., Gibbs, E., & Gleeson, J. G. (2014). Primary cilia in neurodevelopmental disorders. *Nature Reviews Neurology, 10*(1), 27-36. doi: 10.1038/nrneurol.2013.247

van den Hoogen, W. J., Laman, J. D., & 't Hart, B. A. (2017). Modulation of Multiple Sclerosis and Its Animal Model Experimental Autoimmune Encephalomyelitis by Food and Gut Microbiota. *Frontiers in Immunology, 8*(1081). doi: 10.3389/fimmu.2017.01081

Vangeel, L., & Voets, T. (2019). Transient Receptor Potential Channels and Calcium Signaling. *Cold Spring Harb Perspect Biol, 11*(6). doi: 10.1101/cshperspect.a035048

Vercellino, M., Masera, S., Lorenzatti, M., Condello, C., Merola, A., Mattioda, A., . . . Cavalla, P. (2009). Demyelination, inflammation, and neurodegeneration in multiple sclerosis deep gray matter. *J Neuropathol Exp Neurol, 68*(5), 489-502. doi: 10.1097/NEN.0b013e3181a19a5a

Verkhratsky, A., & Parpura, V. (2010). Recent advances in (patho)physiology of astroglia. *Acta Pharmacol Sin, 31*(9), 1044-1054. doi: 10.1038/aps.2010.108

Verkhratsky, A., Reyes, R. C., & Parpura, V. (2014). TRP channels coordinate ion signalling in astroglia. *Rev Physiol Biochem Pharmacol, 166*, 1-22. doi: 10.1007/112_2013_15

Veto, S., Acs, P., Bauer, J., Lassmann, H., Berente, Z., Setalo, G., Jr., . . . Illes, Z. (2010). Inhibiting poly(ADP-ribose) polymerase: a potential therapy against oligodendrocyte death. *Brain, 133*(Pt 3), 822-834. doi: 10.1093/brain/awp337

Viana, F. (2016). TRPA1 channels: molecular sentinels of cellular stress and tissue damage. *J Physiol, 594*(15), 4151-4169. doi: 10.1113/jp270935

Voss, E. V., Skuljec, J., Gudi, V., Skripuletz, T., Pul, R., Trebst, C., & Stangel, M. (2012). Characterisation of microglia during de- and remyelination: can they create a repair promoting environment? *Neurobiol Dis, 45*(1), 519-528. doi: 10.1016/j.nbd.2011.09.008

Walton, R. M. (2012). Postnatal neurogenesis: of mice, men, and macaques. *Vet Pathol, 49*(1), 155-165. doi: 10.1177/0300985811414035

Wang, Z., Li, V., Chan, G. C. K., Phan, T., Nudelman, A. S., Xia, Z., & Storm, D. R. (2009). Adult Type 3 Adenylyl Cyclase–Deficient Mice Are Obese. *PLoS One, 4*(9), e6979. doi: 10.1371/journal.pone.0006979

Wang, Z., Phan, T., & Storm, D. R. (2011). The Type 3 Adenylyl Cyclase Is Required for Novel Object Learning and Extinction of Contextual Memory: Role of cAMP Signaling in Primary Cilia. *The Journal of Neuroscience, 31*(15), 5557-5561. doi: 10.1523/jneurosci.6561-10.2011

Watanabe, M., Ueda, T., Shibata, Y., Kumamoto, N., Shimada, S., & Ugawa, S. (2015). Expression and Regulation of Cav3.2 T-Type Calcium Channels during Inflammatory Hyperalgesia in Mouse Dorsal Root Ganglion Neurons. *PLoS One, 10*(5), e0127572. doi: 10.1371/journal.pone.0127572

Watson, A., Eilers, A., Lallemand, D., Kyriakis, J., Rubin, L. L., & Ham, J. (1998). Phosphorylation of c-Jun is necessary for apoptosis induced by survival signal withdrawal in cerebellar granule neurons. *J Neurosci, 18*(2), 751-762.

Wei, M. C., Lindsten, T., Mootha, V. K., Weiler, S., Gross, A., Ashiya, M., . . . Korsmeyer, S. J. (2000). tBID, a membrane-targeted death ligand, oligomerizes BAK to release cytochrome c. *Genes Dev, 14*(16), 2060-2071.

Wei, M. C., Zong, W. X., Cheng, E. H., Lindsten, T., Panoutsakopoulou, V., Ross, A. J., . . . Korsmeyer, S. J. (2001). Proapoptotic BAX and BAK: a requisite gateway to mitochondrial dysfunction and death. *Science, 292*(5517), 727-730. doi: 10.1126/science.1059108

Werneck, L. C., Lorenzoni, P. J., Kay, C. S. K., & Scola, R. H. (2018). Multiple sclerosis: disease modifying therapy and the human leukocyte antigen. *Arquivos de Neuro-Psiquiatria, 76*, 697-704.

Wheway, G., Nazlamova, L., & Hancock, J. T. (2018). Signaling through the Primary Cilium. *Frontiers in cell and developmental biology, 6*, 8-8. doi: 10.3389/fcell.2018.00008

Widmann, C., Gibson, S., Jarpe, M. B., & Johnson, G. L. (1999). Mitogen-activated protein kinase: conservation of a three-kinase module from yeast to human. *Physiol Rev, 79*(1), 143-180. doi: 10.1152/physrev.1999.79.1.143

Williamson, J. S., Sykes, K. C., & Stohlman, S. A. (1991). Characterization of brain-infiltrating mononuclear cells during infection with mouse hepatitis virus strain JHM. *J Neuroimmunol, 32*(3), 199-207.

Wilson, S. R., Gerhold, K. A., Bifolck-Fisher, A., Liu, Q., Patel, K. N., Dong, X., & Bautista, D. M. (2011). TRPA1 is required for histamine-independent, Mas-related G protein-coupled receptor-mediated itch. *Nat Neurosci, 14*(5), 595-602. doi: 10.1038/nn.2789

Wong, S. T., Trinh, K., Hacker, B., Chan, G. C. K., Lowe, G., Gaggar, A., . . . Storm, D. R. (2000). Disruption of the Type III Adenylyl Cyclase Gene Leads to Peripheral and Behavioral Anosmia in Transgenic Mice. *Neuron, 27*(3), 487-497. doi: 10.1016/S0896-6273(00)00060-X

Woodruff, R. H., & Franklin, R. J. (1999). Demyelination and remyelination of the caudal cerebellar peduncle of adult rats following stereotaxic injections of lysolecithin, ethidium bromide, and complement/anti-galactocerebroside: a comparative study. *Glia, 25*(3), 216-228.

Woodruff, R. H., Fruttiger, M., Richardson, W. D., & Franklin, R. J. (2004). Platelet-derived growth factor regulates oligodendrocyte progenitor numbers in adult CNS and their response following CNS demyelination. *Mol Cell Neurosci, 25*(2), 252-262. doi: 10.1016/j.mcn.2003.10.014

Xia, Z., Dickens, M., Raingeaud, J., Davis, R. J., & Greenberg, M. E. (1995). Opposing effects of ERK and JNK-p38 MAP kinases on apoptosis. *Science, 270*(5240), 1326-1331.

Yasuda, K., Rens-Domiano, S., Breder, C. D., Law, S. F., Saper, C. B., Reisine, T., & Bell, G. I. (1992). Cloning of a novel somatostatin receptor, SSTR3, coupled to adenylylcyclase. *J Biol Chem, 267*(28), 20422-20428.

Ye, F., Nager, A. R., & Nachury, M. V. (2018). BBSome trains remove activated GPCRs from cilia by enabling passage through the transition zone. *217*(5), 1847-1868. doi: 10.1083/jcb.201709041

Zeger, M., Popken, G., Zhang, J., Xuan, S., Lu, Q. R., Schwab, M. H., . . . Ye, P. (2007). Insulin-like growth factor type 1 receptor signaling in the cells of oligodendrocyte lineage is required for normal in vivo oligodendrocyte development and myelination. *Glia, 55*(4), 400-411. doi: 10.1002/glia.20469

Zuo, J., Stohlman, S. A., Hoskin, J. B., Hinton, D. R., Atkinson, R., & Bergmann, C. C. (2006). Mouse hepatitis virus pathogenesis in the central nervous system is independent of IL-15 and natural killer cells. *Virology, 350*(1), 206-215. doi: 10.1016/j.virol.2006.01.027

Zygmunt, P. M., & Hogestatt, E. D. (2014). TRPA1. *Handb Exp Pharmacol, 222*, 583-630. doi: 10.1007/978-3-642-54215-2_23

6. BIBLIOGRAPHY

Articles related to the thesis

Sághy*, É., **Sipos*, É.**, Ács, P., Bölcskei, K., Pohóczky, K., Kemény, A., Sándor, Z., Szőke, É., Sétáló, Gy. Jr., Komoly, S. and Pintér, E. (2016). "TRPA1 deficiency is protective in cuprizone-induced demyelination-A new target against oligodendrocyte apoptosis." *Glia, 64*(12), 2166-2180. doi: 10.1002/glia.23051
*contributed equally

Bölcskei, K., Kriszta, G., Sághy, É., Payrits, M., **Sipos, É.**, Vranesics, A., Berente, Z., Ábrahám, H., Ács, P., Komoly, S. and Pintér, E. (2018). "Behavioural alterations and morphological changes are attenuated by the lack of TRPA1 receptors in the cuprizone-induced demyelination model in mice. " *J Neuroimmunol, 320*, 1-10. doi: 10.1016/j.jneuroim.2018.03.020

Sipos, É., Komoly, S. and Ács, P. (2018). "Quantitative Comparison of Primary Cilia Marker Expression and Length in the Mouse Brain." *J Mol Neurosci, 64*(3), 397-409. doi: 10.1007/s12031-018-1036-z

Abstracts published in cited journals

Pintér, E., Bölcskei, K., Sághy, É., Payrits, M., Kriszta, G., Vranesics, A., **Sipos, É**., Ács, P., Berente, Z., Ábrahám, H., Komoly, S. (2017) "TRPA1 receptor deficiency substantially diminishes the cuprizone-induced demyelination. " *Journal of Neurochemistry* 142 : 1 pp. 171-172., 2 p.

Poster presentations

Sipos, É., Komoly, S., Ács, P. "Expression of primary ciliary markers in satiety centers of the brain. " Department of Neurology, Medical School of Pécs, University of Pécs, Hungary. P91, *IBRO Workshop*, Debrecen, Magyarország, 2014

Sághy É., Bölcskei K., Perkecz A., Sándor Z., Kemény Á., Szőke É., Ács P., **Sipos É.**, Gaszner B., Komoly S., Helyes Zs., Pintér Erika. "A Tranziens Receptor Potenciál Ankyrin 1 (TRPA1) receptor szerepe cuprizone-indukált kísérletes demyelinizáció modellben. " A Magyar Élettani Társaság 79. Vándorgyűlése és a Magyar Mikrocirkulációs és Vaszkuláris Biológiai Társaság Konferenciája, Szeged, Magyarország, 2015.

Sághy É., **Sipos É.,** Ács P., Bölcskei K., Pohóczky K., Kemény Á., Sándor Z., Szőke É., Sétáló Gy. Jr., Komoly S., Pintér E. "A TRPA1 receptor szerepe a sclerosis multiplex kísérletes állatmodelljében. " Magyar Farmakológiai, Anatómus, Mikrocirkulációs és Élettani Társaságok Közös Tudományos Konferenciája, Pécs, Magyarország, 2016.

Sághy É., Bölcskei K., Péter Á., Komoly S., **Sipos É.,** Szőke É., Perkecz A., Gaszner B., Kemény Á., Sándor Z., Helyes Zs., Pintér E. "Transient Receptor Potential Ankyrin 1 (TRPA1) receptor has regulatory role in the cuprizone-induced demyelination in mice. " *IBRO Workshop,* Budapest, Magyarország, 2016.

Oral presentations

Pintér E.**,** Sághy É., Payrits M., Bölcskei K., Perkecz A., Sándor Z., Kemény Á., Szőke É., Ács P., **Sipos É.,** Komoly S., Helyes Zs., Ábrahám I. "A Tranziens Receptor Potencial Ankyrin 1 (TRPA1) Receptor szerepe a neurodegeneratív kórképekben**.** " Magyar Farmakológiai, Anatómus, Mikrocirkulációs és Élettani Társaságok Közös Tudományos Konferenciája**,** Pécs, Magyarország, 2016.

Sághy, É., Bölcskei K., Ács, P., Komoly, S., Perkecz, A., Gaszner, B., **Sipos, É.**, Kemény, A., Szőke, É., Sándor, Z., Helyes, Zs., Pintér, E. "Genetic deletion of the Transient Receptor Potential Ankyrin 1 (TRPA1) receptor inhibits cuprizone-induced demyelination in mice. " Neuropeptides, Aberdeen, Scotland, United Kingdom, 2015.

Sipos É., Ács P., Komoly S. "Elsődleges csillók a központi idegrendszerben."
BAW – Brain Awareness Week/ Agykutatás Hete, Pécsi Tudományegyetem, Általános Orvostudományi Kar, 2017. március 13-19.

7. ACKNOWLEDGEMENT AND FUNDING

7.1 Acknowledgment

I am grateful to my project leader Prof. Sámuel Komoly M.D., Ph.D., D.Sc. and mentor Péter Ács M.D., Ph.D. for their leadership, support, advices and for providing me the opportunity to perform this project.

I wish to thank Prof. Erika Pintér M.D, Ph.D., D.Sc., Kata Bölcskei M.D, Ph.D. and Éva Sághy Pharm.D., Ph.D. for the collaboration throughout the whole study.

I am also grateful to my colleagues and members of the Pathology Department of Pécs University for providing me technical facilities and invaluable practical suggestions during the course of the study.

I owe special thanks to Prof. Miklós Palkovits M.D., Ph.D., D.Sc. and the Department of Neuroanatomy of Semmelweis University for the excellent contribution, support in the studies.

I appreciate the collaboration, support and advices of György Sétáló Jr. M.D., Ph.D.

I am grateful to Ms. Andrea Fábiánkovics M.D., Ms. Krisztina Fülöp, Mrs. Mónika Vecsernyés, Ms. Anikó Perkecz and Mr. Ernő Bognár for their excellent technical assistance.

I wish to thank my family for their support and unconditional love.

7.2 Funding

This study was supported by Hungarian Grants:

National Brain Research Program–A KTIA_NAP_13-1-2013-0001; Gedeon Richter's Talentum Foundation; EFOP 3.6.1.-16.2016.00004; and KA-2015-09 of University of Pécs